

Characterization of the TPR protein family and a putative photosynthetic protein from *Synechocystis* PCC 6803



Dissertation der Fakultät für Biologie
der
Ludwig-Maximilians-Universität München

vorgelegt von

Shao, Lin

München

2012

Characterization of the TPR protein family and a putative photosynthetic protein from *Synechocystis* PCC 6803

Dissertation der Fakultät für Biologie
der
Ludwig-Maximilians-Universität München

vorgelegt von

Shao, Lin

München

2012

Erstgutachter: **Prof. Dr. Jörg Nickelsen**, AG Molekulare Pflanzenwissenschaften

Zweitgutachter: **Prof. Dr. Dario Leister**, AG Molekularbiologie der Pflanzen/Botanik

Tag der mündlichen Prüfung: 22.03.2012

Content

1. SUMMARY	1
2. ZUSAMMENFASSUNG	2
3. INTRODUCTION	4
3.1 SYNECHOCYSTIS SP. PCC 6803 AS A MODEL ORGANISM	4
3.2 PHOTOSYNTHESIS	5
3.2.1 Photosystem II.....	6
3.2.2 Photosystem I.....	9
3.3 RESPIRATION.....	11
3.4 BIOGENESIS OF THYLAKOID MEMBRANES IN CYANOBACTERIA	13
3.4.1 Formation, stabilization and organization of thylakoid membranes	14
3.4.2 Photosystem II assembly.....	14
3.5 THE FUNCTION OF TPR PROTEINS IN PHOTOSYNTHESIS	16
3.6 EFFECTS OF SALT STRESS ON PHOTOSYSTEM II AND I IN CYANOBACTERIA	18
4. AIMS OF THIS WORK.....	20
5. MATERIALS AND METHODS	21
5.1 MATERIALS	21
5.1.1 Chemicals	21
5.1.2 Enzymes	23
5.1.3 Kits	23
5.1.4 Strains, vectors and oligonucleotides	23
5.1.5 Antibodies	24
5.1.6 Culture media	25
5.2 METHODS	25
5.2.1 Bioinformatical and computational analyses tools and websites.....	25
5.2.2 General methods of molecular biology.....	25
5.2.3 Isolation of genomic DNA from Synechocystis 6803.....	26
5.2.4 DNA amplification by Polymerase Chain Reaction (PCR), cloning and sequencing.....	26
5.2.5 Transformation of Synechocystis 6803 with exogenous DNA	27
5.2.6 Estimation of doubling time	27
5.2.7 Analysis of oxygen evolution.....	28
5.2.8 Emission Spectra Measurement.....	28
5.2.9 Chlorophyll Fluorescence Measurement.....	29
5.2.10 General methods of biochemistry	29
5.2.11 Preparation of whole cell protein extracts from Synechocystis 6803	29
5.2.12 Preparation of membrane proteins from Synechocystis 6803.....	30
5.2.13 Two-dimensional blue native (BN)/SDS-PAGE	30
5.2.14 Immunodetection of proteins by Enhanced Chemiluminescence (ECL).....	31
5.2.15 Sucrose density gradient centrifugation.....	32
5.2.16 Overexpression and purification of recombinant GST-tagged fusion proteins.....	32
5.2.17 Thin layer chromatography (TLC).....	33
5.2.18 Pulse labeling.....	33
5.2.19 Transmission electron microscopy (TEM)	33
5.2.20 Fractionation of membranes from Synechocystis 6803 by sucrose density gradient centrifugation.....	33

6. RESULTS.....	34
6.1 CHARACTERIZATION OF THE TPR PROTEIN FAMILY FROM <i>SYNECHOCYSTIS</i> 6803.....	34
6.1.1 <i>Identification of genes encoding putative TPR proteins</i>	34
6.1.2 <i>Generation and selection of tpr mutants</i>	35
6.1.3 <i>Analysis of photosynthetic performances of tpr mutants</i>	36
6.2 MOLECULAR ANALYSIS OF THE TPR PROTEIN SLL1946.....	39
6.2.1 <i>Analysis of Sll1946 amino acid sequence</i>	39
6.2.2 <i>Complementation of sll1946⁻</i>	40
6.2.3 <i>Determination of protein amounts of photosynthetic subunits in sll1946⁻</i>	41
6.2.4 <i>Analysis of PS II complex assembly</i>	42
6.2.5 <i>Membrane sublocalization of PSII subunits and assembly factors</i>	43
6.2.6 <i>Morphology of sll1946⁻</i>	44
6.2.7 <i>Analyses of pigment and lipid composition in sll1946⁻</i>	45
6.3 MOLECULAR ANALYSIS OF SLR0483, A PROTEIN INVOLVED IN THYLAKOID MEMBRANE BIOGENESIS	47
6.3.1 <i>Analysis of Slr0483 amino acid sequence</i>	47
6.3.2 <i>Generation of a slr0483 insertion mutant</i>	48
6.3.3 <i>Topology and quantification of Slr0483</i>	49
6.3.4 <i>Phenotypic characterization of slr0483⁻</i>	50
6.3.5 <i>Protein level analyses of photosynthetic subunits in slr0483⁻</i>	52
6.3.6 <i>Analysis of PS II complex assembly in slr0483⁻</i>	53
6.3.7 <i>Membrane sublocalization of PSII subunits and assembly factors</i>	55
6.3.8 <i>Distribution of Slr0483 in photosynthetic protein complexes</i>	55
6.3.9 <i>Morphology of slr0483⁻</i>	57
6.3.10 <i>Influence of salt stress on Slr0483 accumulation</i>	59
7. DISCUSSION	61
7.1 TPR PROTEIN FAMILY	61
7.1.1 <i>Putative functions of TPR proteins in Synechocystis 6803</i>	61
7.1.2 <i>Evolution of the TPR proteins</i>	62
7.2 SLL1946, A TPR PROTEIN POTENTIALLY INVOLVED IN EARLY STEPS OF PS II ASSEMBLY	64
7.3 SLR0483 IS A THYLAKOID MEMBRANE ORGANIZATION FACTOR	66
7.3.1 <i>Loss of Slr0483 leads to defective TM organization and reduced photosynthetic performance</i>	66
7.3.2 <i>Slr0483 is conserved in photosynthetic organisms</i>	68
7.3.3 <i>Defective respiratory performance</i>	69
7.3.4 <i>Changes of pD1 and CP47 localization in slr0483⁻</i>	69
7.3.5 <i>Crucial role of Slr0483 under salt stress</i>	70
7.4 CONCLUSION	71
8. REFERENCES.....	72
9. LIST OF ABBREVIATIONS.....	85
10. ACKNOWLEDGEMENTS.....	88
11. CURRICULUM VITAE.....	89
12. EHRENWÖRTLICHE VERSICHERUNG.....	90

1. Summary

Photosynthesis, occurring on the thylakoid membranes (TM) of photosynthetic organisms, converts light energy to chemical energy thus generates biomass and oxygen required for many processes on earth. The light reactions of photosynthesis are performed coordinately by photosynthetic protein machineries. The mechanisms regarding the expression, regulation and assembly of these apparatuses are still not fully understood. Interestingly, so-called TPR proteins (tetratricopeptide repeat) mediating protein-protein interactions were often found to play crucial roles in the TMs biogenesis of photosynthetic organisms.

In *Synechocystis* 6803, a model cyanobacterium for genetic and physiological studies of photosynthesis, 23 open reading frames encoding putative TPR proteins have been identified. Eight of these TPR proteins were analyzed previously, thus the present study focuses on the remaining 15 TPR proteins that were investigated by mutagenesis of the respective genes. Among these 15 mutants, 11 of them could be shown to be fully segregated whereas 3 were found to be essential. To estimate the photosynthetic performances, doubling time, oxygen evolution, emission spectra and chlorophyll fluorescence were analyzed. Combining these data with the previously analyzed mutants, at least 12 proteins (52 % of the whole protein family) can be proposed to play roles in photosynthesis or TMs biogenesis.

For more detailed analysis of certain TPR proteins in TMs biogenesis, Sll1946 was chosen to investigate further, since the mutant, *sll1946*⁻, was found to exhibit a strong photosynthetic phenotype. It could be shown that the loss of Sll1946 leads to diminished levels of D1 and CP43 and to a clear reduction of PSII monomers. Thus, the results suggest a potential role of Sll1946 in the early step of PS II assembly.

Additionally, the function of Slr0483, an integral membrane protein that is evolutionarily conserved in all photosynthetic organisms, was analyzed in this study. The generated mutant was found to be fully segregated and loss of Slr0483 led to clear defects in photosynthetic and respiratory performances. The deactivation of *slr0483* specifically reduced the levels of all PS II subunits tested and subsequently the PS II dimer was almost absent in *slr0483* cells. Additionally, changes in membrane fraction localization was observed for pD1 (precursor form of D1) and CP47. Surprisingly, the organization of TMs in *slr0483* cells was highly disordered and no convergence sites between plasma membrane and TMs were detected, indicating a role of Slr0483 in the maintenance of TMs. Moreover, Slr0483 was found to be induced by salt stress leading to a strong sensitivity of the *slr0483* cells to high salt concentrations.

2. Zusammenfassung

Photosynthese findet an den Thylakoidmembranen (TM) von photosynthetischen Organismen statt und wandelt Lichtenergie in chemische Energie um, wodurch Biomasse und Sauerstoff erzeugt werden, welche für eine Vielzahl von Prozessen benötigt werden. Die Lichtreaktion der Photosynthese wird durch eine Reihe von photosynthetischen Proteinmaschinerien durchgeführt. Die Mechanismen, welche zur Expression, Regulierung und Assemblierung dieser Proteinkomplexe führen sind noch nicht vollständig geklärt. Interessanterweise wurde gefunden, dass so genannte TPR Proteine (Tetratricopeptid Repeat), welche Protein-Protein Interaktionen vermitteln, häufig wichtige Rollen in der TM Biogenese von photosynthetischen Organismen spielen.

In dem Cyanobakterium *Synechocystis* 6803, einem Modelsystem für genetische und physiologische Studien der Photosynthese, wurden 23 Leserahmen, welche für mutmaßliche TPR Proteine kodieren, identifiziert. Acht dieser TPR Proteine wurden bereits in früheren Studien analysiert, folglich fokussiert sich die vorliegende Arbeit auf die verbleibenden 15 TPR Proteine, welche durch Mutagenese der entsprechenden Gene untersucht wurden. Für 11 von diesen 15 Mutanten konnte gezeigt werden, dass sie vollständig segregiert waren, wohingegen 3 als essentielle Gene identifiziert wurden. Um die photosynthetische Leistung der generierten Mutanten zu messen, wurden Analysen der Verdopplungszeit, Sauerstoffentwicklung, Emissionsspektren und Chlorophyllfluoreszenz durchgeführt. Kombiniert man die erhaltenen Daten mit früheren Untersuchungen, so kann postuliert werden, dass mindestens 12 Proteine (52% der gesamten Proteinfamilie) Funktionen in der Photosynthese oder TM Biogenese ausüben.

Um einige der TPR Proteine genauer auf ihre Rolle in der TM Biogenese zu untersuchen, wurde *Sll1946* für weitere Analysen ausgewählt, da die *sll1946* Mutante einen deutlichen photosynthetischen Phänotyp aufwies. Es konnte gezeigt werden, dass der Verlust von *Sll1946* zu verringerten D1- und CP43-Mengen sowie zu einer deutlichen Reduzierung der Photosystem II (PSII) Monomere führt. Folglich legen die Ergebnisse eine Rolle von *Sll1946* in frühen Schritten der PSII Assemblierung nahe.

Zusätzlich wurde in dieser Arbeit die Funktion von *Slr0483* untersucht, ein integrales Membranprotein, welches in allen photosynthetischen Organismen konserviert ist. Die hergestellte Mutante war vollständig segregiert und der Verlust von *Slr0483* führte zu deutlichen Defekten in der photosynthetischen und respiratorischen Leistung. Die Deaktivierung von *slr0483* hatte eine spezifische Reduzierung der Mengen aller getesteten PS II Untereinheiten zur Folge und somit konnte fast kein PS II Dimer in den *slr0483* Zellen

mehr detektiert werden. Zusätzlich wurden Änderungen in der Lokalisierung in Membranfraktionen für pD1 (die Vorstufenform von D1) und CP47 gefunden. Überraschenderweise konnte gezeigt werden, dass die Organisation der TMs in *slr0483* Zellen stark gestört war und keinerlei Konvergenzzentren zwischen Plasmamembran und den TMs mehr existierten, was eine Funktion von Slr0483 in der Aufrechterhaltung der TMs nahe legt. Außerdem wurde gefunden, dass Slr0483 durch Salzstress induziert wird, was zu einer drastischen Empfindlichkeit der *slr0483* Zellen gegenüber hohen Salzkonzentrationen führt.

3. Introduction

3.1 *Synechocystis* sp. PCC 6803 as a model organism

Synechocystis sp. PCC 6803 (henceforth referred to as *Synechocystis* 6803), a fresh water inhabitant, is a Gram-negative and a unicellular non-nitrogen-fixing cyanobacterium (Ikeuchi and Tabata 2001). Information about complete genomic sequences of *Synechocystis* 6803 is available and the total length of the genome includes 3,573,470 bp (Kaneko et al 1996). The whole genome comprises 3,168 potential protein coding genes, of which the sequences, locations and additional information are available on the Kazusa website (<http://genome.kazusa.or.jp/cyanobase/Synechocystis>). Of these 3,168 genes, 131 have so far been found to be involved in the various stages of photosynthesis and respiration (Kaneko and Tabata 1997). Table 1 shows an overview about the assigned functions of the products of protein coding genes in *Synechocystis* 6803.

Table 1. Functional categories of the products of putative protein coding genes in *Synechocystis* 6803 (Kaneko and Tabata 1997).

Category	Gene number
Amino acid biosynthesis	84
Biosynthesis of cofactors, prosthetic groups, and carriers	108
Cell envelope	64
Cellular processes	62
Central intermediary metabolism	31
Energy metabolism	86
Fatty acid, phospholipid, and sterol metabolism	35
Photosynthesis and respiration	131
Nucleic acid metabolism	38
General regulatory functions	147
DNA replication, recombination, and repair	49
Transcription	24
Translation	144
Transport and binding proteins	158
Other categories	255
Function unknown	1752
Total	3168

In addition to the availability of the fully sequenced genome, two main properties are the reason for using *Synechocystis* 6803 as a model organism for genetic and physiological studies of photosynthesis: it is naturally capable of high frequency exogenous DNA transformation (Grigorieva and Shestakov 1982) and grows photoheterotrophically in the presence of a carbon source (Rippka et al. 1979).

Based on these advantages, *Synechocystis* 6803 is a useful tool to investigate the roles and functions of photosynthesis-related genes and proteins.

3.2 Photosynthesis

Photosynthesis converts light energy into chemical energy and is thus responsible for production of most of the biomass on earth. In plants, algae and cyanobacteria, the photosynthetic reactions additionally lead to the generation of oxygen. The evolutionary invention of this oxygenic photosynthesis changed the environment fundamentally and allowed the evolution of advanced life on earth by providing the oxidant for respiration (Blankenship 1992). As this process generated the vast majority of the atmospheric oxygen, it is moreover responsible for creation of the ozone layer required to protect the earth from UV irradiation (Blankenship 1992; Xiong and Bauer 2002). Therefore, the process of photosynthesis is widely accepted as the most important chemical reaction on earth.

The light reactions comprise the first stage of photosynthesis and involve the capture of light energy, water oxidation, electron transport, generation of a proton gradient and production of ATP. This light-driven process is performed and coordinated by a series of protein complexes embedded in the energy-transducing thylakoid membrane system of plants and algae chloroplasts, as well as of cyanobacteria. In general, these photosynthetic machineries include Light-Harvesting Complexes (LHCs), Photosystem II (PS II), Cytochrome *b₆f* (Cyt *b₆f*), Photosystem I (PS I) and the ATP Synthase complex (ATPase). So far, three classes of LHCs were characterized: first, in terrestrial plants, light harvesting is carried out by the chlorophyll a/b-binding (CAB) proteins; second, in marine algae such as diatoms, dinoflagellates, brown algae, and chrysophytes, the fucoxanthin-chlorophyll a/c complexes perform light harvesting; third, phycobilisomes (PBS) carry out the light harvesting in the prokaryotic cyanobacteria and eukaryotic red algae (Grossman et al. 1993).

In brief, light energy is absorbed by LHCs and is subsequently transferred to PS II and PS I to drive the photosynthetic electron transport. Water functions as an electron donor in this process and is oxidized to molecular oxygen and four protons within PS II (Nelson and Ben-Shem 2004). The released electrons are further transported through a plastoquinone (PQ) pool and Cyt b_6f complexes to plastocyanin (PC) (Cramer et al. 1996). Light energy absorbed by PS I finally induces the reduction of NADP⁺ to NADPH via ferredoxin (Fd) and ferredoxin-NADP reductase (FNR) at the stromal/cytosolic side (Nelson and Ben-Shem 2004). Additionally, a proton gradient is formed that powers the ATP synthesis by ATPase. A schematic depiction of the light-driven reactions is indicated in Figure1.

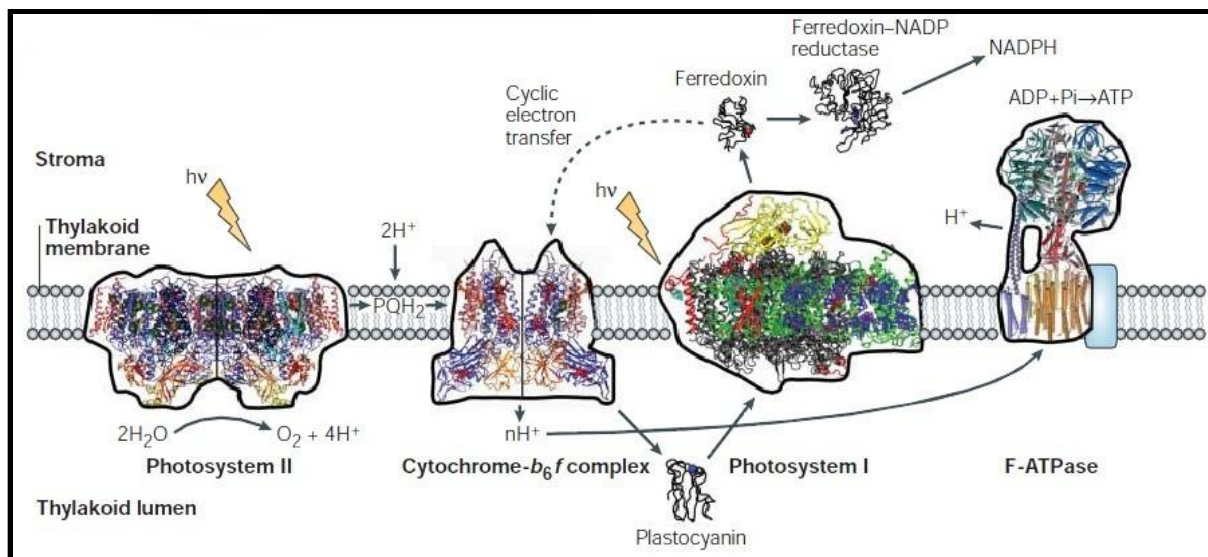


Figure 1. The structures of the four major membrane protein complexes which drive oxygenic photosynthesis. Electron donors and acceptors, plastoquinone, plastocyanin, ferredoxin and ferredoxin-NADP reductase are depicted as well. The linear and cyclic electron flows are indicated by solid and dashed lines, respectively (Nelson and Ben-Shem 2004).

The Calvin cycle, also known as the dark reactions, utilizes the products (ATP and NADPH) of the light reactions to fix atmospheric CO_2 into carbon skeletons that are used directly for starch and sucrose biosynthesis in all photosynthetic bacteria and in all photosynthetic eukaryotes (Raines 2003). This cycle is comprised of 11 different enzymes, catalyzing 13 reactions, and is initiated by the enzyme ribulose-1, 5-bisphosphate carboxylase/oxygenase (Rubisco, EC 4.1.1.39). During the photosynthetic assimilation of CO_2 , one molecule of CO_2 fixed by the Calvin cycle into carbohydrates consumes three molecules of ATP and two molecules of NADPH (Zhu et al. 2008).

3.2.1 Photosystem II

Photosystem II (PS II) catalyzes the chemically and thermodynamically demanding reaction of water oxidation powered by light (Barber 2006). In 1998, Rhee et al. reported a three-dimensional structure of plant PS II reaction center at 8 Å resolution, containing the proteins D1, D2, CP47 and cytochrome b-559 (Rhee et al. 1998). In 2001, Zouni et al. increased the resolution to 3.8 Å using isolated PS II from the thermophilic cyanobacterium *Synechococcus elongatus* and could thus show the spatial organization of protein subunits and cofactors (Zouni et al. 2001). In the following years, the PSII structure has been resolved in much more details (Kamiya and Shen 2003; Loll et al. 2005). So far, the latest study succeeded in obtaining a high resolution structure of PSII from *Thermosynechococcus elongatus* at 1.9 Å

(Umena et al., 2011; Figure 2). Thus it was revealed that each PS II monomer contains at least 20 protein subunits and numerous cofactors, including 35 chlorophylls (Chl), more than 20 lipids, 11 β -carotenes (Car), 4 manganese atoms, 3 or 4 calcium atoms, 3 chloride ions, 2 pheophytins (Pheo), 2 PQs, 2 haem Fe^{2+} , a non-haem Fe^{2+} and a bicarbonate ion (Umena et al. 2011).

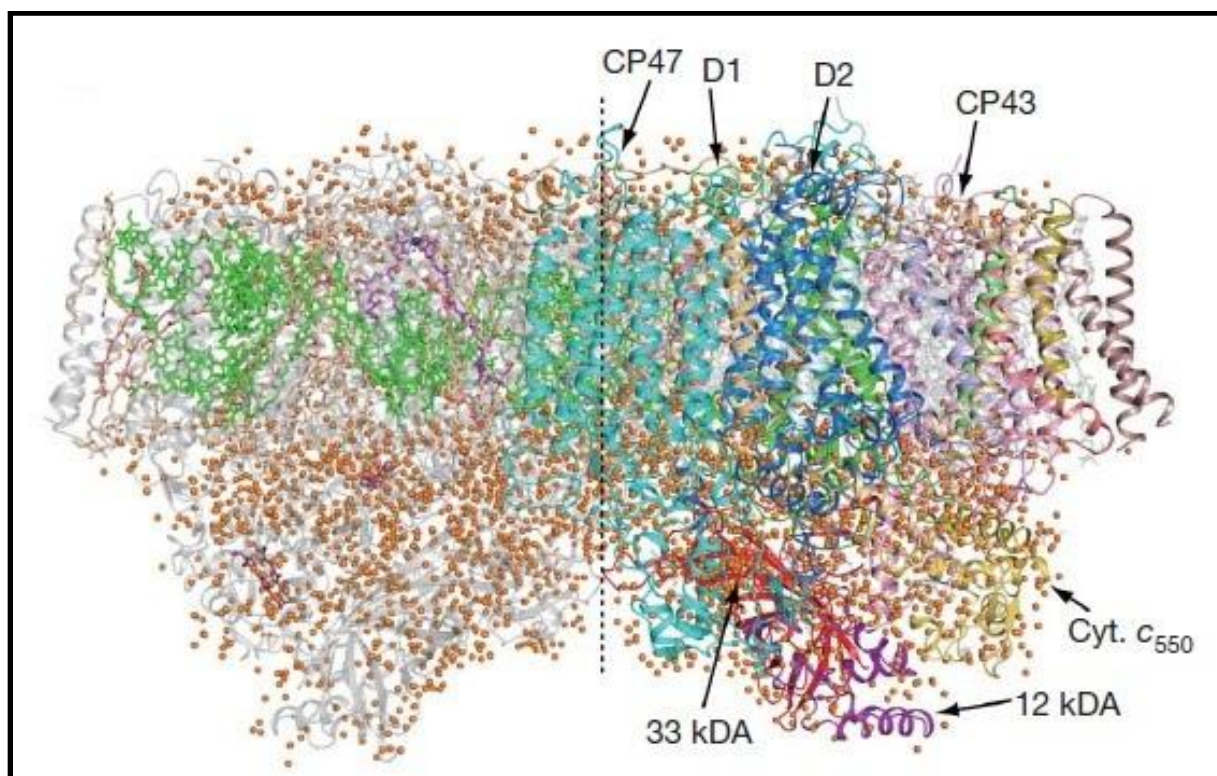


Figure 2. Overall structure of PS II dimer at 1.9 Å resolution from *Thermosynechococcus elongatus*. View from the direction perpendicular to the membrane. The protein subunits are colored individually in the right monomer and in light grey in the left monomer; the cofactors are depicted in color in the left monomer and in light grey in the right monomer. Orange balls represent water molecules. (Umena et al. 2011).

Among the protein subunits, the D1 (PsbA) and D2 (PsbD) proteins that each contains 5 transmembrane helices, form the core reaction center (RC) of the PS II complex. These two proteins are flanked by the CP43 (PsbC) and CP47 (PsbB) subunits, each comprised of 6 transmembrane helices (Ferreira et al. 2004). Table 2 describes the molecular weight, number of transmembrane α -helices and functions of identified PS II subunits in prokaryotes and eukaryotes.

In green algae and higher plants, light photons are captured by chlorophyll *a*, chlorophyll *b* and carotenoids, whereas in red algae and cyanobacteria, phycobilins carry out the light-harvesting. The primary electron donor, P_{680} (4 Chls in the center of D1/D2), is excited and

rapidly transfers the electrons to the acceptor Pheo that passes them on to Q_A and subsequently to Q_B (Barber and Nield 2002). On the oxidizing side of RC, P_{680} is double-reduced by the manganese cluster through a redox-active tyrosine, Y_Z , and accepts electrons derived from water oxidation (Barber and Nield 2002).

Water is oxidized at the metal-containing oxygen evolving complex (OEC) on the luminal side of PS II, catalyzing the reaction as follows:



Table 2. Summary of PS II protein subunits (Nickelsen et al. 2007; Müh et al. 2008; Allen et al. 2011; Data of Eukaryotes are from *A.thaliana* and *C.reinhardtii*).

Gene	Subunit	Mass (kDa)	Number of transmembrane α -helices	Function	Prokaryotes	Eukaryotes
<i>psbA</i>	D1	38	5	Primary reaction	+	+
<i>psbB</i>	CP47	56.3	6	Light harvesting	+	+
<i>psbC</i>	CP43	50.1	6	Light harvesting	+	+
<i>psbD</i>	D2	39.2	5	Primary reaction	+	+
<i>psbE</i>	Cyt b559 subunit α	9.2	1	Photoprotection and assembly	+	+
<i>psbF</i>	Cyt b559 subunit β	4.4	1	Photoprotection and assembly	+	+
<i>psbH</i>		7.7	1	Q_A to Q_B transfer, PS II repair	+	+
<i>psbI</i>	4.4 kDa	4.4	1	Assembly and repair	+	+
<i>psbJ</i>		4.1	1	Assembly	+	+
<i>psbK</i>		4.3	1	Assembly and stabilization	+	+
<i>psbL</i>	5 kDa	4.4	1	Stabilization	+	+
<i>psbM</i>		3.7	1	Stabilization	+	+
<i>psbO</i>	33 kDa	33	0	OEC stabilization	+	+
<i>psbP</i>	23 kDa	23	0	OEC stabilization	+	+
<i>psbQ</i>	16 kDa	16.5	0	OEC stabilization	+	+
<i>psbR</i>		15.1	1	OEC stabilization and repair	-	+
<i>psbS</i>		22	4	Photoprotection	-	+
<i>psbT</i>		3.8	1	Stabilization and repair	+	+
<i>psbU</i>	12 kDa	12	0	OEC Stabilization	+	-
<i>psbV</i>	Cyt c550	15	0	OEC Stabilization	+	-
<i>psbW</i>		6.1	1	Stabilization of PS II dimer	-	+
<i>psbX</i>		4.1	1	Stabilization	+	+
<i>psbY</i>		4	1	Unknown	+	+
<i>psbZ</i>	Ycf9	6.7	2	Supercomplex stabilization	+	+

The protons produced from this reaction are finally transferred to the stroma/cytosol via the ATPase to generate ATP (Figure 1). Four manganese (Mn) ions and one Calcium (Ca) ion have been found to be required for water-splitting and comprise the catalytic center. In addition, 5 oxygen atoms serve as oxo bridges linking the 5 metal atoms (Umena et al. 2011).

Moreover, 4 water molecules were shown to be associated with the Mn_4CaO_5 cluster, suggesting that at least some of these serve as the substrates for water oxidation (Figure 3, Umena et al. 2011).

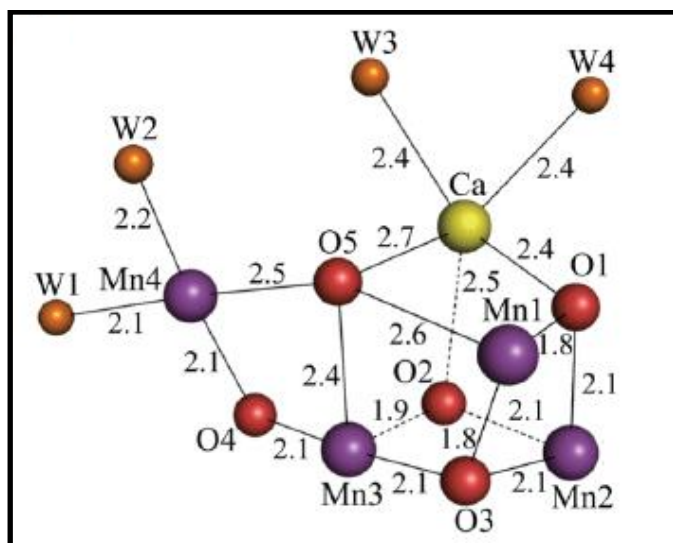


Figure 3. Structure of the Mn_4CaO_5 cluster. The numbers show the distance between metal atoms and oxygen atoms or water molecules. Three Mn, one Ca and four oxygen atoms form a cubane-like structure in which the Ca and Mn atoms occupy four corners and the oxygen atoms occupy the other four (Umena et al. 2011).

Each PS II monomer contains 13 subunits with a molecular weight less than 10 kDa (Low Molecular Mass, LMM). Three extrinsic subunits (PsbO, PsbU and PsbV) are found on the luminal side the PS II. The roles of the LMM subunits and 3 extrinsic subunits are summarized in Table 2.

3.2.2 Photosystem I

Photosystem I (PS I) catalyzes the subsequent light-driven electron transport from the luminal electron carrier plastocyanin (PC) to ferredoxin (Fd) on the stromal/cytosolic side (Figure 1). Several studies contributed in solving the crystal structure of PSI from cyanobacteria and higher plants in great details (Jordan et al. 2001; Amunts et al. 2007; Figure 4). To date, the PSI complex is thought to consist of 17 protein subunits, 173 chlorophylls, 15 carotenoids, 4 LHC I proteins, 3 Fe_4S_4 clusters and 2 phylloquinones.

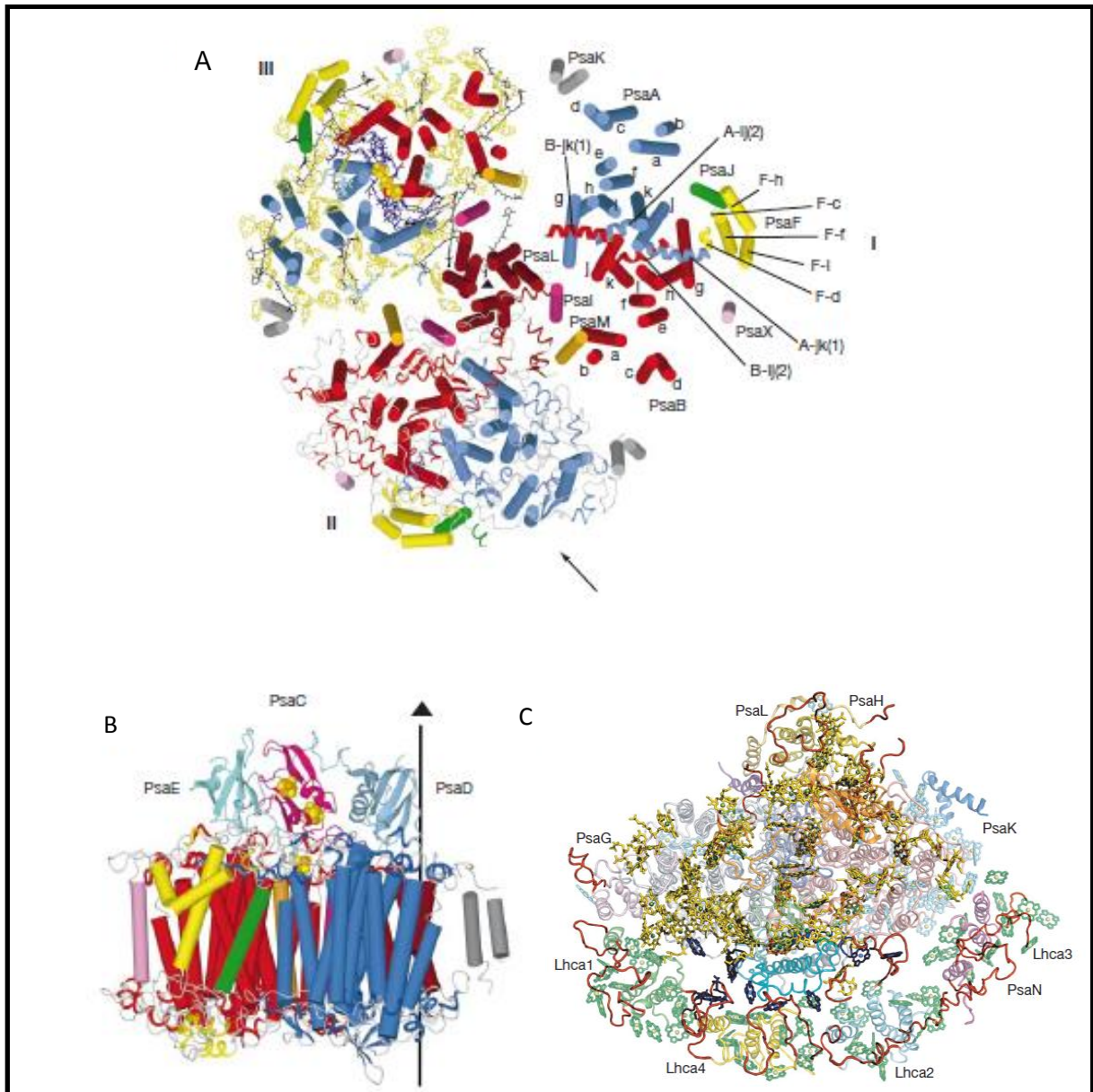


Figure 4. Structural model of PS I trimer. A and B show the cyanobacterial PS I trimer structure at 2.5Å resolution (*Synechococcus elongatus*). In C, the pea PS I structure at 3.3 Å resolution is depicted. A, View along the membrane from the stromal side. For simplification, stromal subunits have been omitted. Different structural elements are shown in each of the three monomers (I, II and III). I, arrangement of the transmembrane α -helices (cylinders). II, membrane-intrinsic subunits. III, complete set of cofactors including the transmembrane α -helices. B, Side view of the arrangement of all proteins in one monomer of PSI (colors as in A), including the stromal subunits PsaC (pink), PsaD (turquoise), PsaE (green) and the Fe_4S_4 clusters. View direction indicated by an arrow (in monomer II in A). The vertical line (right) shows the crystallographic C3 axis. C depicts the view from the stromal side onto the structure of plant PS I at 3.4Å resolution (Jordan et al. 2001; Amunts et al. 2007).

Among the 17 so far identified protein subunits, only PsaA, PsaB and PsaC are directly involved in binding to the electron transport donor P_{700} (a chlorophyll dimer) and to the electron acceptors A_0 (Chl *a*), A_1 (phylloquinone) and F_x (Fe_4S_4 cluster) (Jensen et al. 2007).

The Fe_4S_4 cluster contains FeS_x , FeS_A and FeS_B , of which FeS_A and FeS_B bind to PsaC, an electron carrier between F_x and Fd (Vassiliev et al. 1998). The final step of photosynthetic electron transport is the reduction of NADP^+ to NADPH via the membrane-associated FNR (ferredoxin-NADP-oxidoreductase), which completes the linear electron flow that starts with water oxidation at PS II (Karplus et al. 1991). Table 3 displays a comparison of PS I protein subunits between prokaryotes and eukaryotes.

However, photosynthesis provides an additional electron transfer route, driven solely by PS I, called cyclic electron flow (CEF). In this pathway, electrons are re-transported from either reduced Fd or NADPH to PQ and subsequently to Cyt b_6f complexes (Munekage et al. 2004; Figure 1). The CEF generates a pH gradient across the thylakoid membrane and therefore ATP is produced without the accumulation of reduced ferredoxin or NADPH (Pierre and Johnson 2011). Moreover, a high pH gradient will regulate the efficiency of light capture by the PSII antenna system to protect the cells against photoinhibition (Heber and Walker 1992).

Table 3. Summary of properties and functions of PS I protein subunits (Scheller et al. 2001; Xu et al. 2001; Nickelsen et al. 2007; Allen et al. 2011; Data of Eukaryotes are from *A.thaliana* and *C.reinhardtii*).

Subunit	Mass (kDa)	Number of transmembrane α -helices	Function	Prokaryotes	Eukaryotes
PsaA	83	11	Light harvesting and charge separation	+	+
PsaB	82	11	Light harvesting and charge separation	+	+
PsaC	8.8	0	Electron transfer	+	+
PsaD	17.7	0	Binding of ferredoxin	+	+
PsaE	8.1	0	Binding of ferredoxin and FNR	+	+
PsaF	17.5	2	Binding of PC	+	+
PsaG	10.8	1	Binding of LHC I	-	+
PsaH	10.2	1	Binding of LHC II	-	+
PsaI	4	1	Stabilization of PsaL	+	+
PsaJ	5	1	Stabilization of PsaF	+	+
PsaK	9	2	Binding of LHC I	+	+
PsaL	16.6	3	Trimer formation and stabilization of PsaH	+	+
PsaM	3.4	1	Trimer formation	+	-
PsaN	9.8	0	Docking of PC	-	+
PsaO	10	2	Binding of LHC II	-	+
PsaP	14	2	Not determined	+	+
(TMP14)					
PsaX	4.8	1	Binding with chlorophyll	+	-

3.3 Respiration

Respiration is a process common to living cells in which reduced organic substrates are oxidized at the expense of molecular oxygen (Bennoun 1982). The free energy recovered in this process is partly converted into heat and partly recovered by the coupled

phosphorylation of ADP into ATP, occurring in mitochondria of eukaryotes (Bennoun 1982). All mitochondria have a smooth outer membrane and a highly convoluted inner membrane which contains the respiratory chain. The classical respiratory chain includes complex I (NADH dehydrogenase, NDH-1), complex II (succinate dehydrogenase, SDH), complex III (cytochrome *c* reductase) and complex IV (cytochrome *c* oxidase, OX) in most animals; while in plants five additional so-called “alternative” oxidoreductases were identified, among which four were termed rotenone insensitive NADH dehydrogenases and the remaining represents a terminal oxidase called “alternative oxidase” (Eubel et al. 2004).

Cyanobacteria are among the very few organisms which can perform oxygenic photosynthesis and respiration simultaneously in the same compartment, the thylakoid membrane system, which contains both the photosynthetic and respiratory electron transport chains (Vermaas 2001). Additionally, the respiratory complexes are found as well in the plasma membrane in most cyanobacteria. Thus, photosynthetic electron transport occurs solely in thylakoid membrane, whereas respiratory electron flow takes place in both the thylakoid and plasma membrane systems (Figure 5, Vermaas 2001).

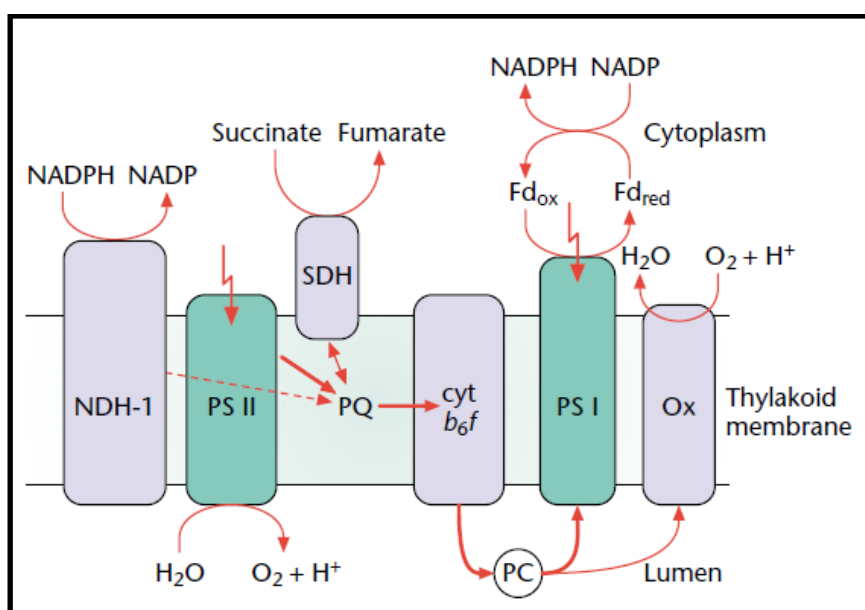


Figure 5. Schematic picture of the intersecting photosynthetic and respiratory electron transport pathways in thylakoid membranes of the cyanobacterium *Synechocystis* 6803. Complexes that are specifically involved in photosynthetic electron transfer are PS II and PS I, whereas those specific for respiratory electron flow include type 1 NADPH dehydrogenase (NDH-1), succinate dehydrogenase (SDH), and the terminal oxidase (OX). PQ, Cyt *b₆f* and PC are shared by both pathways (Vermaas 2001).

3.4 Biogenesis of thylakoid membranes in cyanobacteria

Similar to other Gram-negative bacteria, cyanobacteria possess an envelope layer consisting of an outer membrane (OM), a peptidoglycan layer (PD), and a plasma membrane (PM) (Zak et al. 2001; Figure 6). Using transmission electron microscopy (TEM), the thylakoid membrane system (TM) can be further identified separately from the OM and PM. Unlike the membranes in chloroplasts, the thylakoid membranes in cyanobacteria do not form areas of grana stacks and stromal lamellae, but appear to progress around the cell as concentric layers proximal to the plasma membrane (Liberton et al. 2006). Moreover, it has been postulated that the TM sheets converge at sites adjacent to the PM (van de Meene et al. 2006). In several cases, specific structures named thylakoid centers were found to be located in the convergence sites (van de Meene et al. 2006). It was suggested that these centers might play a role in biogenesis of the TM system (see Chapter 3.4.2.)

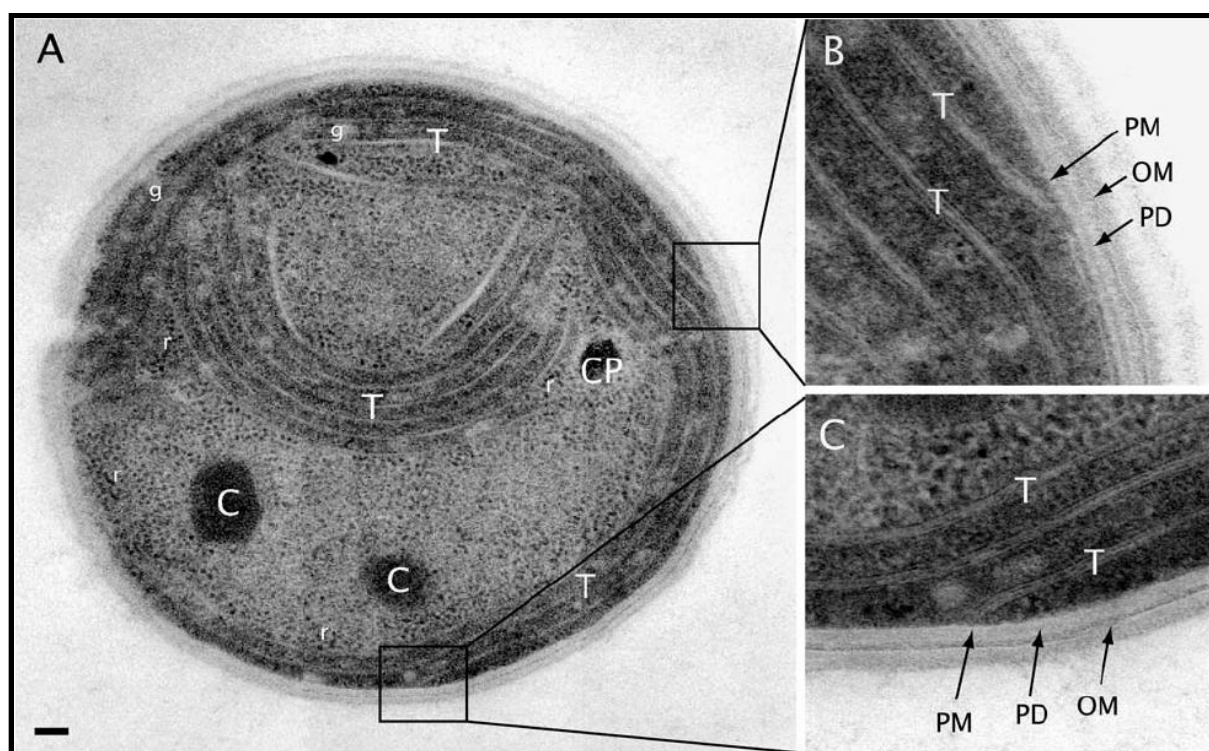


Figure 6. Electron micrograph of a representative cell of *Synechocystis* 6803. A shows an intact cell. B and C show parts of the cell, in which the outer membrane (OM), peptidoglycan layer (PD), plasma membrane (PM), and thylakoid membrane (T) are identified (black arrow). C carboxysome; CP cyanophycin granule; g glycogen granule; r ribosome (Liberton et al. 2006)

As mentioned above (Section Chapter 3.2), photosynthesis occurs exclusively in the thylakoid membrane. Basic questions regarding regulation and biogenesis of the photosynthetic complexes in all photosynthetic organism include: How is the expression of genes encoding photosynthetic subunits regulated? How are newly synthesized proteins

directed to their respective subcellular locations? How are the photosynthetic machineries assembled? As many aspects of these questions remain unanswered yet, the present study mainly focuses on biogenesis and assembly of photosystems using *Synechocystis* 6803 as a model organism.

3.4.1 Formation, stabilization and organization of thylakoid membranes

Thylakoid membranes are exclusive features of both cyanobacteria and chloroplasts, and the precise processes of their formation remain elusive (Fuhrmann et al. 2009). In several recent studies, a variety of proteins have been observed to be involved in the formation of thylakoid membranes. In 2001, Kroll et al. reported that the deletion of *vipp1* (vesicle inducing protein in plastids 1) gene leads to complete loss of thylakoid membranes in *Arabidopsis thaliana* suggesting that Vipp1 is essential for the maintenance of thylakoids (Kroll et al. 2001). In *Synechocystis* 6803, thylakoid membrane formation is strongly affected by disruption of *vipp1*, supporting the role of Vipp1 in this process (Westphal et al. 2001). Recently, Fuhrmann et al. described that *vipp1* deletion in *Synechocystis* 6803 specifically affects biogenesis and/or stabilization of PSI (Fuhrmann et al. 2009). Another factor from *Synechocystis* 6803, for which an important role in thylakoid biogenesis and/or maintenance was revealed is Alb3 (albino3 mutant of *Arabidopsis*, Spence et al. 2004). Moreover, in 2011, Bryan et al. reported the first example of a protein (Slr1768) that affects the maintenance of the TMs specifically under high light, thus displaying a phenotype dependent on light intensity in *Synechocystis* 6803 (Bryan et al. 2011). An additional example of a protein required for TMs biogenesis is Sll1213. Its corresponding gene encodes a fucose synthetase in *Synechocystis* 6803 and its deletion causes alteration of the organization of the TM system (Mohamed et al. 2005). Furthermore, an insertion mutant of *atMDG1* encoding MGDG (monogalactosyldiacylglycerol) synthase 1 lacked galactolipids and exhibits disrupted photosynthetic membranes, leading to the complete impairment of photosynthetic ability and photoautotrophic growth in *Arabidopsis thaliana* (Kobayashi et al. 2007). Taken together, many factors are involved in formation, stabilization, and organization of thylakoid membranes in cyanobacteria and higher plants (Fuhrmann et al. 2009).

3.4.2 Photosystem II assembly

To investigate the function of the various PS II subunits and factors involved in regulation of PSII assembly, targeted mutants have been generated and characterized in previous studies that helped revealing a stepwise assembly including a number of discrete PSII sub-complexes (Figure 7, Nixon et al. 2010). In *Synechocystis* 6803, Cyt b559 seems to act as a

nucleation factor to initiate PS II assembly and initially forms a D2-Cyt b559 subcomplex (Komenda et al. 2004; Komenda et al. 2008). In the next step, the second core reaction center protein D1 together with PsbI is added and a PS II reaction center (RC) pre-complex is built (Dobáková et al. 2007; Komenda et al. 2008). Subsequently, CP47, together with PsbH and small CAB-like proteins (SCPs), attach to the PS II RC subcomplex to form the so-called RC 47 complex (lacking CP43) (Komenda et al. 2004). Attachment of CP43 to RC 47 allows the formation of PS II monomer (RCC I), which is required for light-driven assembly of the Mn_4CaO_5 cluster and attachment of the luminal extrinsic subunits, PsbO, PsbU and PsbV, which act as a 'cap' to protect the cluster (Nixon et al. 2010).

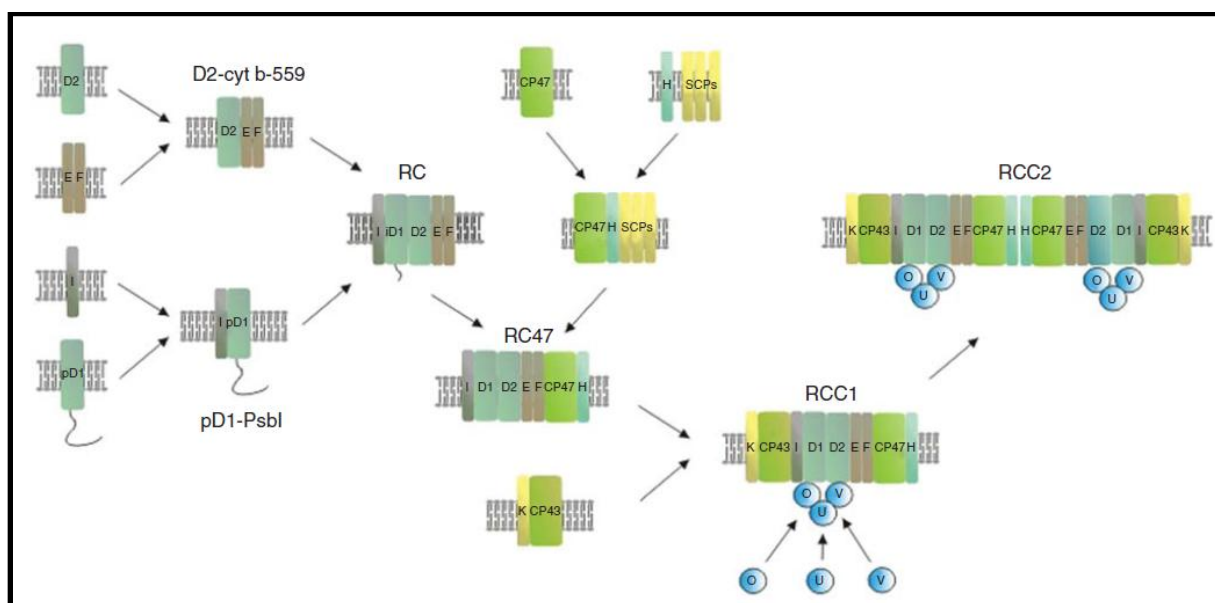


Figure 7. Simplified scheme of PS II assembly in *Synechocystis* 6803 (Nixon et al. 2010). pD1 resembles the precursor form of D1 with a C-terminal extension of 16 amino acids, while iD1 indicates the intermediate form of D1 after removing part of the C-terminal extension. For further details, see text and Nixon et al. 2010.

In addition to the PS II protein subunits, a number of proteins have been identified that function in regulation of PS II assembly, some of which are conserved in cyanobacteria, green algae and plants. These conserved proteins might play crucial roles in PS II biogenesis as they have been retained during evolution (Nixon et al. 2010).

One of these proteins is Ycf48 (hypothetical chloroplast open reading frame number 48), also termed as Hcf136, which was suggested to play a role in PS II assembly or stability (Meurer et al. 1998). In *Synechocystis* 6803, it was found to be a component of PSII RC-like complexes *in vivo* but has not been detected in larger PSII core complexes (Komenda et al. 2008). Moreover, inactivation of *ycf48* retarded the formation of PSII complexes and

decreased the steady state levels of PSII core complexes (Komenda et al. 2008). As Ycf48 was additionally suggested to interact with unassembled pD1 but not with unassembled mature D1 or D2, it was proposed that Ycf48 functions in early steps of PS II biogenesis (Komenda et al. 2008).

Two other PS II assembly factors that have been detected by proteomic analysis of purified PS II complexes from *Synechocystis* 6803 are Psb27 and Psb28 (Kashino et al. 2002). Psb27 is a 10 kDa protein localized on the lumenal side of PS II. As it is known to facilitate the assembly of the Mn_4CaO_5 cluster, it provides a selective advantage for cyanobacterial cells under stressed conditions where Mn_4CaO_5 cluster assembly efficiency is important for survival (Roose and Pakrasi 2008). Recently, Liu et al. described the role of Psb27 as a gate-keeper during the assembly process of the OEC in PSII (Liu et al. 2011). Psb28 (named also Psb13 or Ycf19), a membrane protein, is bound to PSII assembly intermediates containing CP47 and was found to be critical for the synthesis of Chls (Dobáková et al. 2009). Other factors involved in PS II assembly will be introduced below (Chapter 3.5).

3.5 The function of TPR proteins in photosynthesis

For coordination of the assembly of large protein complexes like PS II, controlled protein-protein interactions are prerequisite. These are often mediated by tetratricopeptide repeat (TPR) motifs, a degenerated 34 amino acid sequence identified in a wide range of proteins and present in tandem arrays of 3-16 motifs that form scaffolds to assist in the assembly of multiprotein complexes (Das et al. 1998). Sequence alignment of TPR motifs reveals the consensus sequence defined by a pattern of small and large hydrophobic amino acids (Figure 8A, D'Andrea and Regan 2003). One TPR motif adopts a helix-turn-helix arrangement with adjacent TPR domains packed in a parallel manner, resulting in a superhelix of repeating anti-parallel α -helices (D'Andrea and Regan 2003). In 1998, Das et al. described the first crystal structure of the N-terminal TPR motifs of a protein phosphatase, PP5, at 2.5 Å resolution and the structure provided the basis for understanding the thereby mediated protein-protein interactions (Figure 8B and C, Das et al. 1998; D'Andrea and Regan 2003).

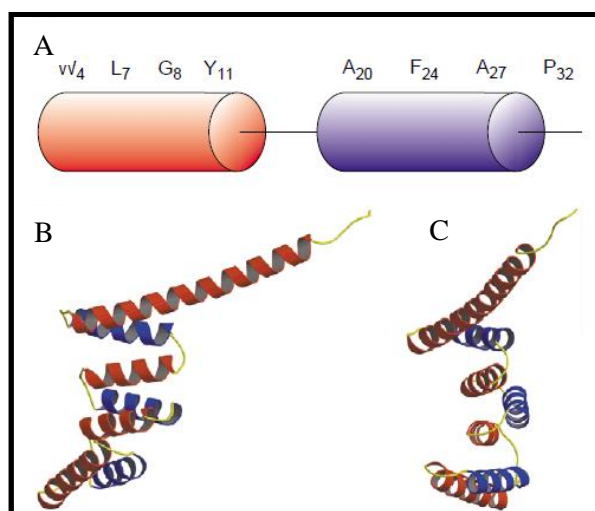


Figure 8. Structure of a TPR motif. A indicates a scheme of the secondary structure arrangement of the 34 amino acids forming a TPR domain. Helix A (red), helix B (blue) and the loop region (black) are shown. The conserved amino acids of the consensus sequence are depicted above. B and C describe the front and perpendicular view of the three TPR motifs of the phosphatase PP5 (D'Andrea and Regan 2003).

During biogenesis of the TMs, a number of photosynthetic multiprotein complexes have to be assembled, in which several TPR proteins are involved and play critical roles. Table 4 includes an overview of TPR proteins functioning in the biogenesis of TMs from *A.thaliana*, *N.tabacum*, *C.reinhardtii* and *Synechocystis* 6803, with this dissertation focusing on the TPR proteins from *Synechocystis* 6803.

Table 4. Overview of TPR proteins involved in the biogenesis of thylakoid membranes.

TPR Protein	Function	Organism	Reference
Mbb1	<i>psbB</i> RNA stability	<i>C.reinhardtii</i>	Vaistij et al. 2000
Nac2	<i>psbD</i> RNA stability	<i>C.reinhardtii</i>	Boudreau et al. 2000
Hcf107	<i>psbH</i> RNA stability	<i>A.thaliana</i>	Felder et al. 2001
Ycf3 (Slr0823)	photosystem I assembly	<i>C.reinhardtii</i>	Boudreau et al. 1997
		<i>N. tabacum</i>	Ruf et al. 1997
		<i>Synechocystis</i>	Wilde et al. 2001
Ycf37 (Slr0171)	photosystem I assembly	<i>Synechocystis</i>	Schwabe et al. 2003
		<i>A.thaliana</i>	Stöckel et al. 2006
LPA1	photosystem II assembly	<i>A.thaliana</i>	Peng et al. 2006
FLU	chlorophyll biosynthesis	<i>A.thaliana</i>	Meskauskiene et al. 2001
Rep27	photosystem II repair	<i>C.reinhardtii</i>	Park et al. 2007
PratA (Slr2048)	photosystem II assembly	<i>Synechocystis</i>	Klinkert et al. 2004
Pitt (Slr1644)	chlorophyll biosynthesis	<i>Synechocystis</i>	Schottkowski et al. 2009
Sll0886	light-activated heterotrophic growth (LAHG)	<i>Synechocystis</i>	Kong et al. 2003

One example of a TPR protein involved in TMs biogenesis in cyanobacteria is PratA (processing associated TPR protein) that contains nine TPR motifs. PratA was found to bind

to both D1 and pD1 C-terminal regions (amino acid numbers 314 to 328), facilitates D1 maturation (Klinkert et al. 2004) and is localized in a special membrane subcompartment, which forms an intermediate between the PM and the TM systems (Schottkowski et al. 2009). Recently, this specialized membrane fraction was characterized and named PDM (Prata defined membrane), in which early steps of PS II biogenesis and chlorophyll synthesis are performed (Rengstl et al. 2011).

Another important cyanobacterial TPR protein required for PSII biogenesis is Pitt (P_{OR} interacting TPR protein), a membrane protein that contains five TPR motifs, interacts with POR (the light-dependent protochlorophyllide oxidoreductase), an enzyme that mediates the light-dependent conversion of protochlorophyllide to chlorophyllide. Hence Pitt affects the accumulation of pD1 and POR (Chew and Bryant 2007; Schottkowski et al. 2009). Pitt was mainly found to be localized in the TMs, although it can also be detected in the PDM, supporting the idea that Pitt is involved in early steps of photosynthetic pigment/protein complex formation (Schottkowski et al. 2009; Rengstl et al. 2011).

In addition to PS II assembly, some TPR proteins were also found to be involved in PS I assembly in cyanobacteria. Ycf37 (hypothetical chloroplast open reading frame number 37), conserved in a variety of algae and containing 3 TPR motifs, was suggested to function in PS I stability and assembly (Wilde et al. 2001). The deletion of another TPR protein, Ycf3 (hypothetical chloroplast open reading frame number 3), conserved from cyanobacteria to higher plants, was found to lead to the complete absence of PS I, thus it was proposed to play a critical role in PS I biogenesis as well (Schwabe et al. 2003).

3.6 Effects of salt stress on photosystem II and I in cyanobacteria

During evolution, cyanobacteria had to adapt to aquatic conditions with various salt concentrations (Hagemann 2011). For instance, *Synechocystis* is able to grow in up to 1.2 M NaCl (Reed and Stewart 1985) by synthesis of the solute glucosylglycerol (Hagemann et al. 1997) in addition to the involvement of ion exchangers, like Na⁺/H⁺ antiporters (Inaba et al. 2001). The physiological response of cyanobacteria to salt stress occurs in three phases. The first phase takes place within seconds and is observed after a sudden increase of NaCl concentration, which involves the influx of Na⁺ and Cl⁻ ions into the cytoplasm. The second phase, occurring within one hour, is characterized by replacement of Na⁺ by K⁺ ions, resulting in a decrease of toxic effects of high concentration of Na⁺ ions. The third and longest phase lasts for several hours, which results in the acclimation of cells to elevated concentrations of ions. This is achieved by the synthesis or uptake of compatible solutes,

required to suppress the toxic effects of salts and to conserve the structures of complex proteins and cell membranes (Reed et al. 1985; Allakhverdiev and Murata 2008). Over a longer period of time, namely, several days, salt stress inhibits cell division (Ferjani et al. 2003).

In natural environments, salt stress often occurs in combination with light stress leading to the inhibition of photosystem activities, known as photoinhibition (Aro et al. 1993; Murata et al. 2007). Previous studies clearly demonstrated that 0.5 M NaCl is able to inhibit the *de novo* synthesis of D1 protein as well as repair of photodamaged PSII (Allakhverdiev et al. 2002; Allakhverdiev and Murata 2004). A study using the cyanobacterium *Synechococcus* sp. PCC 7942 revealed that both osmotic and ionic effects are responsible for the NaCl-induced inactivation of the photosynthetic machinery (Figure 9, Allakhverdiev et al. 2000). The cyanobacterial cells incubated with 0.5 M NaCl showed a rapid and reversible reduction and subsequent slow and irreversible loss of the oxygen-evolving activity of PS II and the electron transport activity of PSI (Allakhverdiev et al. 2000).

Protective mechanisms of tolerance to salt stress have been investigated in great details, with emphasis on the role of Na^+/H^+ antiporters, water and ionic channels, the synthesis of compatible solutes and of salt stress-induced proteins as well as the membrane-lipid composition (for review, see Allakhverdiev and Murata 2008). The Na^+/H^+ antiport system is mainly responsible for maintaining the intracellular concentration of Na^+ ions at a certain low level, however, additional protective pathways exist as well (Allakhverdiev et al. 2000).

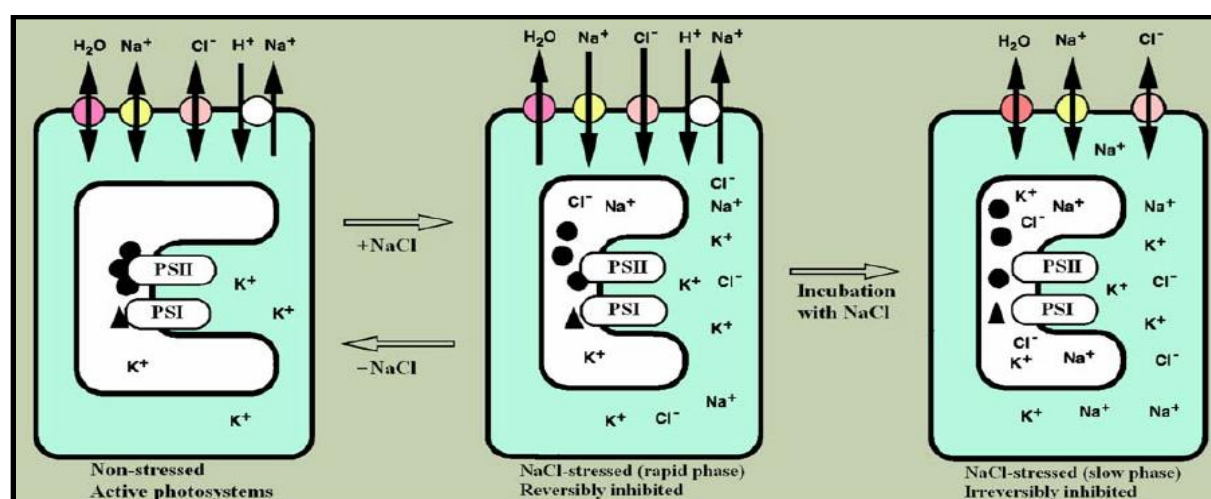


Figure 9. A hypothetical model of the NaCl-induced inactivation of PS II and PSI in cyanobacterial cells. Possible targets for inactivation are the three extrinsic proteins of the oxygen evolving machinery (PsbO, PsbU and PsbV; black solid circle) and plastocyanin (black solid triangle). Thylakoid lumen and cytoplasm are indicated by white and green color, respectively. Red circle, water channel; yellow circle, K^+ (Na^+) channel; pink circle, Cl^- channel; white circle, Na^+/H^+ antiporter (Allakhverdiev and Murata 2008).

4. Aims of this work

TPR proteins play critical and/or essential roles in the biogenesis of thylakoid membranes in all photosynthetic organisms. This work focuses on the physiological characterization of the whole set of TPR proteins present in *Synechocystis* 6803 with regard to their potential photosynthetic roles. Additionally, a membrane protein involved in the development and/or organization of the thylakoid membrane system has been analyzed.

(1) To investigate the function of all TPR proteins from *Synechocystis* 6803, genes encoding these proteins are inactivated by insertion of a kanamycin resistance cassette into the respective open reading frames (ORF). The thereby generated insertion mutants are characterized with focus on putative photosynthetic phenotypes using measurements of doubling time, oxygen evolution, emission spectra and chlorophyll fluorescence. Interesting candidates are selected for further analysis.

(2) The second part of this work deals with the further characterization of Sll1946, one of the cyanobacterial TPR proteins of which the inactivation displayed a photosynthetic phenotype. Detailed analyses by using a combination of molecular biological and biochemical methods will provide further insights into the specific function of Sll1946 and thus into the regulation of thylakoid membrane biogenesis.

(3) The third part comprises the characterization of a membrane protein, Slr0483, whose homologue in *Arabidopsis thaliana* has previously been shown to be involved in organization of the thylakoid membranes. Elucidation of this protein will give insights into the evolutionary conservation of its function and will be useful to understand the connection between the thylakoid membrane biogenesis and the photosynthetic performance.

5. Materials and Methods

5.1 Materials

5.1.1 Chemicals

All chemicals (names of chemicals and companies) used in the experiments are listed in Table 5.

Table 5. Chemicals and corresponding production company

Chemical	Production Company
Aceton	Mallinckrodt Baker B.V. (Deventer, Netherlands)
Agar-Agar	Carl Roth GmbH (Karlsruhe, Germany)
6-aminohexanoic acid	Carl Roth GmbH (Karlsruhe, Germany)
Ammonium bicarbonate	Carl Roth GmbH (Karlsruhe, Germany)
Ammonium persulfate (APS)	Carl Roth GmbH (Karlsruhe, Germany)
Ampicillin	Roche Diagnostics GmbH (Mannheim, Germany)
Bis(2-hydroxyethyl)-amino-tris(hydroxymethyl)-methane (Bis-tris)	Carl Roth GmbH (Karlsruhe, Germany)
Boric acid	Carl Roth GmbH (Karlsruhe, Germany)
Bromophenol blue	AppliChem GmbH (Darmstadt, Germany)
Calcium chloride dihydrate	Merck KGaA (Darmstadt, Germany)
Chloramphenicol	Carl Roth GmbH (Karlsruhe, Germany)
Chloroform	AppliChem GmbH (Darmstadt, Germany)
Citric acid	Sigma-Aldrich Chemie GmbH (Steinheim, Germany)
Cobalt(II) nitrate	Carl Roth GmbH (Karlsruhe, Germany)
Complete Mini EDTA-free (Protease Inhibitor Cocktail Tablets)	Roche Diagnostics GmbH (Mannheim, Germany)
Coomassie Brilliant Blue G-250	AppliChem GmbH (Darmstadt, Germany)
Deoxyribonucleoside triphosphate (dNTPs)	Carl Roth GmbH (Karlsruhe, Germany)
α -D(+)-Glucose monohydrate	Carl Roth GmbH (Karlsruhe, Germany)
Dipotassium phosphate	Carl Roth GmbH (Karlsruhe, Germany)
Dimethyl sulfoxide (DMSO)	Carl Roth GmbH (Karlsruhe, Germany)
Disodium phosphate dihydrate	Carl Roth GmbH (Karlsruhe, Germany)
<i>n</i> -Dodecyl- β -D-Maltoside	Carl Roth GmbH (Karlsruhe, Germany)
D(+)-Sucrose	AppliChem GmbH (Darmstadt, Germany)
Iron(II) sulfate heptahydrate	Merck KGaA
Ammonium ferric citrate	Sigma-Aldrich Chemie GmbH (Steinheim, Germany)
Acetic acid (96%)	Carl Roth GmbH (Karlsruhe, Germany)
Ethanol	Carl Roth GmbH (Karlsruhe, Germany)
Ethidium bromide (1%)	Carl Roth GmbH (Karlsruhe, Germany)
Ethylenediaminetetraacetic Acid, Disodium Salt, Dihydrate ($\text{Na}_2\text{EDTA} \cdot 2\text{H}_2\text{O}$)	AppliChem GmbH (Darmstadt, Germany)
Glycerol	Carl Roth GmbH (Karlsruhe, Germany)
Glycin	Carl Roth GmbH (Karlsruhe, Germany)
GST-Agrose	Biontex (Martinsried, Germany)
Urea	Carl Roth GmbH (Karlsruhe, Germany)
Yeast extract	Carl Roth GmbH (Karlsruhe, Germany)
Isopropyl β -D-1-thiogalactopyranoside	Carl Roth GmbH (Karlsruhe, Germany)
Potassium acetate	Carl Roth GmbH (Karlsruhe, Germany)
Potassium chloride	AppliChem GmbH (Darmstadt, Germany)
Potassium dihydrogen phosphate	Merck KGaA (Darmstadt, Germany)

Potassium hydroxide	Carl Roth GmbH (Karlsruhe, Germany)
Potassium permanganate	Sigma-Aldrich Chemie GmbH GmbH (Steinheim, Germany)
Kanamycin sulfate	Carl Roth GmbH (Karlsruhe, Germany)
Copper(II) sulfate	Merck KGaA (Darmstadt, Germany)
L(-)-Glutathione, reduced	Carl Roth GmbH (Karlsruhe, Germany)
Luminol	Sigma-Aldrich Chemie GmbH GmbH (Steinheim, Germany)
Lysozyme	AppliChem GmbH (Darmstadt, Germany)
Nonfat dried milk powder	AppliChem GmbH (Darmstadt, Germany)
Magnesium chloride hexahydrate	AppliChem GmbH (Darmstadt, Germany)
Magnesium sulfate hexahydrate	Carl Roth GmbH (Karlsruhe, Germany)
Manganese(II) chloride tetrahydrate	Sigma-Aldrich Chemie GmbH GmbH (Steinheim, Germany)
β -mercaptoethanol	Carl Roth GmbH (Karlsruhe, Germany)
Methanol	Carl Roth GmbH (Karlsruhe, Germany)
4-(2-hydroxyethyl)-1-piperazineethanesulfonic acid (HEPES)	Carl Roth GmbH (Karlsruhe, Germany)
3-(N-Morpholino)-2-hydroxypropanesulfonic acid (MPOS)	Carl Roth GmbH (Karlsruhe, Germany)
<i>N,N</i> -Dimethylformamide (DMF)	Carl Roth GmbH (Karlsruhe, Germany)
Tetramethylethylenediamine (TEMED)	Merck KGaA (Darmstadt, Germany)
<i>N</i> -(2-Hydroxy-1,1-bis(hydroxymethyl)ethyl)glycine (Tricine)	Biomol GmbH (Hamburg, Germany)
<i>N</i> -(Tris(hydroxymethyl)methyl)-2-aminoethanesulfonic acid (TES)	Carl Roth GmbH (Karlsruhe, Germany)
Sodium acetate	Merck KGaA (Darmstadt, Germany)
Sodium carbonate	AppliChem GmbH (Darmstadt, Germany)
Sodium chloride	AppliChem GmbH (Darmstadt, Germany)
Sodium dodecyl sulfate	Carl Roth GmbH (Karlsruhe, Germany)
Sodium hydroxide	Carl Roth GmbH (Karlsruhe, Germany)
Sodium molybdate	Merck KGaA (Darmstadt, Germany)
Sodium nitrate	Carl Roth GmbH (Karlsruhe, Germany)
Sodium thiosulfate pentahydrate	AppliChem GmbH (Darmstadt, Germany)
<i>p</i> -Coumaric acid	Sigma-Aldrich Chemie GmbH GmbH (Steinheim, Germany)
Casein pepton	Carl Roth GmbH (Karlsruhe, Germany)
Phenylmethanesulfonylfluoride (PMSF)	AppliChem GmbH (Darmstadt, Germany)
Ponceau S	Carl Roth GmbH (Karlsruhe, Germany)
Isopropyl alcohol	Scharlau GmbH Scharlau GmbH (Hamburg, Germany)
Roti [®] -Quant	Carl Roth GmbH (Karlsruhe, Germany)
Acrylamide/Bis Solution (37, 5:1)	SERVA Electrophoresis GmbH (Heidelberg, Germany)
Rubidium chloride	Sigma-Aldrich Chemie GmbH GmbH (Steinheim, Germany)
Hydrochloric acid	Carl Roth GmbH (Karlsruhe, Germany)
Sulfuric acid	Carl Roth GmbH (Karlsruhe, Germany)
Toluene	Carl Roth GmbH (Karlsruhe, Germany)
Tris(hydroxymethyl)-aminomethan (Tris)	Carl Roth GmbH (Karlsruhe, Germany)
Triton X-100	Carl Roth GmbH (Karlsruhe, Germany)
Tween 20	Carl Roth GmbH (Karlsruhe, Germany)
Hydrogen peroxide	AppliChem GmbH (Darmstadt, Germany)
Zinc sulfate heptahydrate	Carl Roth GmbH (Karlsruhe, Germany)

5.1.2 Enzymes

All restriction enzymes and T4 DNA ligase were purchased from Fermentas GmbH (St. Leon-Rot, Germany).

5.1.3 Kits

For DNA purification prior to sequencing, the QIAquick PCR Purification Kit (QIAGEN GmbH, Hilden, Germany) and for purification of DNA fragments from agarose gels, the QIAquick Gel Extraction Kit (QIAGEN GmbH, Hilden, Germany) were used. Genomic DNA isolation was performed with the DNeasy Plant Mini-Kit (QIAGEN GmbH, Hilden, Germany).

5.1.4 Strains, vectors and oligonucleotides

The Glucose-adapted *Synechocystis* sp. PCC 6803 HP (*Synechocystis* 6803) strain was used as the wild type (WT) (Rippka et al. 1979).

For cloning of DNA fragments in *Escherichia coli* (*E.coli*), the DH5 α and XL1 Blue and for recombinant protein overexpression in *E.coli*, the BL21 (DE3) and BL21 (Rosetta) strains were used.

Genes of interest were cloned into the vectors pJET1.2/blunt (Fermentas GmbH, St. Leon-Rot, Germany), pBluescript KS (+) (Stratagene, Waldbronn, Germany), pGEX-4T-1 (for recombinant protein overexpression; GE Healthcare, Munich, Germany).and pVZ321 (for complementation in *Synechocystis* 6803; Zinchenko et al. 1999).

All oligonucleotides were ordered from Metabion International AG (Martinsried, Germany) or purchased from Fermentas GmbH (St. Leon-Rot, Germany) as shown in Table 6.

Table 6. Sequences and applications of the oligonucleotides

Name	Sequence (5'-3')	Plasmid	Application
pJET1.2 forward primer	CGACTCACTATAGGGAGAGCGGC		
pJET1.2 reverse primer	AAGAACATCGATTTTCCATGGCAG		sequencing
sll1628-FW	GCTAATTCAGATTCGATCGCCTC	pKS-sll1628Kan	
sll1628-RV	GGGCAAATTGTCTGGGGTTCGT		
sll1946-FW	ATCAATTGGCGATCGGCTGCA	pKS-sll1946Kan	
sll1946-RV	CAAAGGCCAGGTTTGCACAGC		
slr0626-FW	CAATGACATCCAGTAGCTCAC	pKS-slr0626Kan	
slr0626-RV	GGTTTTTCTCTTTATATTCGCAATTAATC		
sll1667-FW	AAAATTCGGCCGCATCAACAAG	pKS-sll1667Kan	insertion mutant generation

sll1667-RV	AGAAGAACTAGCCCCCATGGA		
sll0910-FW	TACGGGAAATTTTAGCTAGTTGGG	pKS-sll0910Kan	
sll0910-RV	AGCATCTTTTATTACGTTCAATCATGCG		
slr1968-FW	TAAACCTGGGGACCGTCAATG	pKS-slr1968Kan	
slr1968-RV	CAATACCTCCAGGAGGGGAAAAT		
slr0483-FW	GAAGCCTATTTAGCTAAGGCCGAAAG	pKS-slr0483Kan	
slr0483-RV	TAGTACCTGGTCTTCCATGGCGT		
sll1946com-FW	<u>CTCGAGAGGATTACCAAAATGATT</u> <i>XhoI</i>	pVZ321-sll1946com	complementation
sll1946com-RV	<u>CTCGAGGTAATAATTGAGCAG</u> <i>XhoI</i>		
sll1946AB-FW	<u>AAGGATCCGTTGCTGATCCTAAGCAAGTT</u> <i>BamHI</i>	pGEX4T1-sll1946	overexpression for antibody generation
sll1946AB-RV	<u>AAGTCGACAGGATCGTATAAATTAATCCGG</u> <i>SalI</i>		
slr0483AB-FW	<u>AAGGATCCGTGGGCCGTAAACATTCAA</u> <i>BamHI</i>	pGEX4T1-slr0483	overexpression for antibody generation
slr0483AB-RV	<u>AAGTCGACGCACTTCCCACACCGGTTGTA</u> <i>SalI</i>		

5.1.5 Antibodies

All polyclonal antibodies were generated from rabbits by Biogenes (Berlin, Germany) or Pineda (Berlin, Germany). Alternatively, antibodies were purchased from Agrisera (Vännäs, Sweden). Information about antibody applications is listed in Table 7.

Table 7. Antibodies used in this thesis

Name	Dilution	Production Company
α D1	1:1000	Biogenes (Schottkowski et al. 2009)
α D2	1:1000	Biogenes
α CP43	1:1000	Agrisera
α CP47	1:2000	Agrisera
α Cyt f	1:2000	Agrisera
α PsaA	1:1000	Agrisera
α RbcL	1:5000	Agrisera
α PratA	1:625	Biogenes (Klinkert et al. 2004)
α Pitt	1:1000	Biogenes (Schottkowski et al. 2009)
α POR	1:1000	A kind gift of Prof. Dr. J. Soll (Dept. Biology I, Botany, LMU München)
α HCF136	1:500	Biogenes (Rengstl et al. 2011)
α Sll0933	1:625	Biogenes (Rengstl et al. 2011)
α Sll1946		Pineda (this study)
α Slr0483	1:2000	Pineda (this study)

5.1.6 Culture media

For cultivation of *E.coli* strains, liquid LB medium (1 % Pepton, 0.5 % Yeast extract, 1 % NaCl, w/v, pH 7.5) and solid LB medium (1 % Pepton, 0.5 % Yeast extract, 1 % NaCl, 1.5 % Agar, w/v, pH 7.5) were used.

Synechocystis 6803 cells were cultivated in liquid BG11 medium (0.47 % (w/v) $\text{Na}_2\text{S}_2\text{O}_3$, 1x BG-FPC, 6×10^{-4} % (w/v) $\text{FeNH}_4\text{citrate}$, 0.19 mM Na_2CO_3 , 0.175 mM K_2HPO_4 , 5 mM Glucose) and on solid BG11 medium (liquid medium with additional 10 mM TES-KOH, pH 8.2 and 1.5 % Agar). BG-FPC was diluted from 100 x BG-FPC containing 1.76 M NaNO_3 , 30.4 mM MgSO_4 , 24.5 mM CaCl_2 , 3.12 mM Citric acid, 9.15 mM $\text{Na}_2\text{-EDTA}$ and 100 x mineral nutrients, while 1000 x mineral nutrients solution contains 46.3 mM H_3BO_3 , 9.15 mM MnCl_2 , 0.77 mM ZnSO_4 , 1.61 mM NaMoO_4 , 0.32 mM CuSO_4 and 0.17 mM $\text{Co}(\text{NO}_3)_2$.

5.2 Methods

5.2.1 Bioinformatical and computational analyses tools and websites

The amino acid sequences of *Synechocystis* 6803 were obtained from CyanoBase (<http://genome.kazusa.or.jp/cyanobase/Synechocystis>). Amino acid sequences of other organisms were retrieved from NCBI/BLAST (<http://blast.ncbi.nlm.nih.gov/Blast.cgi>). Number and position of TPR motifs and transmembrane domains (TMD) based on the amino acid sequences were predicted by TPRpred (<http://toolkit.tuebingen.mpg.de/tprpred>) and TMHMM2.0 (<http://www.cbs.dtu.dk/services/TMHMM/>), respectively. For generation of multiple alignment of amino acid sequences, the program Clustal W2 was used (<http://www.ebi.ac.uk/tools/clustalw2>). Sequence conservation of predicted TPR motifs from all TPR proteins was analyzed using the Weblogo server (<http://weblogo.berkeley.edu/>). Phylogenetic tree for evolutionary analysis was built using the Neighbor-Joining method by MEGA software version 5 (<http://www.megasoftware.net/>; Tamura and Peterson 2011). Quantitative analysis of immunoblots was performed by AIDA Image Analyzer V3.25 (Raytest Isotopenmessgeräte GmbH, Straubenhardt Germany). The cell size was calculated using ImageJ 1.45 (<http://rsbweb.nih.gov/ij/>).

5.2.2 General methods of molecular biology

General methods of molecular biology like growing conditions of bacteria (*E.coli*), preparation of competent bacteria (*E.coli*), DNA precipitation, measurement of DNA concentration, and

bacterial (*E.coli*) transformation (Heat shock) were performed as described (Sambrook and Russell, the 3rd Edition, 2001). Minipreparation of plasmid DNA (Alkaline Lysis with SDS), restrictions, ligations, and gel electrophoresis of DNA were performed as described (Sambrook and Russell, the 3rd Edition, 2001) according to the manufacturers' instructions from the corresponding kits.

5.2.3 Isolation of genomic DNA from *Synechocystis* 6803

Synechocystis 6803 cells (200 ml) were harvested by centrifugation at 5000 *g* for 10 min. Preparation of genomic DNA was performed with the DNeasy Plant Mini-Kit (QIAGEN GmbH, Hilden Germany) according to the manufacturer's instructions. The genomic DNA was used as the template in the following PCR reactions.

5.2.4 DNA amplification by Polymerase Chain Reaction (PCR), cloning and sequencing

For construction of plasmids used for generation of insertion mutants and overexpression of recombinant GST fusion proteins (SlI1946 and Slr0483), various DNA fragments were amplified by PCR, of which the programs are shown in Table 8. For each reaction (50 μ l), 80 ng of template DNA, 5 μ l of 10 x PCR Buffer with 15 mM MgCl₂, 1 μ l of each primer, 1 μ l of dNTPs (10 mM) and 1 μ l of Taq-Polymerase were used. Amplification was performed for 35 cycles.

Table 8. PCR programs

	Initialization	Denaturation	Annealing	Elongation	Final elongation	Length (bp)
slI1946 inactivation		95 °C 60 s	57 °C 40 s	72 °C 90 s		1842
slr0626 inactivation		95 °C 60 s	57 °C 40 s	72 °C 90 s		1797
slI1667 inactivation		95 °C 60 s	60 °C 40 s	72 °C 90 s		1401
slI0910 inactivation		95 °C 60 s	60 °C 60 s	72 °C 90 s		1962
slr1968 inactivation		95 °C 60 s	62 °C 60 s	72 °C 90 s		1714
slI1628 inactivation	95 °C 3 min	95 °C 60 s	58 °C 40 s	72 °C 90 s	72 °C 5 min	1755
slr0483 inactivation		95 °C 60 s	56 °C 60 s	72 °C 60 s		1050
slI1946 complementation		95 °C 60 s	57 °C 60 s	72 °C 90 s		2611
slI1946 overexpression		95 °C 60 s	57 °C 60 s	72 °C 60 s		441
slr0483 overexpression		95 °C 30 s	55 °C 30 s	72 °C 30 s		174

The PCR products were extracted from the agarose gel with QIAquick Gel Extraction Kit, sub-cloned into the vector pJET1.2/blunt and transformed into *E.coli* XL1 Blue. Correct insertion of DNA fragments into the plasmids was monitored by double digestion with two

different restriction enzymes flanking the insertion site (*Xba* I and *Xho* I) and by sequencing performed by the Sequencing Lab (Dept. Biology I, Genetics, LMU München, <http://www.gi.bio.lmu.de/sequencing>).

To construct the donor plasmids for mutant generation, the insertion sites of kanamycin resistant cassette (Km^R) differed according to the gene sequences, shown in Table 9.

Table 9. Insertion sites of Km^R

	Insertion site/Restriction site	Location (bp, from start codon)
sll1946	<i>Bsm</i> I	392
slr0626	<i>Bam</i> H I	606
sll1667	<i>Bsm</i> I	611
sll0910	<i>Hind</i> III	221
slr1968	<i>Xma</i> I	552
sll1628	<i>Bam</i> H I	32
slr0483	<i>Age</i> I	159

5.2.5 Transformation of *Synechocystis* 6803 with exogenous DNA

Transformation of *Synechocystis* 6803 with exogenous DNA was basically performed as described (Williams 1988). Fresh culture (50 ml) was harvested by centrifugation at 5,000 g for 10 min and the cell pellet was resuspended in fresh BG11 medium, adjusting the optical density at 730 nm (OD_{730}) to 2.5. Cell suspension (400 μ l) was mixed with 10-40 μ g DNA, incubated at 25 °C for 3 h without shaking followed by incubation with shaking (120 rpm) for 3 h. Upon addition of 1ml fresh BG11 medium, the mixture was incubated with continuous shaking overnight. Afterwards, 400 μ l of the sample was added onto a BG11 solid medium plate containing 5 μ g/ml kanamycin and plates were incubated at 25 °C at a photon irradiance of 15 μ mol m⁻² s⁻¹.

Subsequently, the transformants were selected stepwise on BG11 solid medium plate containing higher concentrations of kanamycin (50 μ g/ml, 100 μ g/ml, 200 μ g/ml, 300 μ g/ml and 400 μ g/ml).

5.2.6 Estimation of doubling time

In addition to the mutants (*slr1968*⁻, *sll1946*⁻, *sll1667*⁻, *slr0626*⁻ and *slr0483*⁻) generated in this study (for details of cloning strategy, see Table 6, Table 8 and Table 9), the *tpr* mutants (*slr0314*⁻, *slr0183*⁻, *slr1956*⁻, *sll0499*⁻, *sll1251*⁻, *sll1882*⁻, and *slr0751*⁻) generated before

by our group were also used to measure the photosynthetic parameters (methods are described in Chapter 5.2.6, 5.2.7, 5.2.8 and 5.2.9).

WT and mutants were cultivated under either photoheterotrophic (with 5 mM glucose as carbon source) or photoautotrophic conditions (without carbon source). All cultures (50 ml each) were inoculated at $OD_{730} = 0.005$ and OD_{730} was measured everyday within 7 days using a Novaspec III visible spectrophotometer (Amersham Biosciences, Cambridge, England). The doubling time was calculated according to the following equation:

$$\text{Doubling Time} = t / \log_2 (N_t / N_0 + 1) \quad (1)$$

In equation (1), N_0 is the initial cell number and N_t is the final cell number during the period of time t (Korzyńska and Zychowicz 2008).

5.2.7 Analysis of oxygen evolution

Cells (10 ml) were harvested as described in Chapter 5.2.5, resuspended in 1 ml DMF and incubated in dark for 30 min. After centrifugation at 5000 g for 10 min at 4 °C, chlorophyll *a* concentrations were calculated by formula (2):

$$\text{Chlorophyll } a \text{ (}\mu\text{g/ml)} = 12.1 \times OD_{664} - 0.17 \times OD_{625} \text{ (Wang et al. 2008)} \quad (2)$$

Cells of wild-type and mutant strains (*tpr* mutants and *slr0483* mutant, 25 ml of each) were collected at $OD_{730}=0.6-0.8$. Samples containing 25 $\mu\text{g/ml}$ chlorophyll *a* were washed three times with BG11 medium (without Glucose) and resuspended in 1 ml BG11 medium. Measurements during illumination with saturating white light were performed with a Clark-type oxygen electrode (Hansatech Instruments Ltd., Norfolk England) upon stirring gently at 30 °C (Klinkert et al. 2004).

5.2.8 Emission Spectra Measurement

Photosystem stoichiometry was analyzed by means of emission spectra at low temperature (77 K) and quantified by the ratio of PS I / PS II (725 nm / 695 nm). Cells of wild-type and mutant strains (*tpr* mutants and *slr0483* mutant, 25 ml of each) were collected at $OD_{730}=0.6-0.8$. Chlorophyll *a* concentrations were measured as described above (Chapter 5.2.7). Samples containing 5 $\mu\text{g/ml}$ chlorophyll *a* were resuspended in 1 ml BG11 medium mixed

with glycerol (30 %, v/v). Fluorescence emission spectra at 77 K were recorded with a Spex Fluorolog 1680 0.22 m Double Spectrometer (Spex Industries Inc., Edison NJ USA; excitation at 435 nm; Klinkert et al. 2004).

5.2.9 Chlorophyll Fluorescence Measurement

Precultures of wild-type and mutant strains (*tpr* mutants and *slr0483* mutant) were grown until $OD_{730} = 0.6-0.8$. Cells (10 ml) were harvested by centrifugation at 5,000 *g* for 10 min and the cell pellet was resuspended in 20 μ l fresh BG11 medium, making $OD_{730} = 0.1$. The 20 μ l aliquot of each strain was dropped onto a BG11 solid medium plate. After incubation at 22 °C at a photon irradiance of 50 μ mol m⁻² s⁻¹ for 5 days, the plates were subjected to the chlorophyll fluorescence measurement. For this purpose, cells were incubated in the dark for 15 min and were subsequently placed into a kinetic imaging fluorometer (FluroCam 800MF, Photon Systems Instruments, Czech Republic). The maximum PSII quantum yield (Fv/Fm) was measured according to manufacturer's instructions.

5.2.10 General methods of biochemistry

SDS-PAGE, immunoblots (Western blot) and gels stained with Coomassie Brilliant Blue R250 were performed according to Molecular Cloning (Sambrook and Russell, the 3rd Edition, 2001). Soluble protein concentrations were determined with Roti[®]-Quant according to Bradford (Bradford 1976).

5.2.11 Preparation of whole cell protein extracts from *Synechocystis* 6803

Cell cultures (50 ml if not stated otherwise) were harvested by centrifugation at 5,000 *g* for 10 min and the cell pellet was resuspended in 1 ml Breaking Buffer (50 mM Tris HCl pH 7.0; 20 mM MgCl₂; 20 mM KCl) including Triton X-100 (0.1 %, v/v), glass beads (0.5 cm height in the 2 ml Eppendorf tube; 0.4-0.5 mm diameter) and protease inhibitor (1 %, v/v). Whole cell proteins were extracted using a Mini-BeadBeater (3 x 20 sec; Glen Mills Inc., Clifton NJ USA) with intervals of 1 min on ice between each turn and subsequent incubation on ice for 15 min. The insoluble material was removed by centrifugation at 20,000 *g* for 1 min and the supernatant was taken for further experiments.

5.2.12 Preparation of membrane proteins from *Synechocystis* 6803

Cell cultures (1 L if not stated otherwise) were harvested by centrifugation at 5,000 *g* for 10 min and the cell pellet was resuspended in 3 ml Thylakoid Buffer (50 mM HEPES/NaOH pH 7.0; 5 mM MgCl₂; 25 mM CaCl₂; 10 % Glycerin (v/v)) supplemented with glass beads (0.5 cm height in the 2 ml Eppendorf tube; 0.4 -0.5 mm diameter) and protease inhibitor (1 %, v/v). For extraction of membranes, cells were disrupted by 3 bursts of 20 sec in a Mini-BeadBeater (Glen Mills Inc., Clifton, NJ, USA) with intervals of 1 min on ice between each turn. The supernatant was transferred to a new tube and centrifuged at 20,000 *g* for 1 min at 4 °C. Subsequently, the supernatant was centrifuged once more at 20,000 *g* for 30 min at 4 °C. Afterwards, the pellet was washed twice with 700 µl thylakoid buffer and centrifuged at 20 000 *g* for 20 min at 4 °C. The pellet was finally resuspended in 600 µl thylakoid buffer.

The concentration of chlorophyll was determined according to Arnon 1949. In brief, the samples (20 µl) were mixed with 980 µl 80% acetone and incubated for 30 min in the dark. The mixture was then centrifuged at 2,800 *g* for 10 min at 4 °C and the chlorophyll concentration was calculated according to formula (3):

$$\text{Chlorophyll a (mg/ml)} = \text{OD}_{652} \times 1.45 \text{ (Arnon 1949)} \quad (3)$$

5.2.13 Two-dimensional blue native (BN)/SDS-PAGE

Membrane pellet (equivalent to 20 µg of chlorophyll) was solubilized in 50 µl ACA-Buffer (50 mM Bis-Tris, pH 7.0; 750 mM aminocaproic acid; 0.5 mM EDTA) including 1.3% (w/v) n-Dodecyl-β-D-Maltoside. After incubation on ice for 30 min, samples were centrifuged at 20,000 *g* for 30 min at 4°C. The supernatant was supplemented with 8 µl Loading Buffer (5 % Coomassie Brilliant Blue G-250, w/v; 750 mM aminocaproic acid) and loaded on a 4.5-12 % polyacrylamide gradient gel (Table 10).

Table 10. Composition of solutions used for first dimension of Blue native PAGE/SDS PAGE

	separating gel		stacking gel
	4.5 %	12 %	4 %
Acrylamide/Bis Solution (37, 5:1)	1.87 ml	5 ml	1.05 ml
3 x Gel-Buffer (150 mM Bis-Tris, pH 7.0, 1.5 M Aminocaproic acid)	5.5 ml	5.5 ml	3.5 ml
H ₂ O	8.63 ml	2.5 ml	5.85 ml
Glycerin 50%	-	3 ml	-
TEMED	10 µl	10 µl	10 µl
APS 10 % (w/v)	60 µl	60 µl	75 µl

The samples were subjected to electrophoresis at constant current (40 mA) overnight at 4 °C using cathode running buffer (50 mM Tricine; 15 mM Bis-Tris, pH 7.0; 0.02% Coomassie Brilliant Blue G-250 (w/v)) and anode running buffer (50 mM Bis-Tris, pH 7.0). After ~1/3 of the run, the cathode running buffer was replaced by colorless cathode running buffer (50 mM Tricine; 15 mM Bis-Tris, pH 7.0), adjusting the voltage to 300 V. For the second dimension (SDS-PAGE), the lanes of the first dimension (BN-PAGE) were cut off and incubated for 20 min in solubilization buffer (2% SDS (w/v); 66 mM Na₂CO₃; 0.67% β -mercaptoethanol (v/v)), followed by incubation for 20 min in SDS-PAGE running buffer (25 mM Tris; 192 mM glycine; 0.1% SDS). Each gel strip was then horizontally applied to a SDS-PAGE gel (Table 11). Electrophoresis was performed at 20 mA for 30 min, followed by a constant current of 8 mA overnight at RT.

Table 11. Composition of solutions used for second dimension of Blue Native PAGE/SDS PAGE

	separating gel 15 %	stacking gel 4 %
Acrylamide/Bis Solution (37, 5:1)	11.25 ml	0.61 ml
Urea	7.21 g	-
Lower Buffer (Separating Gel Buffer)	7,5 ml	-
Upper Buffer (Stacking Gel Buffer)	-	2.54 ml
H ₂ O	6.5 ml	1.85 ml
TEMED	10 μ l	10 μ l
APS 10 % (w/v)	100 μ l	75 μ l

5.2.14 Immunodetection of proteins by Enhanced Chemiluminescence (ECL)

Transfer of proteins onto nitrocellulose membrane was performed using a semidry blotter (Fastblot B34, Biometra, Biomedizinische Analytik GmbH, Göttingen, Germany) with 0.8 mA/cm² for 1.5 h in Transfer Buffer (48 mM Tris, pH 8.3, 39 mM Glycin, 0.037 % SDS (w/v), 20 % Methanol (v/v)). Subsequently, the membrane was blocked with Blocking Buffer (5 %, w/v, nonfat dried milk powder (AppliChem GmbH, Darmstadt, Germany) in TBS (10 mM Tris/HCL, pH 7.5, 150 mM NaCl) for 1 h at RT. Afterwards, the membrane was incubated with the primary antibody (Table 7) in Blocking Buffer at 4 °C overnight. The next day, the membrane was washed 3 times with TBST (TBS including 0.1 % Tween 20) for 10 min. Then the membrane was incubated with the secondary antibody (dilution of 1:20,000, anti-rabbit IgG HRP, GE Healthcare, München, Germany) in Blocking Buffer at RT for 1 h. Peroxidase-conjugated antibody signals were detected by ECL reagents mixed 1:1 (Solution A: 13.3 μ l 90 mM *p*-Coumaric acid in DMSO; 1.66 μ l 35 % H₂O₂; 3 ml 100 mM Tris/HCl, pH 8.5; Solution B: 30 μ l 20 mM Luminol in DMSO; 3 ml 100 mM Tris/HCl, pH 8.5). The nitrocellulose membrane was incubated in the ECL reagents for 1 min in the dark. After removal of the

reagent, the luminescence was detected and visualized with a FUJI Medical X-Ray Film (FUJIFILM Europe GmbH, Düsseldorf, Germany).

5.2.15 Sucrose density gradient centrifugation

Linear sucrose density gradient centrifugation was applied to separate the membrane protein complexes according to Rögner et al. 1990. Membrane proteins (200 µg) extracted (described in 5.2.12) from fresh cell culture (100 ml) were loaded onto a linear 10-30% sucrose density gradient (20 mM MES, pH 6.5; 10 mM CaCl₂; 10 mM MgCl₂; 0.03 % n-Dodecyl-β-D-Maltoside (w/v)) and centrifuged at 160,000 *g* for 16h at 4°C. The gradient contained three clearly visible bands, an upper yellow/orange one and two lower, green bands. The three bands were collected and analyzed by SDS-PAGE and immunoblots.

5.2.16 Overexpression and purification of recombinant GST-tagged fusion proteins

For heterologous expression of N-terminal GST fusion proteins, the coding regions of *sll1946* (amino acid 584-730) and *slr0483* (amino acid 1-58) were cloned into the pGEX-4T-1 vector (see Chapter 5.2.4). Overexpression was carried out in *E.coli* BL21 (DE3) and BL21 (Rosetta) cells at 37 °C for 4 h (*sll1946*) or overnight at 12 °C (*slr0483*), respectively. For this purpose, one liter culture of each strain (OD₆₀₀≈0.6) was induced with 1 mM IPTG and cultivated under the abovementioned conditions. The cells were collected by centrifugation at 6000 *g* for 10 min and suspended in 10 ml PBS Buffer (1.4 M NaCl; 27 mM KCl; 100 mM Na₂HPO₄; 18 mM KH₂PO₄, pH 7.3). Afterwards, the cell suspension was disrupted by M-110L Microfluidizer Processor (Microfluidics, Newton, MA, USA) and centrifuged at 15,000 *g* for 15 min at 4 °C. The supernatant containing the soluble recombinant fusion protein was then incubated with 150 µl GST-Agarose (Biontex, Germany) for 30 min at RT. After centrifugation at 500 *g* for 5 min at 4 °C, the beads were washed 5 times with 2 ml PBS Buffer each. Elution was performed with fresh elution buffer (50 mM Tris/HCl pH 9.5; 13.33 mM reduced L(-)-Glutathione; final pH 8.0) and samples were analyzed via SDS-PAGE. For generation of specific antibodies, the elution fractions were dialysed against 2 L 50 mM NH₄HCO₃ at 4 °C overnight, followed by a second dialysis for 1 h at 4 °C. The protein was freeze-dried using a MicroModulyo Freeze Dryer YO-230 (ThermoSavant, Holbrook, NY, USA), and 0.8 mg of protein were sent to Pineda (Berlin Germany) for antibody production (in rabbit).

5.2.17 Thin layer chromatography (TLC)

For analysis of lipid and hydrophobic pigment composition (Rengstl et al., 2011), 50 ml of *Synechocystis* 6803 culture was harvested as mentioned above (Chapter 5.2.2). The lipids and hydrophobic pigments were extracted using 2 ml chloroform and 1 ml methanol by shaking on a vortex for 3 min after adding each solvent. Afterwards, 3 ml H₂O, 3 ml chloroform and 200 µl saturated NaCl solution were added, mixed gently and centrifuged at 3 000 g for 5 min at 4 °C. After removing the upper phase and evaporating all solvent using compressed air, the lipids/pigment mixture was dissolved in 100 µl chloroform and 20 µl of each sample was applied onto a TLC-plate SIL G-25 UV254 (Wiegand International GmbH, Hamburg Germany). The plate was dipped into the solvent mixture (acetone /toluol /H₂O = 91 /30 /8, v/v/v) in a sealed container at 17 °C. Upon finishing the chromatographic run, the plate was dried for several minutes, sprayed with Color Reagent (36 mM FeSO₄; 5.7 mM KMnO₄; 56 mM H₂SO₄) and incubated at 120°C for 10 min for detection of lipids.

5.2.18 Pulse labeling

Pulse-Chase Labeling of *Synechocystis* 6803 cells, preparation of total membranes, and gel electrophoresis were performed by Dr. Anna Stengel in our group according to Klinkert et al. 2004.

5.2.19 Transmission electron microscopy (TEM)

The whole procedure of TEM experiments were performed by Dr. Irene L. Gügel (Dept. Biology I, Botany, LMU München) according to Reynolds 1963, Spurr 1969, Pfeiffer and Krupinska 2005, van de Meene et al. 2006 and Stengel et al. 2012.

5.2.20 Fractionation of membranes from *Synechocystis* 6803 by sucrose density gradient centrifugation

Membrane fractionation of *Synechocystis* 6803 cells and immunoblot analysis were carried out by Birgit Rengstl in our group according to Schottkowski et al. 2008 and Rengstl et al. 2011.

6. Results

6.1 Characterization of the TPR protein family from *Synechocystis* 6803

6.1.1 Identification of genes encoding putative TPR proteins

Assembly of supramolecular complexes such as PS II requires the assistance of a variety of regulatory proteins. Interestingly, many of those factors have been found to contain TPR motifs which mediate protein-protein interactions required for such assembly processes. Computer-assisted similarity searches, using the TPR-consensus motif as template ($W_4 L_7 G_8 Y_{11} A_{20} F_{24} A_{27} P_{32}$; Sikorski et al. 1990), have revealed 23 ORFs encoding putative TPR proteins within the completely sequenced genome of *Synechocystis* 6803. A schematic overview of the number and location of the TPR motifs, as well as the predicted transmembrane domains (TMD), is shown in Figure 10A. Based on a multiple alignment of the TPR motifs from these 23 proteins, the frequency and conservation of amino acids constituting the TPR units can be determined (Figure 10B). Residues were found to be highly conserved at position 8 (Gly or Ala), position 20 (Ala) and position 27 (Ala), corresponding to the general features of the TPR motif (D'Andrea and Regan 2003).

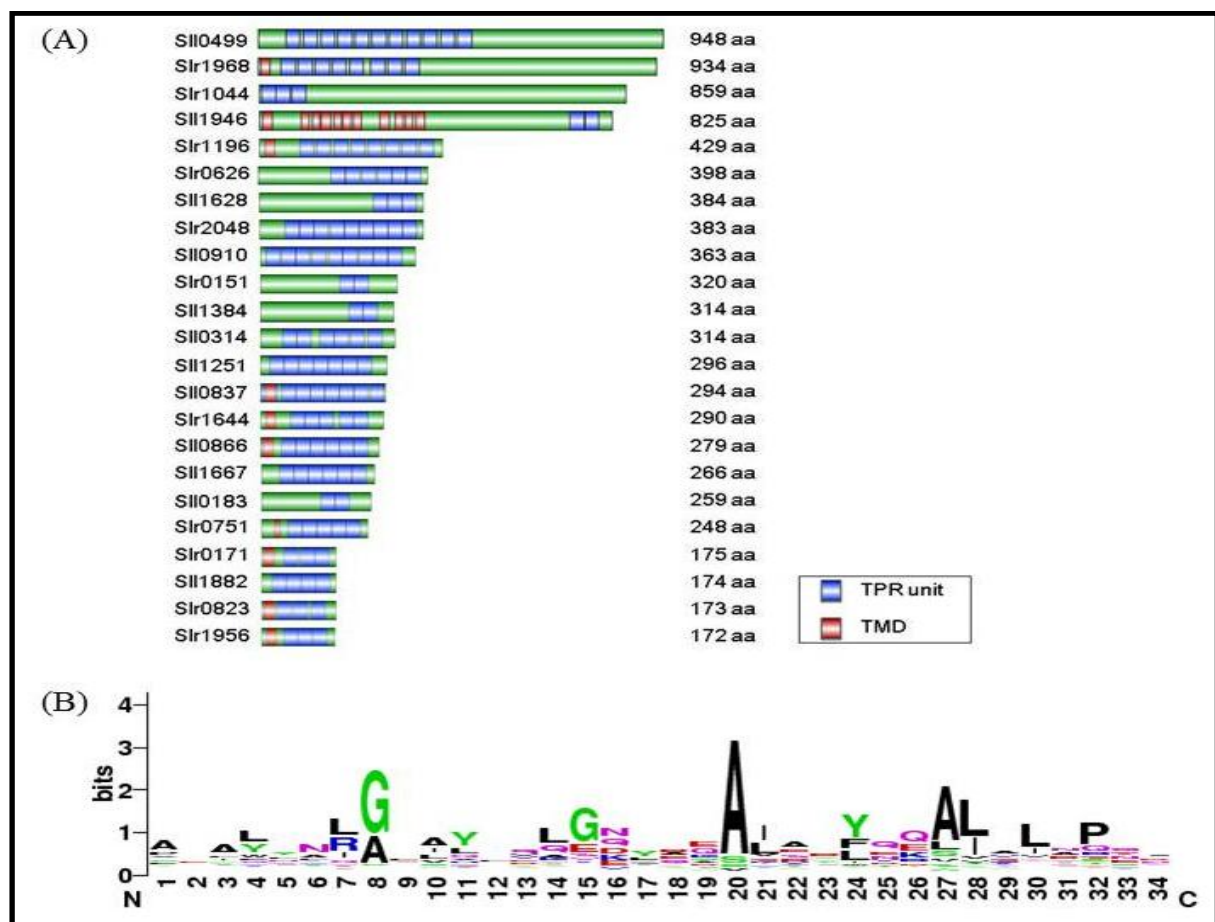


Figure 10. Amino acid sequence analyses of 23 TPR proteins from *Synechocystis* 6803. (A) Schematic arrangement of the predicted TPR motifs (blue) and transmembrane domains (TMD, red). (B) Amino acid conservation of all TPR motifs from the 23 TPR proteins depicted upon analysis with WebLogo (Croops et al. 2004).

6.1.2 Generation and selection of *tpr* mutants

Among 23 *tpr* mutants, mutants of 8 genes were generated and reported by different groups in previous studies (Table 14), 9 mutants (*sll0183*⁻, *slr1956*⁻, *sll0499*⁻ and *slr1196*⁻, *slr0751*⁻, *sll1251*⁻ *sll1882*⁻, *sll0837* *slr0314*⁻) were generated by former colleagues in our group (AG Nickelsen). In this study, 6 genes were cloned and disrupted by inserting a kanamycin resistance cassette (Km^r) into a single restriction site (Figure 11). After subsequent transformation of the constructs into WT *Synechocystis* cells and selection with increasing concentrations of kanamycin, the resulting transformants were tested by PCR analyses (Figure 11). The *Synechocystis* 6803 genome was found to contain 3 essential genes encoding TPR proteins (Table 12). Thus, 6 mutants of TPR proteins from *Synechocystis* were generated successfully.

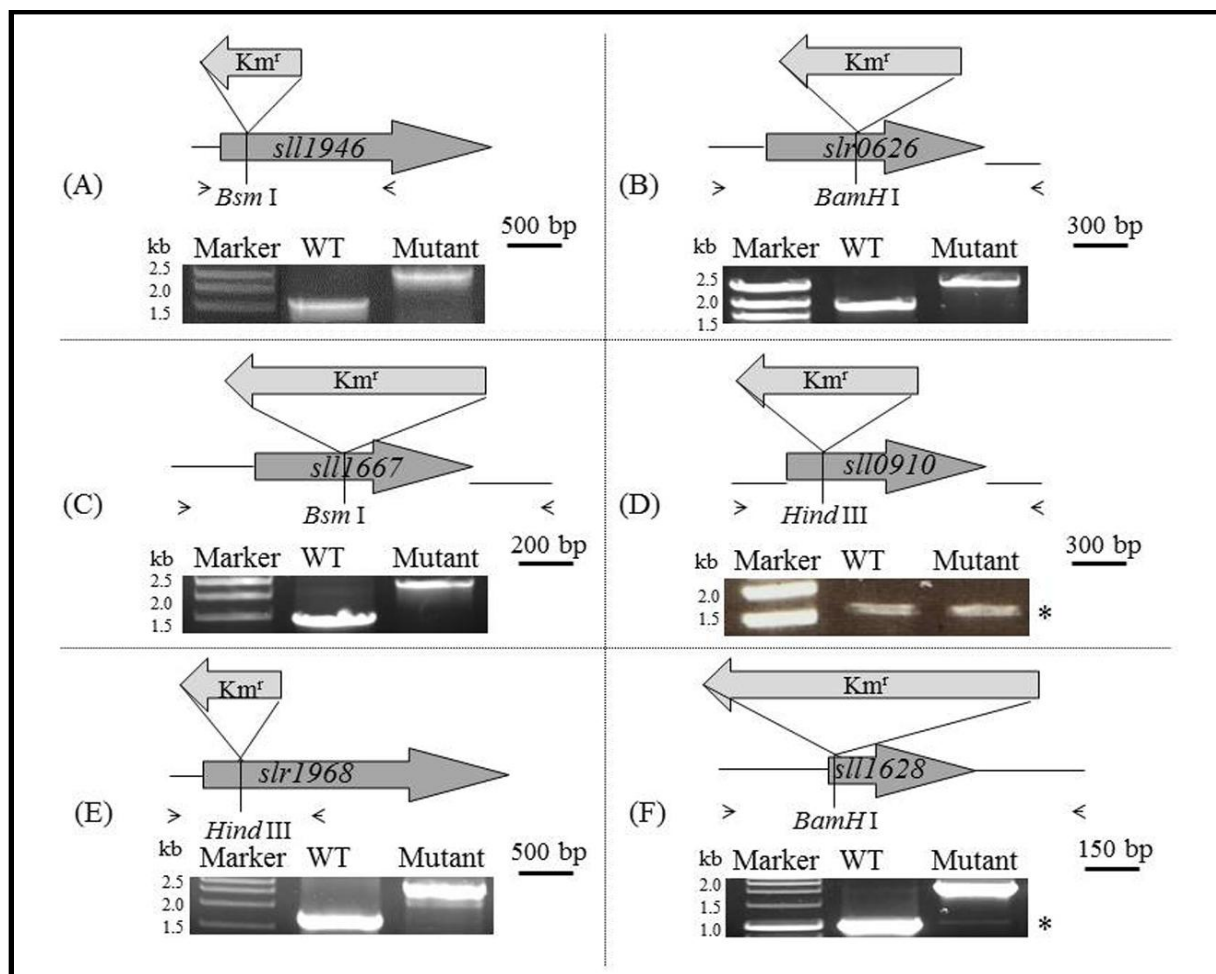


Figure 11. Cloning strategy of *tpr* insertion mutants. The strategy for constructing donor plasmids with inactivated *tpr* gene is shown above (A-F). Km^r, kanamycin resistance cassette. The solid arrows represent the primers used for PCR amplification (Table 6). The kanamycin resistance cassette was inserted upstream of the ORF. For the mutant generation, the PCR product usually contains the target ORF and the flanking regions of 300 bp on both sides with the exception of *slr1946* and *slr1968*. The PCR products of *slr1946* and *slr1968* are 1842 bp (300 bp 5'UTR plus 1542 bp ORF) and 1714 bp (300 bp 5'UTR plus 1414 bp ORF) respectively (Table 8). Examinations of *tpr* insertion mutants by PCR with the primers in Table 6 are shown below in each figure (A-F). The asterisks in *slr0910*⁻ (D) and *slr1628*⁻ (F) indicate the WT bands.

6.1.3 Analysis of photosynthetic performances of *tpr* mutants

Since mutants of all non-essential TPR genes from *Synechocystis* 6803 were available, in the next step these mutants were screened in regard to potential photosynthetic phenotypes. Thus, the photosynthetic performances were analyzed by measuring the double time, oxygen evolution, emission spectra and chlorophyll fluorescence of the *tpr* mutants (Figure 12, Table 12). Investigation of the doubling time revealed no differences of growth rates of any analyzed mutant compared to the WT under photoheterotrophic conditions (Figure 12A); however three of them (*slr0183*⁻, *slr1946*⁻ and *slr1251*⁻) exhibited longer doubling time under photoautotrophic conditions (Figure 12B).

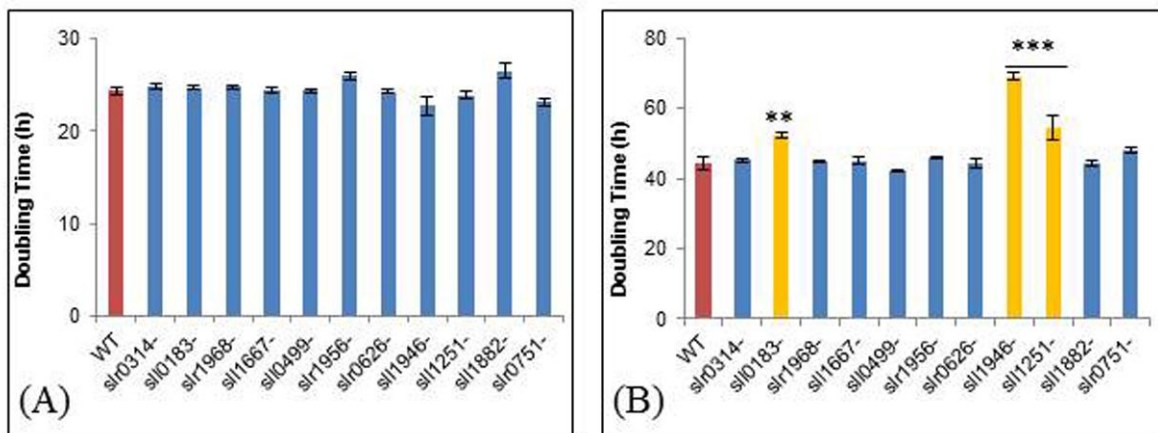


Figure 12. Measurement of doubling time of TPR mutants from *Synechocystis* 6803. (A) and (B) Doubling time (h) of WT and mutant strains based on the growth rate measured under either photoheterotrophic (A) or photoautotrophic (B) conditions. The mutants showing increased doubling time from the WT are colored in yellow. Data shown are mean \pm s.d. (n = 3, * $P \leq 0.05$, ** $P \leq 0.005$ and *** $P \leq 0.0005$, Student's t-test).

From the oxygen evolution measurements, representing the PS II activity, 8 mutants (*slr0314*⁻, *slr1968*⁻, *slr1667*⁻, *slr0499*⁻, *slr1946*⁻, *slr1251*⁻, *slr1882*⁻, and *slr0751*⁻) showed slower oxygen production rates in comparison to the WT (Figure 13A). Moreover, measurement and quantification of photosystem stoichiometry, indicating the ratio of PS I / PS II, depicted an

increase in PSI for three mutants (*slr1946*, *slr1667* and *slr0499*) and a lower PSI / PSII ratio for two mutants (*slr1882*, and *slr0751*) (Figure 13B). Finally, the analyses of chlorophyll fluorescence, representing the potential quantum yield of PS II, exhibited that 4 mutants (*slr1968*, *slr1667*, *slr0499* and *slr1946*) possessed a decreased Fv/Fm value (Figure 13C). Interestingly, the *slr1946* mutant showed differences in all analyzed photosynthetic parameters, and the *slr1667* mutant was altered in all measurements except analysis of the doubling time. Thus these two mutants exhibited the most obvious photosynthetic phenotypes.

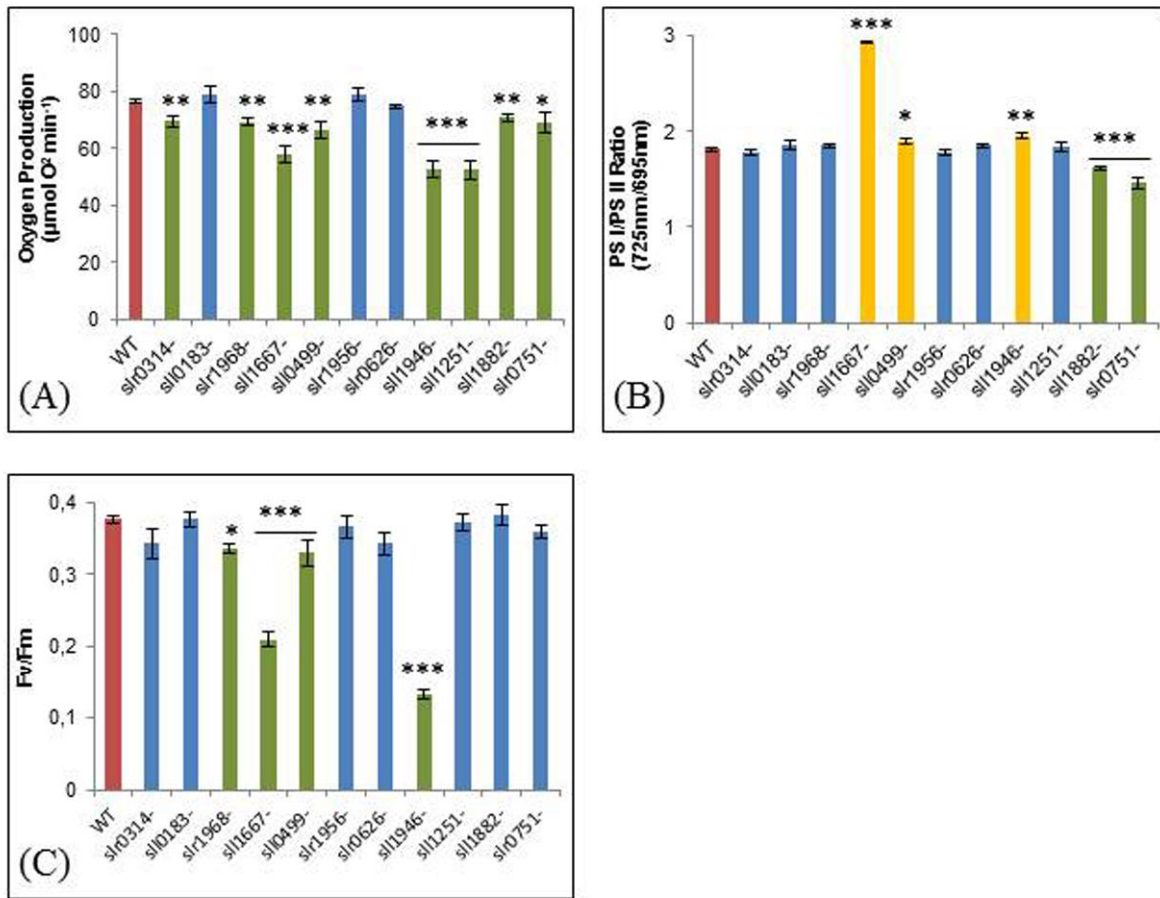


Figure 13. Measurements of oxygen evolution, emission spectra and chlorophyll fluorescence of TPR mutants from *Synechocystis* 6803. (A) Photosystem II activity measured as oxygen evolution rate using whole cells of WT and mutants. (B) Photosystem stoichiometry, indicated by the PS I/PS II ratio was analyzed based on the emission spectra measurement at 77 K. (C) Maximum PSII quantum yield (Fv/Fm), recorded from dark-adapted cells of WT and mutants. $F_v/F_m = (F_m - F_0)/F_m$, in which F_m and F_0 are maximum and minimum chlorophyll *a* fluorescence, respectively, while F_v represents the maximum variation of fluorescence. The mutants showing increased and decreased values from the WT are colored in yellow and green respectively. For (A) - (C), data shown are mean \pm s.d. ($n = 3$, * $P \leq 0.05$, ** $P \leq 0.005$ and *** $P \leq 0.0005$, Student's t-test).

In all, 7 proteins (Slr1968, Sll1667, Sll0499, Sll1946, Sll1251, Sll1882, and Slr0751) were found to possess a photosynthesis-related phenotype in *Synechocystis* 6803 (Table 12). The phenotype was distinguished based on the analyses of significant levels between WT and mutants.

Table 12. Characterization of TPR protein family from *Synechocystis* 6803.

Protein	Segregation	Doubling Time (photoautotrophic) (% of WT)	Oxygen Evolution (% of WT)	PS I/ PS II ratio (% of WT)	Chlorophyll Fluorescence (% of WT)
Sll0314	+	101.983 ± 5.676	91.096 ± 1.836	97.911 ± 1.796	95.415 ± 1.581
Sll0183	+	117.542 ± 3.719	103.338 ± 4.128	102.276 ± 2.017	103.858 ± 7.092
Slr1968	+	100.966 ± 3.465	90.764 ± 0.514	102.040 ± 0.321	92.810 ± 5.341
Sll1667	+	101.573 ± 6.517	76.109 ± 3.148	161.668 ± 1.777	57.914 ± 4.609
Sll0499	+	95.360 ± 3.505	87.155 ± 3.106	104.367 ± 1.979	91.033 ± 8.110
Slr1956	+	103.742 ± 5.291	103.121 ± 3.823	97.854 ± 2.093	104.709 ± 4.348
Slr0626	+	100.022 ± 1.513	94.883 ± 2.760	102.012 ± 1.750	94.515 ± 2.745
Sll1946	+	155.573 ± 8.962	68.954 ± 3.424	108.105 ± 2.410	36.699 ± 0.531
Sll1251	+	122.360 ± 1.943	68.606 ± 0.040	101.585 ± 2.845	101.076 ± 5.683
Sll1882	+	100.189 ± 6.010	91.941 ± 1.265	89.231 ± 1.488	105.684 ± 7.312
Slr0751	+	108.072 ± 2.553	90.484 ± 4.188	80.471 ± 3.456	98.272 ± 4.161
Slr1196	-	Essential			
Sll0837	-				
Sll1628	-				
Sll0910	/	Undermined			

Data are shown as the percentage (%) of WT. Proteins which might be involved in photosynthesis and the significant differences from WT levels are highlighted in bold.

Including the 5 proteins (Ycf3 (Slr0823), Ycf37 (Slr0171), PratA (Slr2048), Slr1644 (Pitt) and Slr0151), which were elucidated before, there are totally at least 12 proteins (52 % of the whole protein family) that might play roles in photosynthesis or TMs biogenesis. Moreover, 3 genes (slr1196, sll0837 and sll1628) are supposed to be essential because they are not fully segregated in the corresponding mutants. Furthermore, during the process of mutant generation, *sll0190* is an exception because the kanamycin resistance cassette was not inserted into the right site of the *sll0190* ORF in the genome by homologous recombination after being selected on BG11 solid medium of 400 µg/ml kanamycin (Figure 11D).

6.2 Molecular analysis of the TPR protein Sll1946

6.2.1 Analysis of Sll1946 amino acid sequence

Sll1946 belongs to the family of TPR proteins in *Synechocystis* 6803. Screening of mutants of all TPR proteins that have not been analyzed yet in regard to photosynthetic phenotypes revealed that *sll1946* possesses the most drastic alterations of photosynthetic parameters in comparison to WT (see 6.1). Thus this mutant was chosen for further molecular characterization.

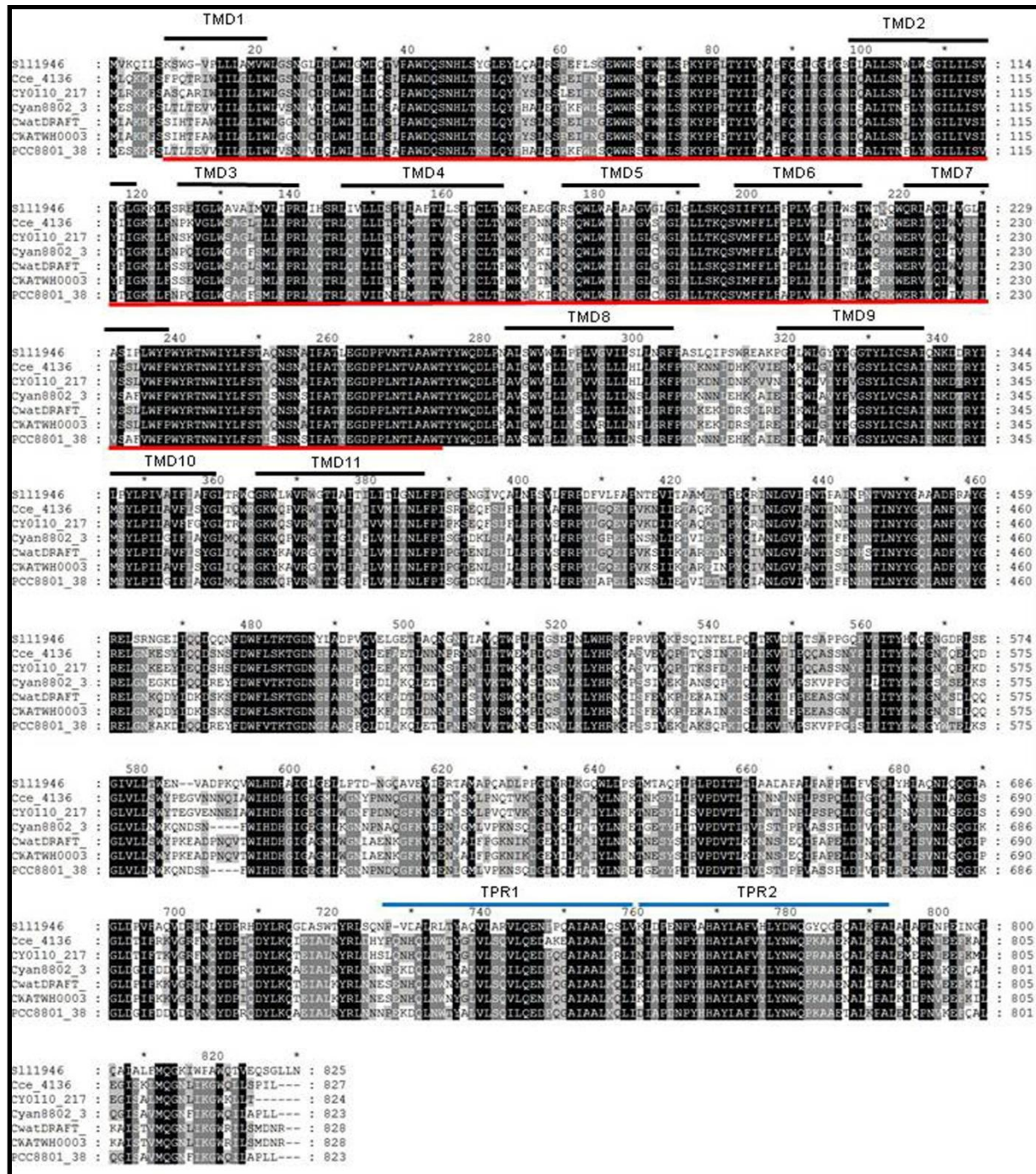


Figure 14. Multiple sequence alignment based on the Sll1946 orthologues CwatDRAFT_5595 (GI: 67921297, *Crocospaera watsonii* WH 8501), Cce_4136 (GI: 172039049, *Cyanothece* sp. ATCC 51142), PCC8801_3896 (GI: 218248630, *Cyanothece* sp. PCC 8801), CY0110_21702 (GI: 126656362, *Cyanothece* sp. CCY0110) and Cyan8802_3946 (GI: 257061697, *Cyanothece* sp. PCC 8802). Black and grey boxes indicate highly conserved and closely related amino acids, respectively. The alignment was generated with Clustal W2. The predicted transmembrane domains (TMDs, amino acids of Sll1946: 9-31, 99-118, 125-142, 146-168, 175-192, 197-214, 221-239, 283-305, 318-337, 342-359 and 366-388) and hypothetical TPR domains (amino acids of Sll1946: 727-760 and 761-794) are marked with black lines above the sequences. The hypothetical PMT domain is marked with a red line (amino acids 7-274 of Sll1946).

Protein sequence of Sll1946 contains 11 predicted transmembrane domains (TMD) on the N-terminus and 2 hypothetical TPR units on the C-terminus (Figure 10A). Homology searches from BLASTP reveal several proteins with similarity to Sll1946 exclusively in cyanobacteria, whereas orthologues in eukaryotes were not found. Among these, CwatDRAFT_5595 (GI: 67921297, *Crocospaera watsonii* WH 8501), Cce_4136 (GI: 172039049, *Cyanothece* sp. ATCC 51142), PCC8801_3896 (GI: 218248630, *Cyanothece* sp. PCC 8801), CY0110_21702 (GI: 126656362, *Cyanothece* sp. CCY0110) and Cyan8802_3946 (GI: 257061697, *Cyanothece* sp. PCC 8802), show maximum identity of 50 % with Sll1946. These five proteins and some of the proteins with lower identity contain a hypothetical PMT domain (Protein O-mannosyltransferases, EC 2.4.1.109) and TPR domains as well (Figure 14).

6.2.2 Complementation of *sll1946*

In a next step, the *sll1946* mutant was complemented with the full-length *sll1946* gene (Table 6). Measurements of the doubling time (Figure 15A) under photoautotrophic conditions as well as of chlorophyll fluorescence (Figure 15B) were performed. Data obtained for *sll1946* and *sll1946*^{com} (complemented strain) revealed that the photosynthetic parameters in *sll1946*^{com} were restored to WT levels (1.14 fold for doubling time and 0.87 fold for chlorophyll fluorescence). Therefore, it can be concluded that complementation was successful and that the declined photosynthetic performance of *sll1946* was caused by inactivation of *sll1946*.

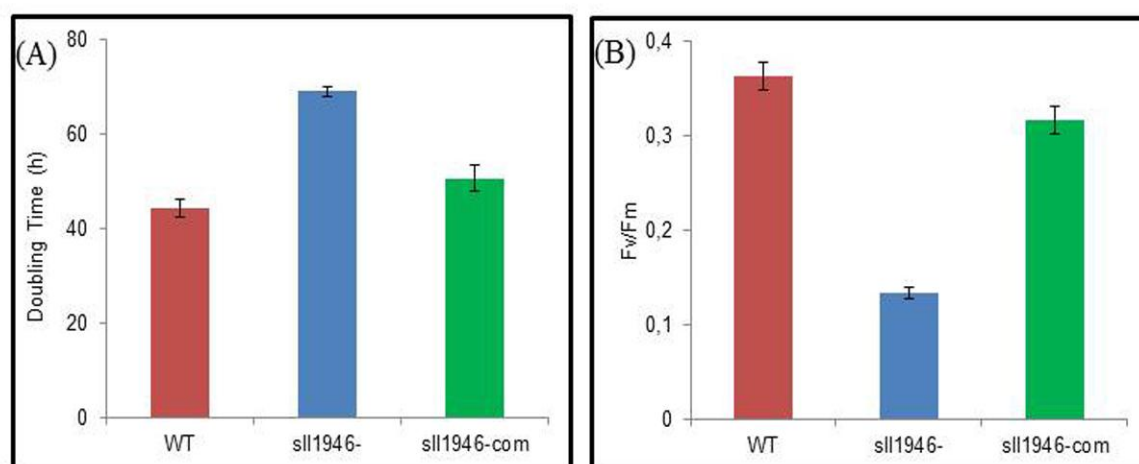


Figure 15. Photosynthetic performance analyses of WT (red), *sll1946*⁻ (blue) and *sll1946*⁻com (complemented strain; green). (A) Doubling time (h) based on the growth rate measured under photoautotrophic conditions. (B) Maximum PSII quantum yield (F_v/F_m), recorded from dark-adapted cells. F_v/F_m=(F_m-F₀)/F_m, in which F_m and F₀ are maximum and minimum chlorophyll *a* fluorescence, respectively, while F_v represents the maximum variation of fluorescence. For (A) and (B), data shown are mean ± s.d. (n= 3).

6.2.3 Determination of protein amounts of photosynthetic subunits in *sll1946*⁻

The so far obtained results suggest that *sll1946* might be involved in regulation of the photosynthetic performance. To further investigate whether Sll1946 plays a role in assembly and stabilization of photosynthetic complexes, the protein levels of PS II and PS I subunits from whole cell proteins were analyzed by semiquantitative immunoblots (Figure 16). Quantification of the observed signals using AIDA Image Analyzer V3.25 revealed a reduction of D1 and CP43 levels of 22.42 ± 4.97 % and 28.42 ± 4.68 %, respectively, in *sll1946*⁻ compared to WT. Additionally, an increase of 11.8 ± 4.38 % of CP47 level was found while the level of PsaA maintained unchanged. Hence, the levels of PS II subunits were specifically affected by the inactivation of *sll1946*, whereas the amount of PSI proteins was not altered.

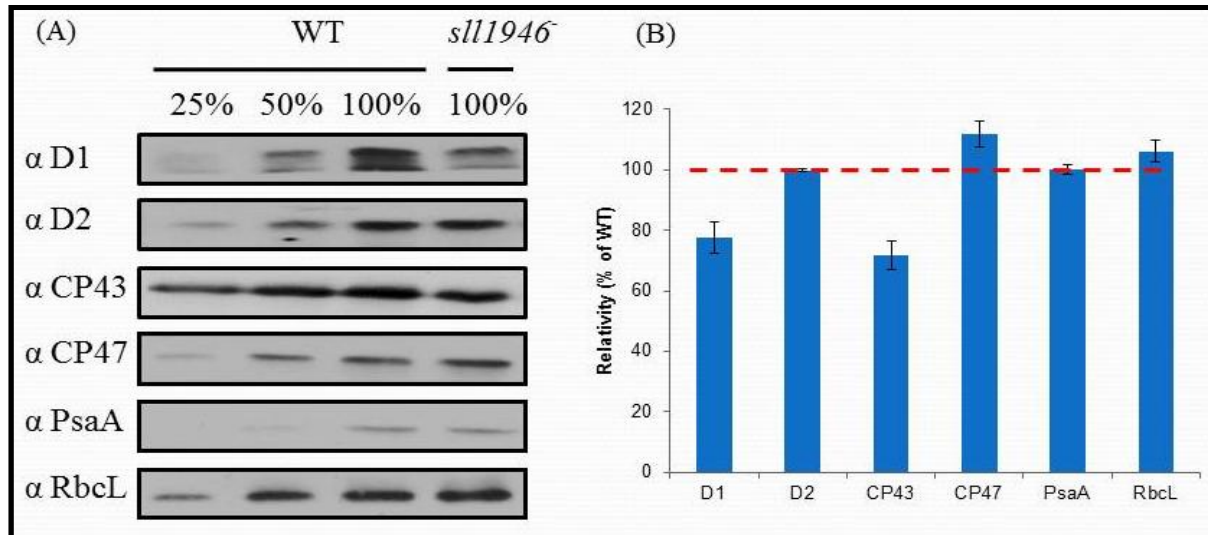


Figure 16. Analyses of protein amounts of photosynthetic subunits in *sll1946*⁻. (A) Whole cell proteins (30 μ g) from WT and *sll1946*⁻ were probed by indicated antibodies. Detection of the RbcL protein served as loading control. The experiment was performed three times, the depicted immunoblots show one representative result. (B) Quantification of the immunoblots using the AIDA Image Analyzer V3.25, estimated from 3 independent experiments. Data shown are mean \pm s.d. (n = 3). The values obtained for WT were arbitrarily set to 100% (red line), and the protein levels in *sll1946*⁻ cells were calculated relative to it.

6.2.4 Analysis of PS II complex assembly

To analyze a potential role of Sll1946 in PS II assembly, the formation of PS II complexes was monitored by 2-dimensional BN-PAGE/SDS-PAGE. In a first approach, TMs (300 μ g proteins) of WT and *sll1946*⁻ were isolated and photosynthetic complexes were separated by a 4.5-12 % BN-PAGE in the first dimension followed by a 15 % SDS-PAGE gel in the second dimension. Subsequently, the PS II dimers (RCC II), monomers (RCC I) and precomplexes (e.g. RC47) were detected by immunoblots using specific D1 and CP43 antibodies as markers (Figure 17A). Interestingly, the amount of RCC I was found to be reduced clearly in *sll1946*⁻ compared to WT; however, the RCC II complex was not affected. Differences in formation of PSII precomplexes were not observed. To further study the kinetics of PSII assembly, Cells from WT and *sll1946*⁻ were labeled with [³⁵S] Met for 20 min before separating the protein complexes by the BN-PAGE/SDS-PAGE system described above (performed by Dr. Anna Stengel; Figure 17B). The results demonstrate that most of the assembled radiolabeled PSII subunits were found in RC47 and RCC I in WT. However, in *sll1946*⁻, the amount of the precomplexes RC47 and RC appeared reduced compared to the RCC I amount, suggesting that the incorporation of D1 into RC or RC47 might be affected in *sll1946*⁻.

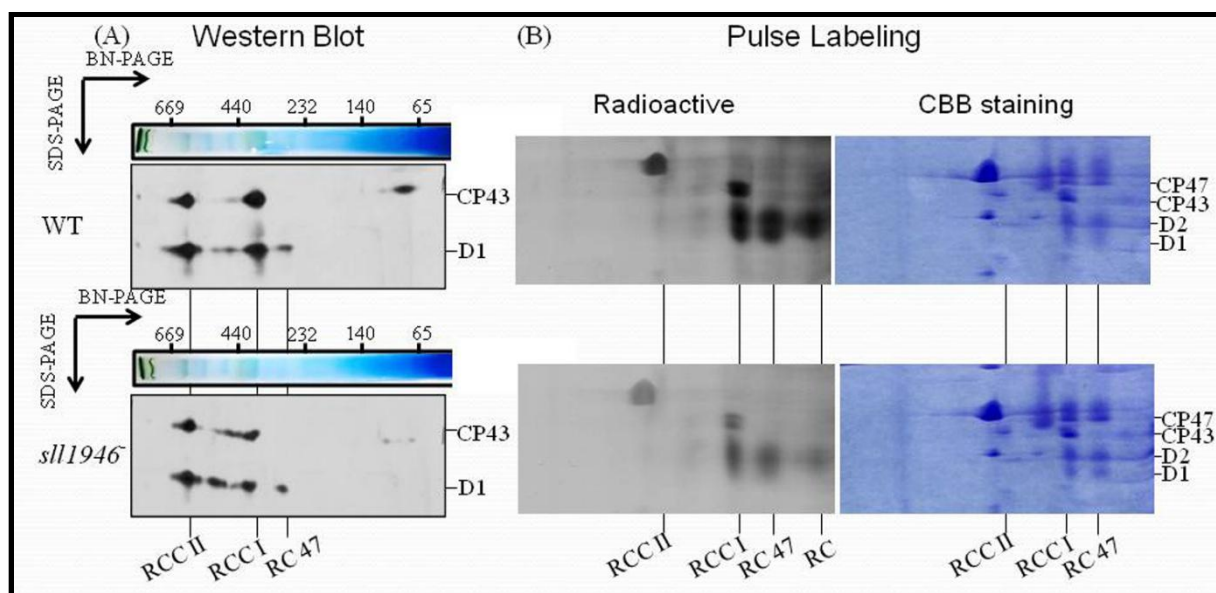


Figure 17. Analysis of PS II assembly using a two-dimensional gel system. For this purpose, 300 μ g thylakoid protein extracts of WT and *sll1946* were subjected to 4.5-12 % BN-PAGE followed by 15 % SDS-PAGE. The separated proteins were either investigated by (A) immunoblots using specific D1 and CP43 antibodies or (B) pulse labeling. RC = the PS II complex containing D1, D2, PsbE, PsbF and PsbI; RC47 = PS II core complex lacking CP43; RCC I = PS II monomer; RCC II = PS II dimer. CBB = Coomassie Brilliant Blue.

6.2.5 Membrane sublocalization of PSII subunits and assembly factors

As Sll1946 seems to play a role in the assembly of PSII monomers (Figure 17), in the next experiments the distribution of PS II subunits and various assembly factors was investigated by fractionation of *Synechocystis* WT and *sll1946* membranes using two consecutive rounds of sucrose density gradient centrifugation (Schottkowski et al. 2009; Rengstl et al. 2011; performed by Birgit Rengstl; Figure 18). Among the PS II subunits and the assembly factors examined in this experiment, only the distribution of Sll0933 was found to be affected in *sll1946*, as it shifted towards the PDM fractions compared to the WT (Figure 18). The localization of all other proteins analyzed was unaltered upon inactivation of *sll1946*. Sll0933 is a homolog of PAM68 from *Arabidopsis thaliana* that was shown to be involved in the early steps of PS II assembly (Armbruster et al. 2010). These data suggest a possible interplay of Sll1946 and Sll0933, thus, together with reduction of the amount of D1 and CP43 in *sll1946* (Figure 16) and the effects on PS II assembly (Figure 17), a role of Sll1946 in early steps of PS II assembly can be hypothesized.

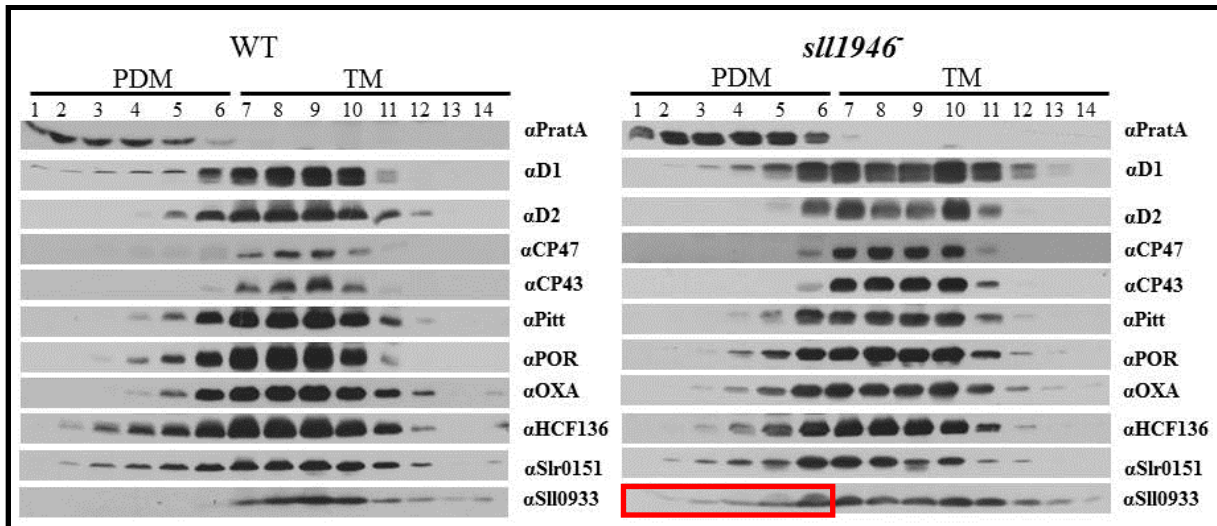


Figure 18. Membrane sublocalization of PSII subunits and assembly factors in WT and *sll1946*. Fractions 1–6 represent PDMs, and fractions 7–14 represent TMs (Schottkowski et al. 2009; Rengstl et al. 2011). To facilitate comparison between gradients, sample volumes were normalized to the volume of fraction 7 that contained 40 g of protein. The indicated proteins were detected using the respective antibodies. The red box marks the shift of SII0933 towards the PDM fractions compared to the WT. The data of the WT were published in Rengstl et al. 2011.

During this study, two antibodies were generated against two different sequence regions of SII1946 to analyze its roles in PS II assembly steps and membrane fractionations. However, these antibodies could not be used in the experiments due to the poor specificity. Hence, the localization of SII1946 in the PS II assembly steps and the membrane sublocalization are still unknown yet. Production of a third antibody is in progress.

6.2.6 Morphology of *sll1946*

In addition to the molecular characterization of SII1946, a potential effect on thylakoid biogenesis was also analyzed morphologically by electron microscopy (performed by Dr. Irene Gügel, Dept. Biology I, Botany, LMU München). For this purpose, ultrathin sections of WT and *sll1946* cells were harvested, high-pressure frozen, cryofixed, infiltrated, dehydrated and cut into 30–60 nm (for references, see 5.2.19). Interestingly, the electron microscope pictures revealed a dramatically increased number of inclusion bodies of unknown composition in *sll1946* compared to WT (Figure 19). These structures possess a low contrast and are localized between the TM sheets and have a diameter of about 20-40 nm. Apart from these differences, the organization and structure of the thylakoid membrane system showed no obvious differences.

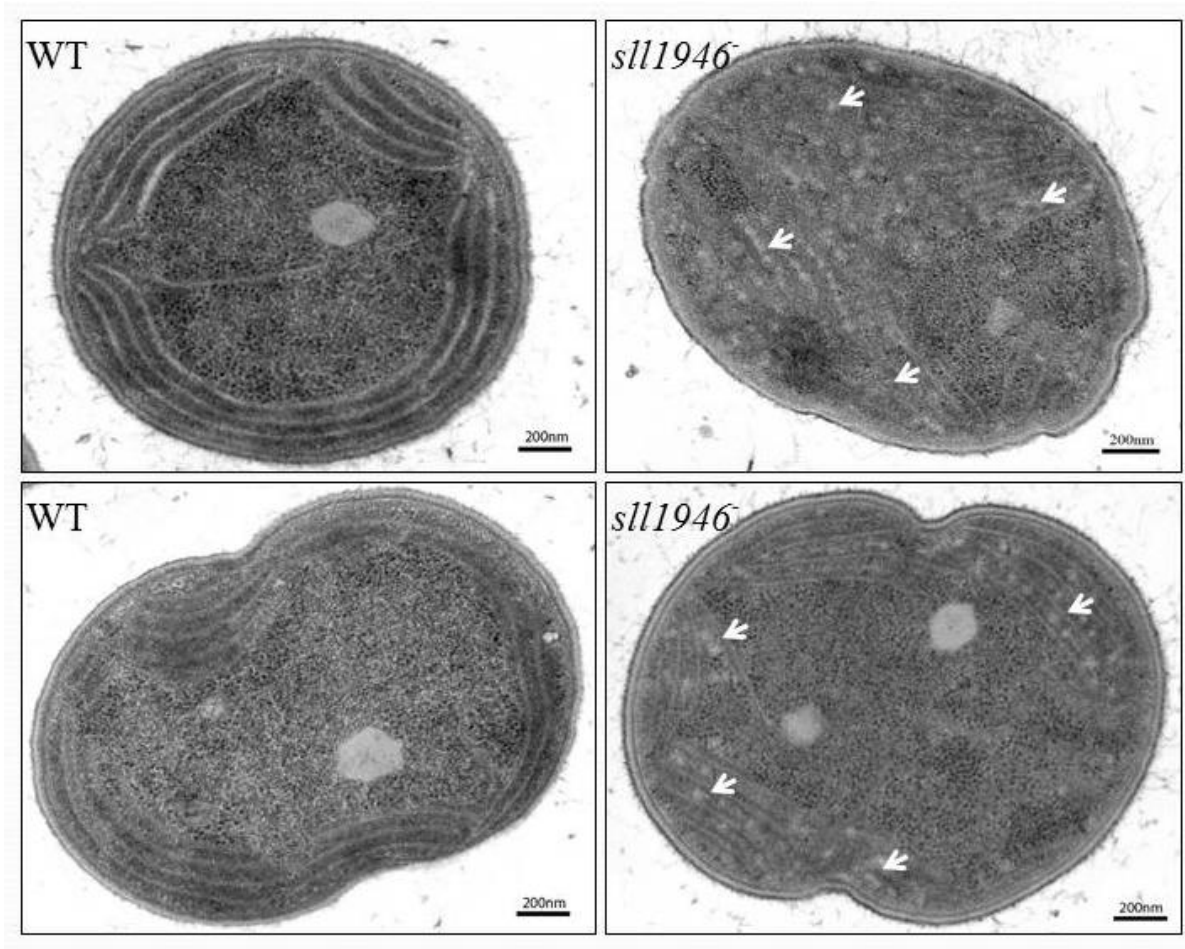


Figure 19. Transmission Electronic Microscopy (TEM) images of WT and *sll1946*⁻. Two non-dividing cells (above) and two cells in early division phase (below) are shown. At both stages of *sll1946*⁻, the inclusion bodies appearing in *sll1946*⁻ are indicated with white arrows. Bars = 200 nm.

6.2.7 Analyses of pigment and lipid composition in *sll1946*⁻

To gain information about the nature and composition of the inclusion bodies detected by the electron microscopic pictures, the pigments and lipids of WT and *sll1946*⁻ cells were analyzed using thin layer chromatography (TLC). With this method, the pigment and lipid components, like chlorophyll, carotenoids and the two major lipid classes monogalactosyldiacylglycerol (MGDG) and digalactosyldiacylglycerol (DGDG) can be separated and visualized (5.2.17; Awai et al. 2006). However, upon determination of the amount of each pigment and lipid by comparing the density of corresponding bands, no differences could be observed, suggesting that the synthesis of pigments and lipids is not affected by the inactivation of *sll1946* (Figure 20).

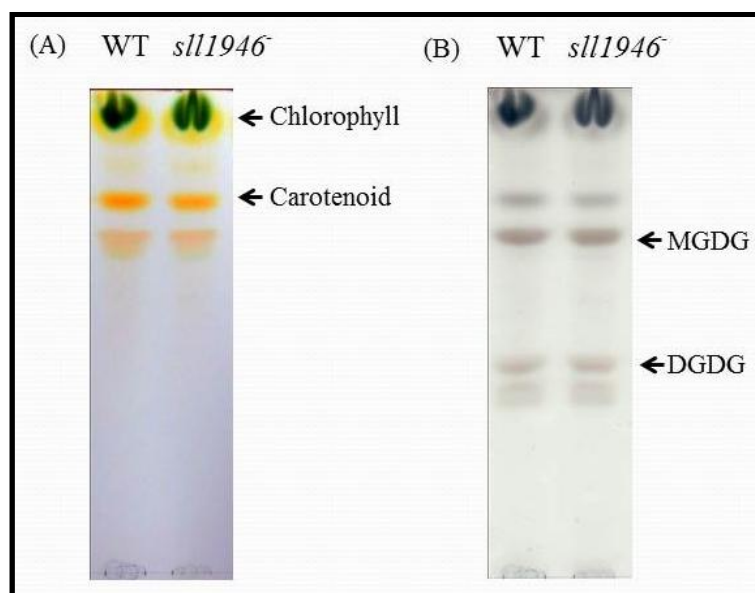


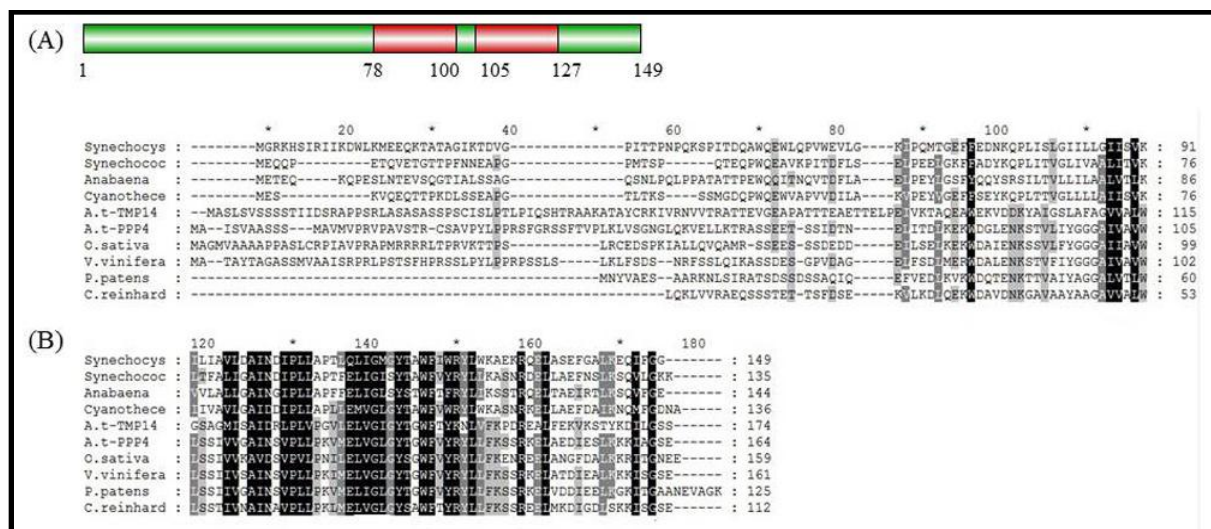
Figure 20. Analyses of pigments (A) and lipids (B) by thin layer chromatography in WT and *sll1946*⁻. In brief, pigments and lipids were extracted and dissolved by chloroform from WT and *sll1946*⁻ cells (50 ml, OD₇₃₀ = 0.8) and 20 µl samples of each strain were loaded onto the plate. To detect the lipids, the plate was sprayed with Color Reagent (36 mM FeSO₄; 5.7 mM KMnO₄; 56 mM H₂SO₄) and incubated at 120°C for 10 min.

To summarize, the TPR protein, Sll1946, was chosen to study further about the role of TPR proteins in TMs biogenesis, because the insertion mutant, *sll1946*⁻, was found to exhibit a strong photosynthetic phenotype. It could be shown that the loss of Sll1946 leads to diminished levels of D1 and CP43 and to a clear reduction of PSII monomers. Thus, the results suggest a potential role of Sll1946 in the early step of PS II assembly.

6.3 Molecular analysis of Slr0483, a protein involved in thylakoid membrane biogenesis

6.3.1 Analysis of Slr0483 amino acid sequence

Slr0483 is a homolog protein to PPP4 (P_utative P_hotosynthetic P_rotein 4) and TMP14 (T_hylakoid M_embrane P_hosphoprotein of 14 kDa, Hansson and Vener 2003) in *Arabidopsis thaliana*, which were found to be co-regulated with groups enriched with photosynthetic genes and were supposed to be involved in photosynthesis (Armbruster and Leister, unpublished results). The ORF of *slr0483* encodes a protein of 149 amino acids that contains two predicted transmembrane domains (amino acids 78 - 100 and 105 - 127; TMHMMServer V2.0; Figure 21A). A protein BLAST search against the non-redundant protein sequences (nr) revealed that the protein sequence of Slr0483 is conserved in all photosynthetic organisms. The sequences of the retrieved homologous proteins from the cyanobacteria *Anabaena* sp. PCC 7120, *Cyanothece* sp. ATCC 51142, *Synechococcus* sp. PCC 7002, the green algae *Chlamydomonas reinhardtii*, the moss *Physcomitrella patens*, *Oryza sativa* (rice), *Vitis vinifera* (grapevine) and *Arabidopsis thaliana* were aligned with the Slr0483 sequence using the Clustal W2 program. The alignment clearly demonstrates that the C-terminal regions of the Slr0483-related proteins are well conserved, whereas the N-terminal domains show a high variation (Figure 21B). Among this C-terminal region with high identity and similarity, polar (N₁₀₁, P₁₀₄, M₁₁₅, Y₁₁₇, T₁₁₈, Y₁₂₄) and charged (R₁₂₃, R₁₃₂, E₁₃₄) amino acids preferentially cover the surface of the molecule (Engelman et al. 1986). Based on this alignment, an evolutionary tree was built using the MEGA software V5 that revealed grouping of the Slr0483-like proteins into two major clades, a eukaryotic and a cyanobacterial clade (Figure 21C). This suggests that these homolog proteins were originated from a common ancestor during evolution.



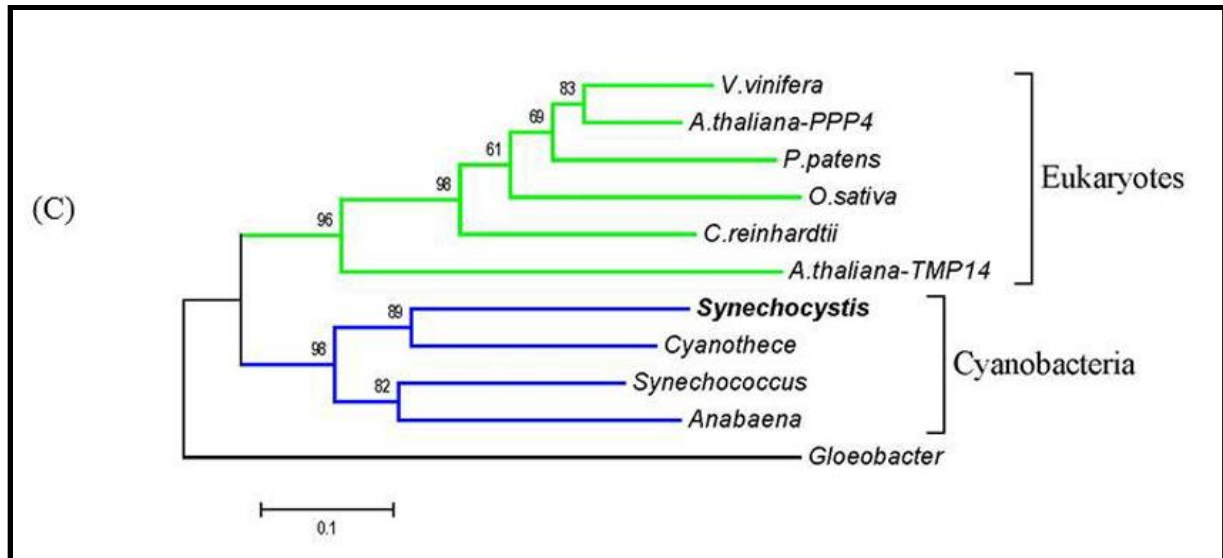


Figure 21. Analyses of the amino acid sequence and evolution of the Slr0483 protein. (A) Schematic overview of the Slr0483 sequence including the predicted transmembrane domains (TMD; red). The amino acid numbers indicate the TMD location (B) Multiple alignment based on the Slr0483 orthologues of *Arabidopsis thaliana* PPP4 (At4g01150) and TMP14 (At2g46820), *Oryza sativa* (Os08g040600), *Vitis vinifera* (GI: 147805130), *Physcomitrella patens* (GI: 168048886), *Chlamydomonas reinhardtii* (GI: 158271317), *Cyanothece* sp ATCC 51142 Cce_0494, *Anabaena* sp. PCC 7120 Alr0805, *Synechococcus* sp. PCC 7002 SYNPPC7002_A2448. Black and grey boxes indicate highly conserved and closely related amino acids, respectively. The alignment was generated with Clustal W2. (C) Unrooted phylogenetic analysis based on the multiple alignment of the amino acid sequences in (B), using the Neighbor-Joining method (MEGA software V5, Tamura et al. 2011). The tree was rooted with *Gloeobacter violaceus* PCC 7421 Gll2934 as the outgroup, which was predicted to be the NADP-thioredoxin reductase. Gll2934 was suggested to be a homolog protein of Slr0483; however, the identity and E-value (Expect value) between two protein sequences are 23 % and 0.005 respectively. Node support was inferred from 1000 bootstrap replicates. Branch lengths represent phylogenetic distances. Bar represents 0.1 substitutions per site.

6.3.2 Generation of a *slr0483* insertion mutant

To analyze the function of Slr0483, an insertion mutant was generated. For this purpose, the DNA sequence containing ORF (450 bp) and flanking sides of 300 bp was amplified by the primers slr0483-FW and slr0483-RV (see chapter 5.1.4), subsequently cloned into pJET1.2 and disrupted by inserting a kanamycin resistance cassette (Km^r) into the unique *Age* I site 159 bp downstream of the start codon (Figure 22A). After transformation of WT cells with this construct (Williams 1988), complete segregation of the mutated gene was confirmed by PCR analysis with the primers mentioned above (Table 6; Figure 22B).

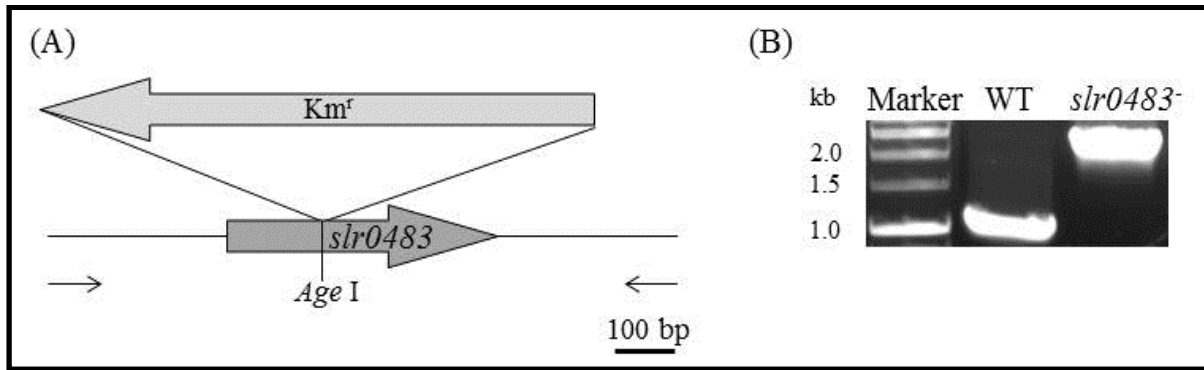


Figure 22. Inactivation of *slr0483*. (A) Strategy for constructing donor plasmids with inactivated Slr0483. Direction of transcripts is indicated by open arrows. The solid arrows represent the primers used for PCR-based segregation analysis of WT and *slr0483*⁻ DNA. The insertion site (*Age* I site) of *Km*^r is at 159 bp downstream of the start codon. Bar = 100 bp. (B) PCR analysis of WT and *slr0483*⁻ with the primers *slr0483*-FW and *slr0483*-RV. The PCR products in both strains are 1050 bp and 1804 bp respectively.

6.3.3 Topology and quantification of Slr0483

Analysis of the protein sequence (Chapter 6.3.1) predicted two transmembrane domains in the C-terminal region of Slr0483 (Figure 21), suggesting that Slr0483 is an integral membrane protein. To confirm this prediction, isolated membranes (50 µg proteins) of WT cells were treated with various potential solubilizing agents and were subsequently separated into soluble proteins (S) and membrane proteins (M). The results make clear that treatment of membranes with 0.1 M Na₂CO₃, 4 M urea, or 1 M NaCl failed to release Slr0483 from the membranes, whereas it was partly solubilized in the presence of the non-ionic detergent Triton X-100, which suggests that Slr0483 is indeed an integral membrane protein (Figure 23A). This was also supported by analysis of the well-known integral membrane protein, CP47, containing 6 transmembrane α-helices, which exhibited the same behavior as Slr0483 under the applied conditions and thus served as control in these experiments. To roughly determine the abundance of Slr0483 in *Synechocystis* cells, relative quantification of Slr0483 was performed, in which the recombinant GST fusion protein was used for calculation of the Slr0483 amount. The data demonstrated that Slr0483 makes up 0.428 ± 0.01 % of the whole cell proteins (Figure 23B).

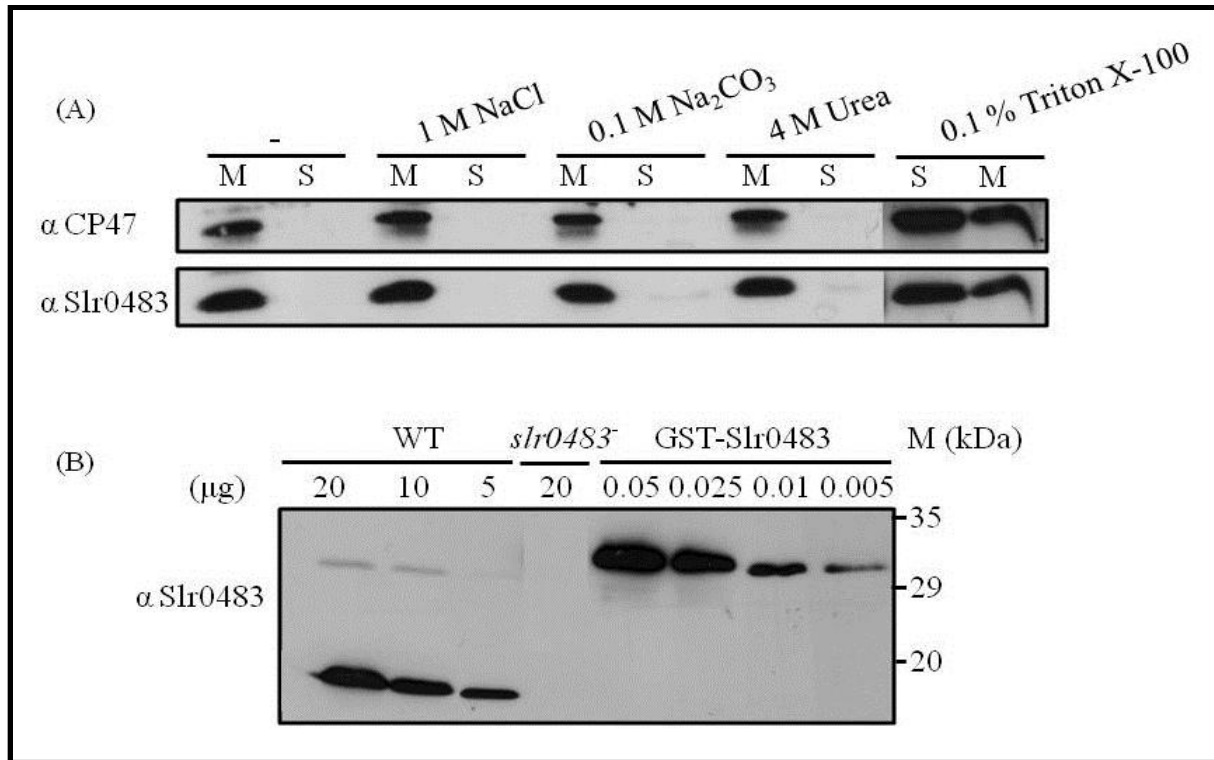


Figure 23. (A) Topology and abundance of Slr0483. Samples of membrane fractions (50 μ g proteins) from WT cells were treated with the indicated compounds for 30 min and separated into membrane (M) and soluble (S) fractions by centrifugation. CP47 was used as control for integral membrane proteins. (B) Relative quantification of Slr0483 (16 kDa) in whole cell protein extracts. A concentration series of recombinant GST fusion protein (32 kDa) was used as standard (50 ng, 25 ng, 10 ng and 5 ng) and whole cell proteins (20 μ g, 10 μ g and 5 μ g) were loaded onto 15% SDS-PAGE and subsequently subjected to immunodecoration. Protein extract of *slr0483*⁻ (20 μ g) served as negative control for the immunodetection. The antibody against Slr0483 was applied with a dilution of 1:2000 in both experiments.

6.3.4 Phenotypic characterization of *slr0483*

As a fully segregated insertion mutant of *slr0483* was successfully generated, the *slr0483* strain was in the next steps characterized with regard to a potential photosynthetic phenotype. Under both photoheterotrophic and photoautotrophic conditions, the doubling time of *slr0483* was found to be clearly increased compared to WT (1.5-fold and 2.0-fold, respectively; Figure 24A). As this is a first indication that the loss of Slr0483 might affect the photosynthetic performance, the light-dependent oxygen evolution in *slr0483* was measured, and indeed found to be reduced to 79.86 ± 1.18 % of the WT rate (Figure 24B). Surprisingly, when the respiratory performance was analyzed in the dark (30 min), a clear decrease (54.63 ± 3.22 %) of oxygen consumption was observed in *slr0483*, indicating that respiration is affected by the disruption of *slr0483* as well (Figure 24B). Moreover, measurement of chlorophyll fluorescence was performed, giving information about the potential quantum yield

of PS II. The obtained F_v/F_m value in *slr0483* was found to be declined to 51.52 ± 0.17 % of the WT level (Figure 24C), suggesting that the maximum photochemical efficiency of PSII was affected. Amount and composition of pigments, especially chlorophyll *a*, were also analyzed by measuring the absorption spectra from 320 to 800 nm using a Spex Fluorolog 1680 0.22 m Double Spectrometer (Spex Industries Inc., Edison, NJ, USA; excitation at 435 nm; Klinkert et al. 2004). The two absorption maxima of chlorophyll *a* at 430 nm and 662 nm (Almela et al. 2000), were clearly reduced in *slr0483* compared to WT, suggesting that chlorophyll synthesis or stability is affected in the mutant (Figure 24D).

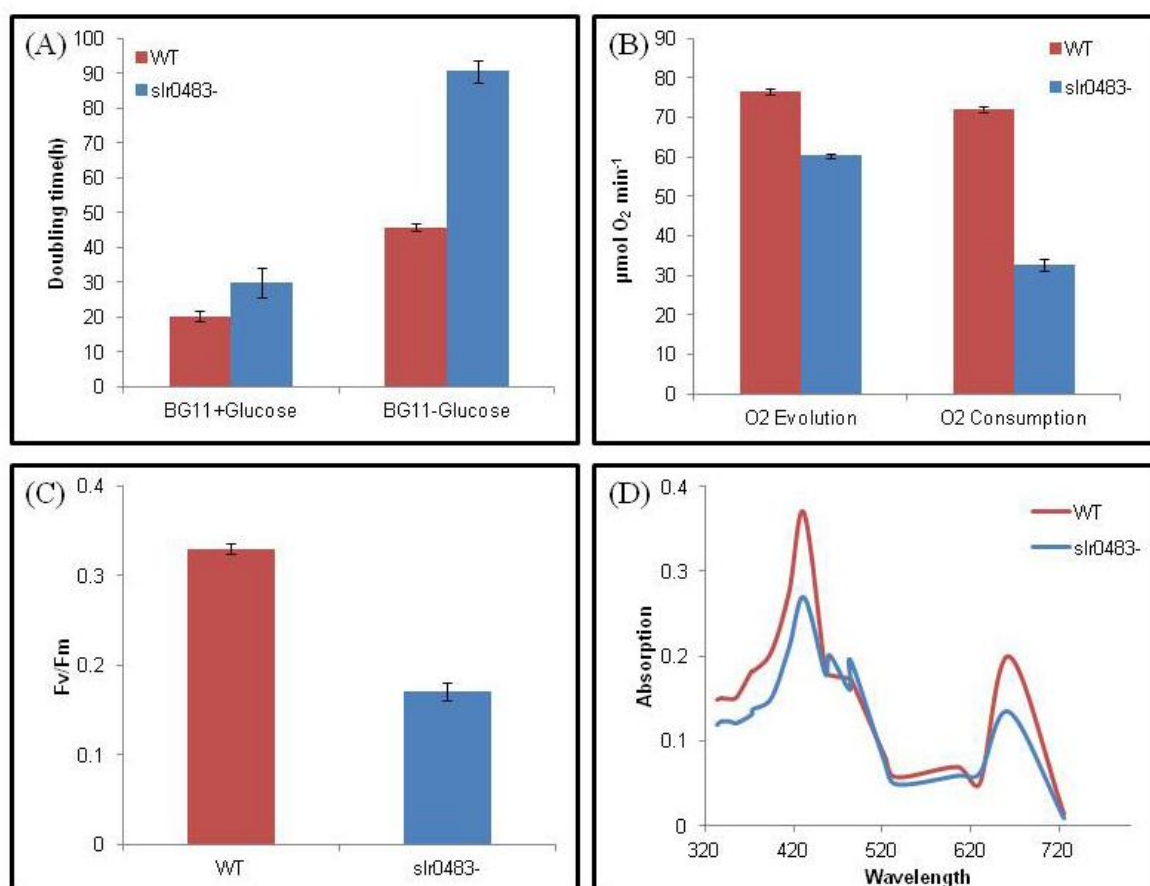


Figure 24. Phenotypic characterization of *slr0483* from *Synechocystis* 6803. (A) Doubling time (h), based on the growth rate measured under either photoheterotrophic (left) or photoautotrophic (right) conditions. (B) Determination of oxygen evolution rate (left) as indicator for photosystem II activity and of the respiratory performance (oxygen consumption rate; right). In both measurements, whole cells equal to 25 $\mu\text{g/ml}$ chlorophyll *a* were used. (C) Maximum PS II quantum yield (F_v/F_m), recorded from dark-adapted cells (15 min) of WT and *slr0483*. $F_v/F_m = (F_m - F_0)/F_m$, in which F_m and F_0 are maximum and minimum chlorophyll *a* fluorescence, respectively, while F_v represents the maximum variation of fluorescence. For (A) - (C), data shown are mean \pm s.d. ($n = 3$). (D) Pigments analyses observed by the absorption spectra from 320 to 800 nm measured by UV/Visible Spectrophotometer (Ultrospec 3000, Pharmacia Biotech, Cambridge England). In (A) - (D), the WT is depicted in red, whereas *slr0483* is shown in blue.

Finally, measurement and quantification of photosystem stoichiometry, i.e. the PS I / PS II ratio, shows a lower value of 20.40 % compared to WT (Table 13). The summary of the physiological parameters is depicted in Table 13.

Table 13. Summary of physiological characterization of *slr0483*.

Strain	Doubling Time (h)		Oxygen Evolution ($\mu\text{mol O}_2 \text{ min}^{-1}$)	Oxygen Consumption ($\mu\text{mol O}_2 \text{ min}^{-1}$)	PS I/ PS II Ratio ^c	Fv/Fm
WT	20.25±1.43 ^a	45.80±0.96 ^b	76.43±0.76	72.07±0.51	2.372	0.33±0.006
<i>slr0483</i> ⁻	30.00±4.13 ^a	90.60±3.25 ^b	61.04±0.90	32.70±1.64	1.888	0.17±0.001

(a),(b) Doubling time measured within 5 days in the presence (a) or absence (b) of glucose, the initial OD₇₃₀=0.005. (c) 5 $\mu\text{g/ml}$ Chlorophyll *a* were used. Data shown are mean \pm s.d. (n = 3).

6.3.5 Protein level analyses of photosynthetic subunits in *slr0483*

Previous results nicely demonstrated an effect of the loss of Slr0483 on photosynthetic performance (Chapter 6.3.4). Thus it was next investigated whether assembly or stability of photosynthetic proteins is altered in *slr0483*⁻. To test this, the protein levels of PS II, Cyt *b₆f* and PS I subunits were analyzed by semiquantitative immunoblots (Figure 25). Quantification of the observed signals revealed a clear reduction of D1, D2, CP43 and CP47 levels to about 43.34 \pm 6.73 %, 41.47 \pm 0.92 %, 44.25 \pm 6.74 % and 56.37 \pm 3.97 %, respectively, in *slr0483*⁻ compared to WT, indicating that the whole PS II complex is affected. Moreover, a decrease of the amount of the PSII-associated factors PratA and POR to about 66.56 \pm 3.66 % and 58.12 \pm 2.74 %, respectively, was observed, together with an accumulation of the Pitt protein to about 131.32 \pm 15.81 % of WT. However, the levels of Cyt *f* and PsaA, which serve as markers for the Cyt *b₆f* and PS I complex, remained unchanged. Therefore, the inactivation of *slr0483* specifically affected the amount of PSII subunits and PSII assembly factors, correlating to changes in the photosynthetic performance as described in 6.3.4.

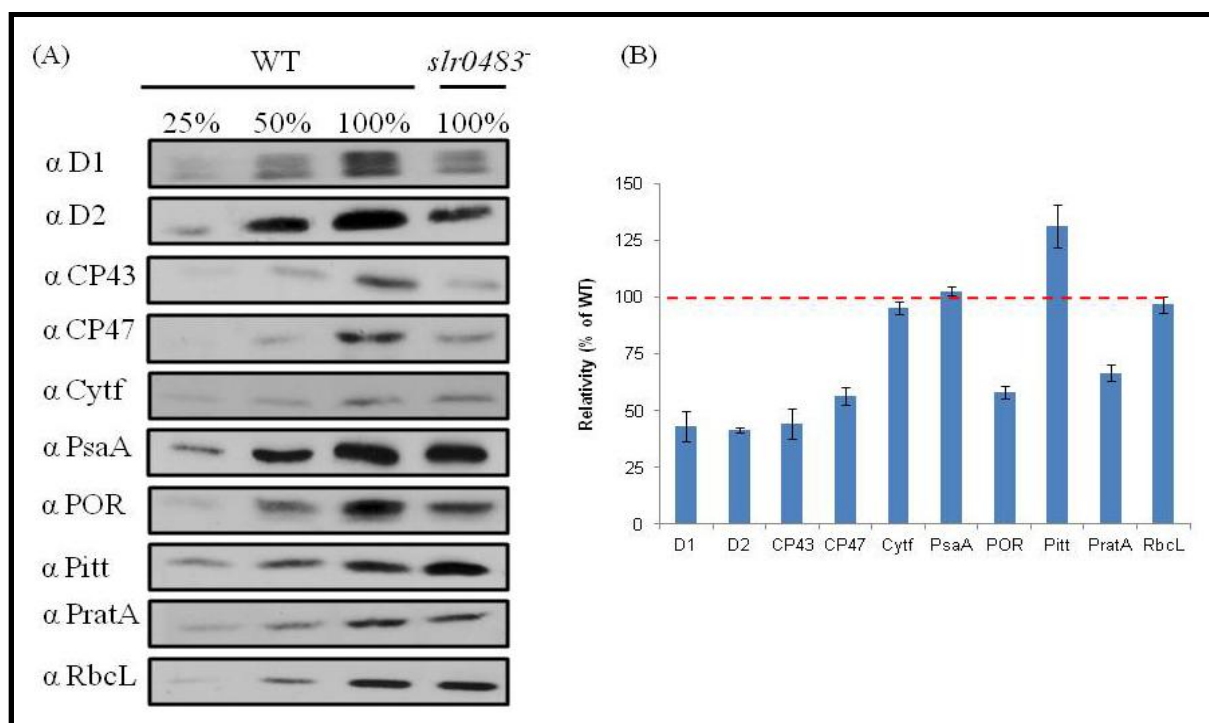


Figure 25. Protein amount analyses of photosynthetic subunits and associated factors in *slr0483*. (A) Whole cell proteins (30 µg) from WT and *slr0483*⁻ were separated by SDS-PAGE and probed with the indicated antibodies. Determination of the RbcL protein level was used as loading control. The experiment was performed three times; the immunoblots show one representative result. (B) Quantification of the protein amounts from (A) estimated from 3 independent experiments. Data shown are mean ± s.d. (n = 3). The values obtained for WT were arbitrarily set to 100% (red line), and the protein levels in *slr0483*⁻ cells were calculated relative to it.

6.3.6 Analysis of PS II complex assembly in *slr0483*

As the above presented experiments suggest a specific effect on the amount of PS II subunits in *slr0483*, it remains to investigate whether the synthesis or assembly of PS II subunits causes these differences. Hence, the PS II assembly process was investigated with BN-PAGE/SDS-PAGE, CN-PAGE/SDS-PAGE (performed by Birgit Rengstl) and pulse labeling (performed by Dr. Anna Stengel). From the BN-PAGE/SDS-PAGE (300 µg membrane proteins) and subsequent immunoblot analyses, the RCC II complexes (PS II dimer) were found to be nearly absent in *slr0483* compared to WT, concluded from the signals detected for D1, D2, CP43 and CP47. By contrast, the PS II monomers and pre-complexes were not drastically affected (Figure 26A). Moreover, analysis of the membrane samples using CN-PAGE/SDS-PAGE exhibited identical results (Figure 26B). Compared with BN-PAGE, CN-PAGE is able to retain labile supramolecular assemblies of membrane protein complexes that are dissociated under the conditions of BN-PAGE (Wittig and Schagger 2005). In both two-dimensional gel systems applied, the vast majority of Slr0483 was not found to co-migrate with PS II complexes, but accumulated in several complexes of

smaller size (below 140 kDa), demonstrating that Slr0483 is not or unstably attached to any PS II complexes. Only a minor fraction co-localized with the monomeric form of PS II, however a specific role of Slr0483 in PS II monomer stability remains questionable. To further study the kinetics of PSII assembly, thylakoid membrane proteins from WT and *slr0483* were separated by BN-PAGE/SDS-PAGE after being labeled with [³⁵S]Met for 20 min (performed by Dr. Anna Stengel; Figure 26C). After pulse labeling, most of the assembled radiolabeled PS II subunits were detected in RC47 and RCC I in WT and *slr0483*, and no clear differences were observed in *slr0483*, suggesting that the synthesis rates and incorporation of each protein into PS II complexes are not affected. Taken together, it can be hypothesized that Slr0483 plays a role in formation or stability of functional PS II dimers.

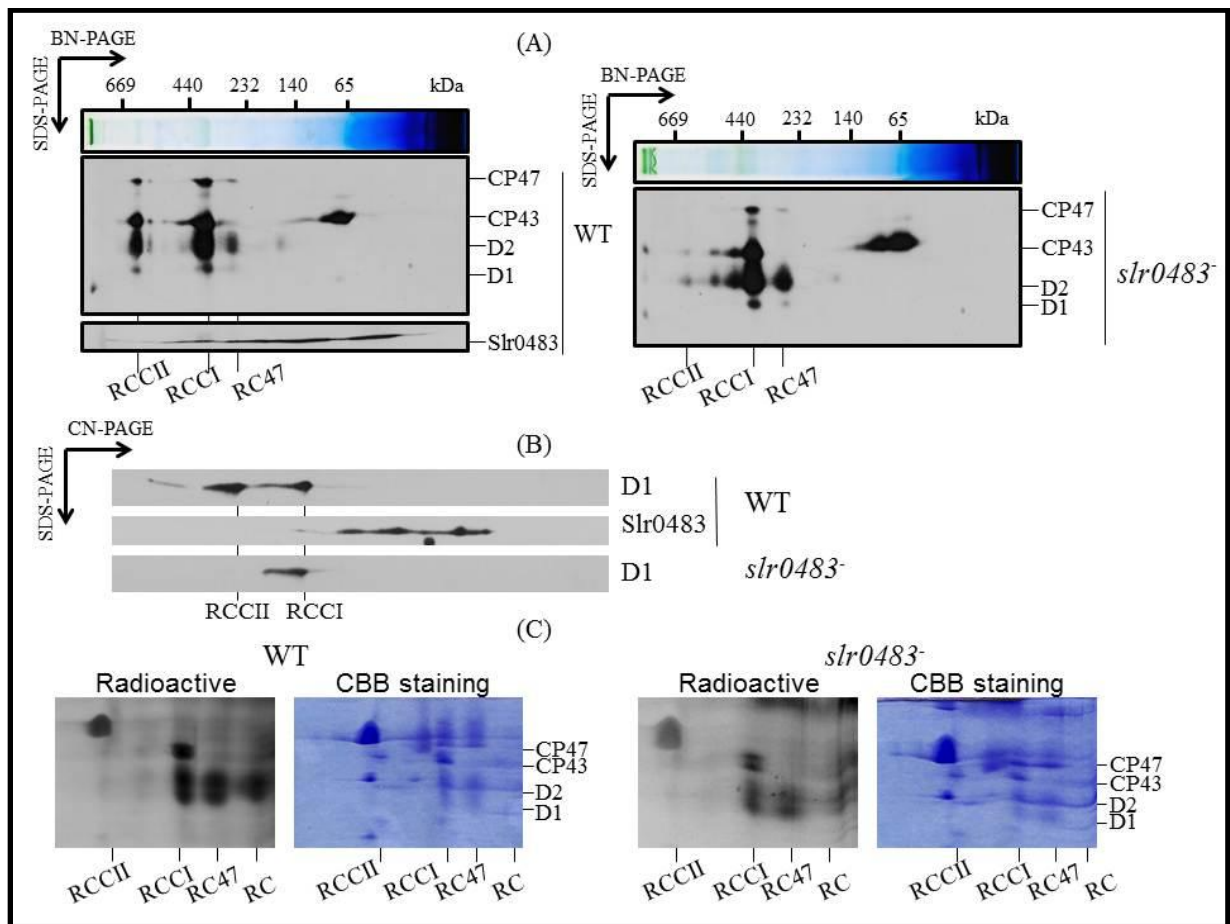


Figure 26. Analyses of PS II assembly using two-dimensional native gel systems. For this purpose, 300 µg thylakoid protein extract of WT and *slr0483* were subjected to 4.5-12 % BN-PAGE or 4-16 % CN-PAGE followed by 15 % SDS-PAGE. (A) BN-PAGE/SDS-PAGE, (B) CN-PAGE/SDS-PAGE followed by immunoblot of WT and *slr0483*. (C) Pulse labeling of newly synthesized thylakoid membrane proteins from WT and *slr0483* after incubation of whole cells with [³⁵S] Met for 20 min and subsequent separation of membrane proteins on a 5-12% BN-PAGE (1st dimension) and a 12.5% SDS-PAGE gel (2nd dimension). RC = the PS II complex containing D1, D2, PsbE, PsbF and PsbI; RC47 = PS II core complex lacking CP43; RCC I = PS II monomer; RCC II = PS II dimer. The indicated proteins were detected using the respective antibodies.

6.3.7 Membrane sublocalization of PSII subunits and assembly factors

Analysis of steady-state amounts of photosynthetic complexes had revealed specific reduction of the amount of PS II proteins, in contrast to PS I and Cyt *b₆f* subunits, that remained unaltered in *slr0483* compared to WT (Chapter 6.3.5). In the next step, the membrane distribution of PS II subunits and various assembly factors was investigated using membrane fractionation by sucrose density gradient centrifugation of WT and *slr0483* cells (Schottkowski et al. 2009; Rengstl et al. 2011; performed by Birgit Rengstl). Interestingly, the distribution of several tested proteins was found to be altered: the pD1 protein was surprisingly totally missing in the PDM fractions, whereas CP47 was found to be present in higher amounts in the PDMs in *slr0483* compared to WT (Figure 27). Moreover, slight changes of the distribution of the assembly factors Pitt and POR towards the PDMs were also observed in *slr0483*. Furthermore, Slr0483 itself was localized in both PDM and TM fractions, but mainly accumulates in TMs.

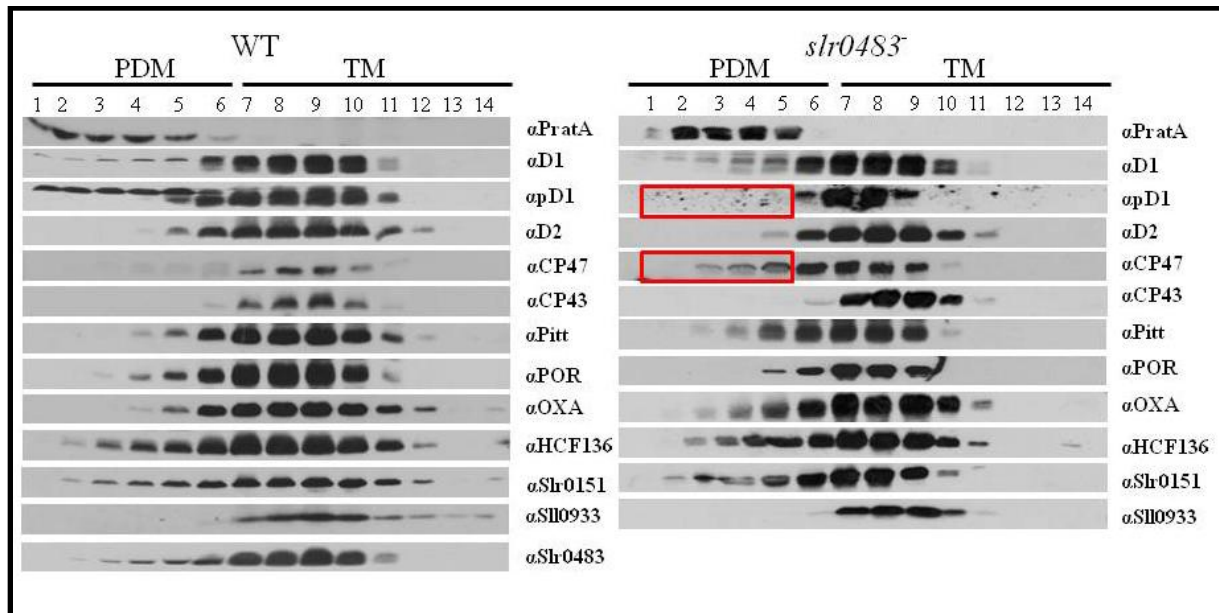


Figure 27. Membrane sublocalization of PSII subunits and assembly factors in WT and *slr0483*. Membrane fractions were isolated according to Schottkowski et al. 2009, where 1–6 represent PDMs, and fractions 7–14 represent TMs. To facilitate comparison between gradients, sample volumes were normalized to the volume of fraction 7 that contained 40 g of protein. The indicated proteins were detected using the respective antibodies. The red box shows the absence of pD1 signal and the shift of CP47 to the PDMs compared to WT. The distribution of proteins in WT was published earlier (Rengstl et al. 2011).

6.3.8 Distribution of Slr0483 in photosynthetic protein complexes

The two-dimensional native gels used for investigation of the migration behavior of Slr0483 revealed no obvious co-localization with the PS II complexes so far (Chapter 6.3.6). To apply

a different method and to further analyze the localization of Slr0483 in various protein complexes, the photosynthetic protein machineries were separated by a sucrose density gradient (Figure 28A), which separated the protein/pigment complexes according to the density (Figure 28B). When membrane proteins (200 μ g) from WT and *slr0483* were extracted and separated using a 10-30 % linear gradient, specific fractions containing certain components of the photosystems could be observed: free pigments (band I), PS I /PS II monomers (band II) and PS I trimers (band III) accumulate to the respective bands according to their densities (Fuhrmann et al. 2009). In *slr0483*, less pigments were detected, however the localization of photosynthetic complexes in the gradient were not changed compared to WT. The composition of band II and band III were further identified by detection of PS I and PS II proteins via immunoblotting. Indeed, band II contains marker proteins for both PS II (D1 and CP47) and PS I complexes (PsaA), whereas band III contains exclusively PsaA, indicating that band II is a mixture of PS I and PS II in contrast to band III that merely contains PS I complex. Furthermore, Slr0483 could be detected in band I and band II with the majority being found in the free-pigment containing band I, suggesting that Slr0483 mainly exists in a free form or bound to yet unidentified non-PS complexes. This result is correlated to the two-dimensional gel systems (6.3.6, Figure 26), suggesting that Slr0483 is not a stable part of the PS II or PS I complexes.

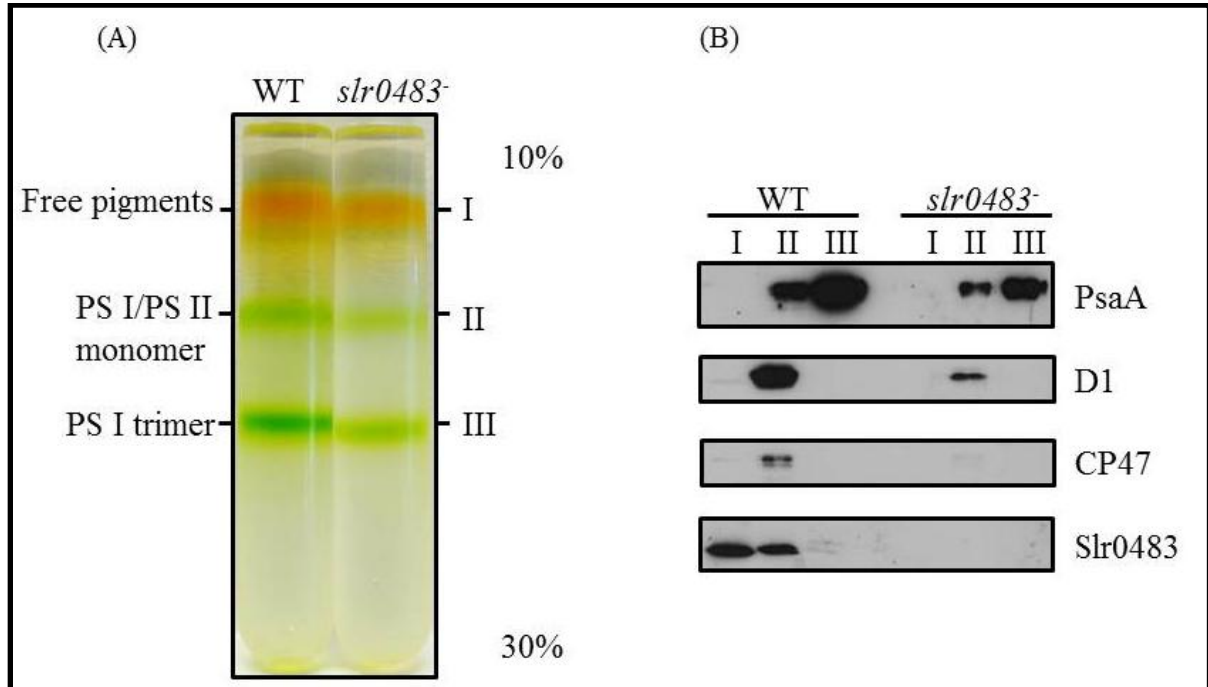


Figure 28. Separation of membrane protein complexes from WT and *slr0483*. (A) Membrane proteins were solubilized with 1.3% (w/v) β -DM and membrane protein complexes were separated on a 10% to 30% linear sucrose density gradient. Three colored bands (I–III) were clearly resolved. (B) Analysis of bands I–III by immunoblot. The membrane protein complexes were identified using antibodies

directed against PSI (PsaA) and PSII (D1 and CP47) subunits. The antibody against Slr0483 was applied for determination of the localization.

6.3.9 Morphology of *slr0483*⁻

Investigation of the physiological parameters revealed an influence of the *slr0483* mutation on the photosynthetic performance, which was found to be clearly reduced in *slr0483*⁻. To gain first insights whether these differences influence also the morphology of the cells ($OD_{730} = 0.6-0.8$), their shape and size were analyzed under an optical microscope (Leica DM 1000, Leica Microsystems CMS GmbH, Wetzlar Germany). Interestingly, the size of *slr0483*⁻ cells was found to be 1.852 ± 0.072 times enlarged compared to WT cells ($n = 50$ cells analyzed; Figure 29). This indicates a general influence of the *slr0483* mutation on the cell morphology and potentially the membrane structure.

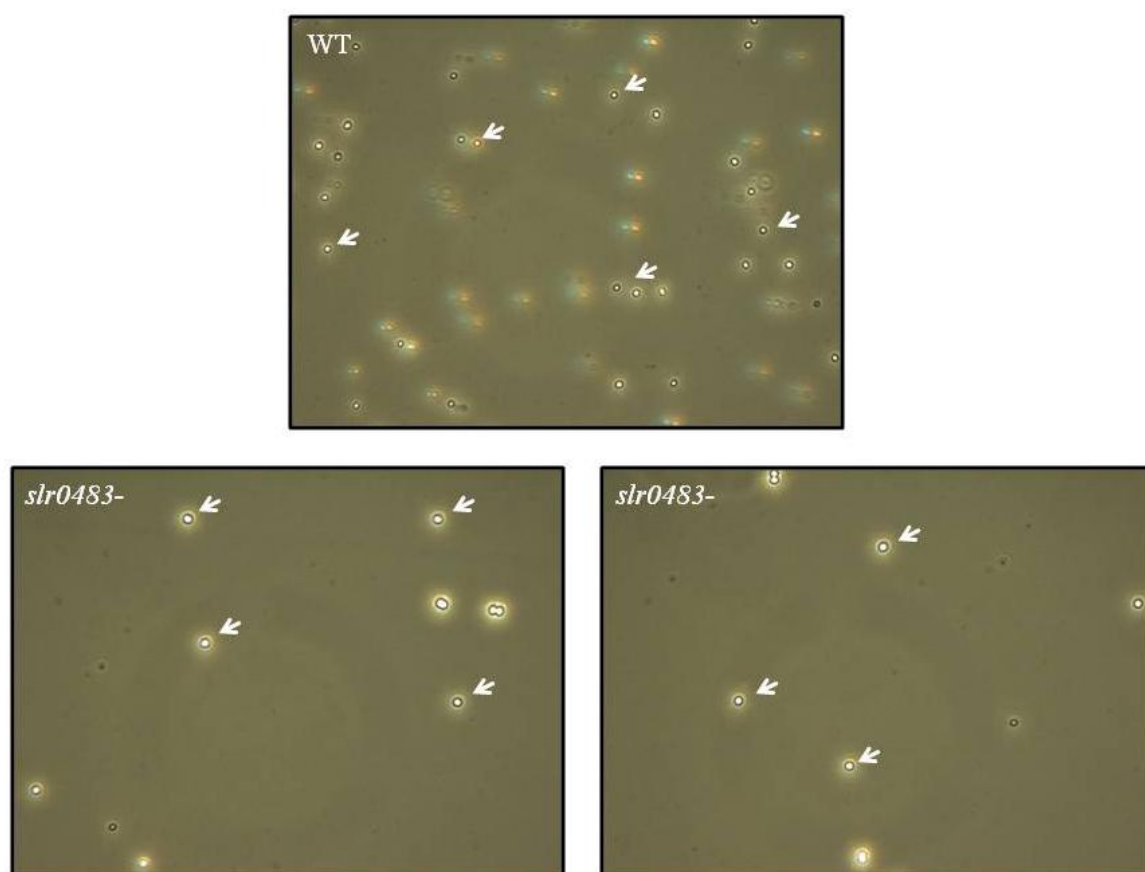


Figure 29. Optical microscope images of WT and *slr0483*⁻ cells with 400 x magnification. The non-dividing cells of each strain are indicated by white arrows.

Investigation of the cell size using an optical microscope had revealed an enlargement of the cells in *slr0483*⁻ compared to WT. As this might suggest alterations in the cell morphology,

the cell structure was analyzed in detail via electron micrographs of ultrathin sections of WT and *slr0483* cells (performed by Dr. Irene Gügel, Dept. Biology I, Botany, LMU München). With this method the cell structure, especially the membrane structure, can be clearly resolved. Interestingly, drastic differences were observed in the membrane organization of *slr0483*: the TMs were found to be irregularly arranged and formed several cyclic layers clearly separated from the PM, whereas the TMs possess several convergence sites in WT (Figure 30). Moreover, the enlargement of *slr0483* cells was also observed in accordance with the optical microscope images (Figure 29). These dramatic effects on TM organization suggest a critical role of Slr0483 in TM development. Furthermore, it can be speculated that the photosynthetic phenotype observed in the abovementioned experiments (see 6.3.4) might be caused directly by the abnormal arrangement of TMs in *slr0483* cells.

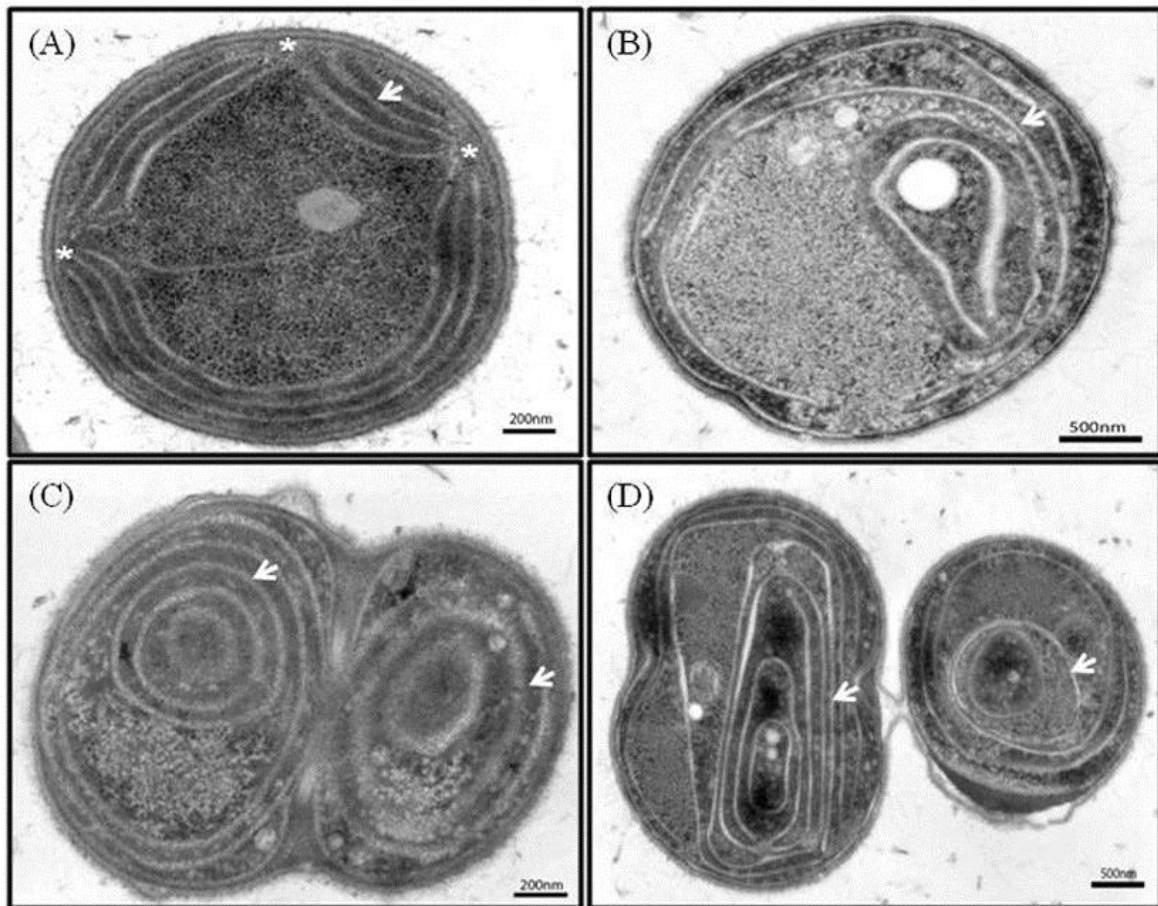


Figure 30. Transmission Electronic Microscopy (TEM) images of WT (A) and *slr0483* (B, C, D). The TMs are indicated by white arrows in both strains and the convergence sites are marked with white asterisks in WT. (C) and (D) exhibit cells in two different division steps. The scale bars represent 200 nm (A, C) and 500 nm (B, D), respectively.

6.3.10 Influence of salt stress on Slr0483 accumulation

In a previous study, Slr0483 was found to be induced by salt stress (4% NaCl, w/v) in the PM (Huang et al. 2006). Thus the effects of salt stress was also analyzed in the present study by treating WT and *slr0483* cells with different NaCl concentrations (0.3 %, 0.6 %, 1 %, 2 %, 3 %, 4 % and 5 %, w/v) and the OD₇₃₀ was measured after 5 days of growth. WT cells depicted no obvious changes in cell density upon incubation with 1 % and 2 % NaCl compared to cells incubated without addition of NaCl (Fig. 31A). When increasing the salt concentration to 3 %, 4 % or 5 % NaCl, a clear decrease in cell number was observed (to 35.44 ± 1.82 %, 17.05 ± 0.99 % and 3.61 ± 3.1 % of the untreated control, respectively). By contrast, the *slr0483* cells were dramatically sensitive to NaCl treatment: Even upon incubation with 1 % NaCl, the *slr0483* cell number decreased to 10.83 ± 0.77 % of the untreated control, and for 2 % to 5 % NaCl, addition of the salt seemed to lead to almost complete cell death (Figure 31A). Within 1 % NaCl (0.3 % and 0.6 % NaCl) treatment, an obvious decline was detected as well, suggesting the high sensitivity of *slr0483* cell to the salt stress (Figure 31B). To analyze the effects of salt stress on protein accumulation, WT cells treated with 1 %, 2 % and 3 % NaCl were harvested, whole proteins (30 µg) were isolated and protein levels detected using immunoblots (WT cells incubated with 4 % and 5 % NaCl as well as all *slr0483* samples could not be analyzed due to the low cell number). Quantification of the immunodetection revealed a reduction of the D1 amount to about 59.5 ± 4.14 % in cells treated with 3% NaCl and a concomitant increase in the Slr0483 level to about 124.44 ± 5.06 % compared to the untreated control. The results confirm that Slr0483 is a salt-induced protein and suggest that it might play a critical role for cell viability under salt stress indicated by the high sensitivity of *slr0483* to NaCl.

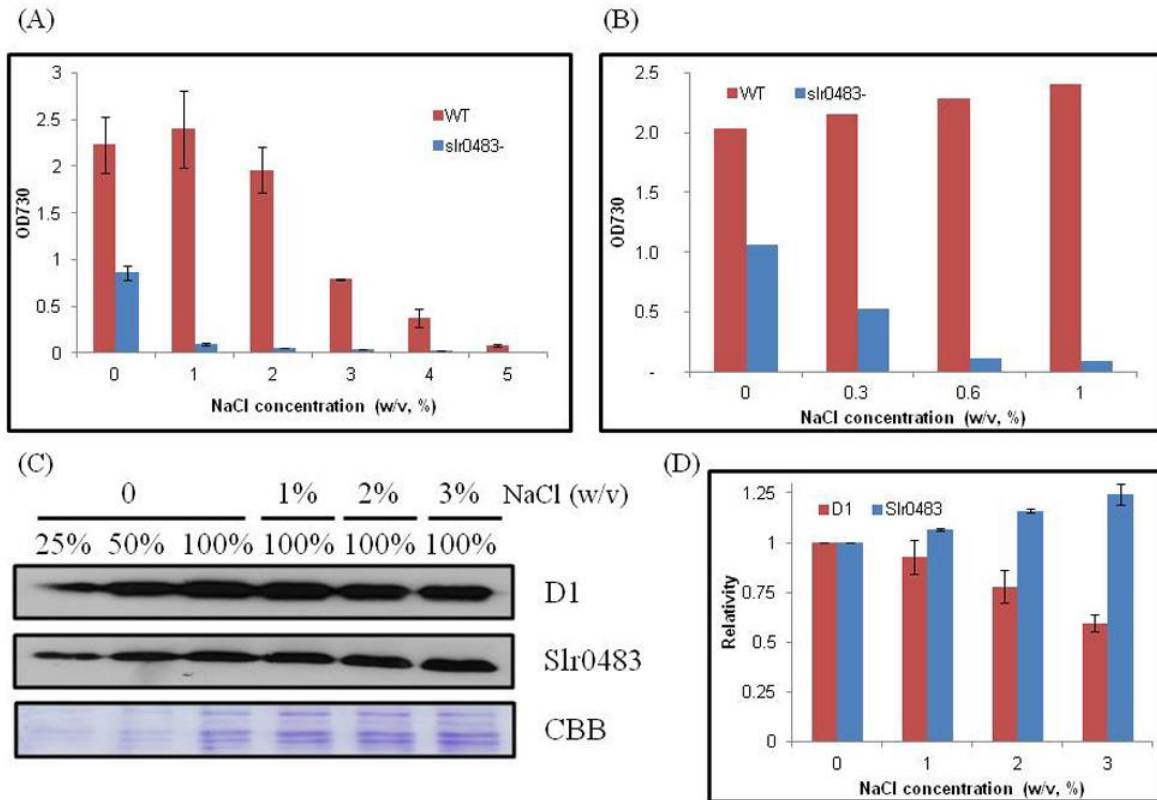


Figure 31. Analyses of WT and *slr0483*⁻ cells under salt stress. (A) Measurement of OD₇₃₀ of WT and *slr0483*⁻ cells upon treatment with different NaCl concentrations (1 %, 2 %, 3 %, 4 % and 5 %) for five days. (B) Measurement of OD₇₃₀ of WT and *slr0483*⁻ cells upon treatment with different NaCl concentrations (0.3 %, 0.6 %, and 1 %) for five days. For (A) and (B), cells grown in BG11 medium without extra NaCl were used as control (0 %). (C) Whole cell proteins from salt-stressed WT cells were extracted and probed by indicated antibodies. The corresponding SDS gel stained with coomassie (CBB) was used as loading control. (D) Quantification of protein levels from 3 independent experiments according to (C). Data shown are mean \pm s.d. (n=3).

To sum up, Slr0483, an integral membrane protein, is evolutionarily conserved in all photosynthetic organisms. The insertion mutant was found to be fully segregated and loss of Slr0483 leads to clear defects in photosynthetic and respiratory performance. The deactivation of *slr0483* specifically reduced the levels of all PS II subunits tested and subsequently the PS II dimer was almost absent in *slr0483*⁻ cells. Additionally, changes in membrane fraction localization were observed for pD1 (precursor form of D1) and CP47. Surprisingly, the organization of TMs in *slr0483*⁻ cells was highly disordered and no convergence sites between plasma membrane and TMs were detected, indicating a role of Slr0483 in the maintenance of TMs. Moreover, Slr0483 was found to be induced by salt stress leading to a strong sensitivity of the *slr0483*⁻ cells to high salt concentrations.

7. Discussion

7.1 TPR protein family

7.1.1 Putative functions of TPR proteins in *Synechocystis* 6803

The data so far accumulated for TPR proteins revealed their basic function in protein-protein interactions. A well-known example is Hop (Hsp70 and Hsp90 organizing protein), also known as p60 or Sti1p, containing 9 TPR motifs forming 2 TPR regions, in which the N-terminal TPR region (3 TPR motifs) is responsible for the interaction with the C terminus of Hsp70 and the C-terminal TPR region (6 TPR motifs) primarily mediates the interaction with Hsp90 (Chen et al. 1996; Lässle et al. 1997; Demand et al. 1998). Concerning the thylakoid membrane biogenesis in *Synechocystis* 6803, several TPR proteins have been found to be involved in this process, e.g., PrtA which interacts directly with D1 and participates in D1 processing (Klinkert et al. 2004; Schottkowski et al. 2009). Other TPR proteins were shown to function in protein complex formation or stability, like Ycf3 interacting with PsaA and PsaD (Naver et al. 2001) or Ycf37 involved in formation or stabilization of PS I (Dühning et al. 2007).

One major goal of this thesis was to investigate the functions of TPR proteins from *Synechocystis* 6803 in thylakoid membrane biogenesis. Interestingly, when combining previously published work with the results of this study, more than half of the TPR proteins in *Synechocystis* 6803 seem to be involved in photosynthesis (Ycf37, Wilde et al. 2001; Ycf3, Schwabe et al. 2003; PrtA, Klinkert et al. 2004; Pitt, Schottkowski et al. 2009; Slr0151, Wegener et al. 2008; Table 14). This high proportion suggests that at least some of these TPR proteins play important roles in the thylakoid membrane biogenesis. Promising candidates should further be investigated in more details regarding their photosynthetic roles, like it was done for Slr1946 (Table 14).

In this study, a mutant is considered to depict a potential photosynthetic phenotype if it exhibits differences in at least two of the photosynthetic parameters measured (doubling time, oxygen evolution, PS I / PS II ratio, chlorophyll fluorescence) compared to WT. Thus this study includes a comprehensive investigation of the photosynthetic phenotypes defined by quantification of the photosynthetic parameters of a whole protein family. However, there are several contradicted aspects among the results. For example, *slr1667* and *slr0499* differ clearly from WT regarding oxygen evolution, emission spectra and chlorophyll fluorescence, but do not depict differences in doubling time under photoautotrophic conditions. Cell division, estimated by measuring the doubling time, is a complex process that utilizes the energy and organic material supplied by photosynthesis, but that is additionally regulated by many other

proteins. Hence, it is difficult to explain why the doubling time is not affected by the decreased efficiency of photosynthesis.

Table 14. Summary of the photosynthetic functions of TPR proteins from *Synechocystis*.

Protein	Segregation	Function/Phenotype	Reference
Slr1044 (Crt1/PilJ)	+	Chemotaxis	Chung et al. 2001
		Pilus assembly	Yoshihara et al. 2002
Slr0171 (Ycf37)	+	PS I assembly	Wilde et al. 2001
Sll0886	-	light-activated heterotrophic	Kong et al. 2003
Slr0823 (Ycf3)	+	PS I assembly	Schwabe et al. 2003
Slr2048 (PratA)	+	PSII assembly	Klinkert et al. 2004
Slr0151	+	PSII assembly	Wegener et al. 2008
Slr1644 (Pitt)	+	Chlorophyll biosynthesis	Schottkowski et al. 2009
Sll1384	+	Phototaxis	Chen et al. 2009
Slr1968	+	photosynthetic phenotype	This study
Sll1667	+		
Sll0499	+		
Sll1946	+		
Sll1251	+		
Sll1882	+		
Slr0751	+		
Sll0314	+	no obvious photosynthetic phenotype	This study
Sll0183	+		
Slr1956	+		
Slr0626	+		
Slr1196	-	essential	This study
Sll0837	-		
Sll1628	-		

7.1.2 Evolution of the TPR proteins

One important feature of the TPR protein family is its occurrence in both prokaryotic and eukaryotic organisms (Smith et al. 1995). Thus, as the TPR domain is present universally among Bacteria, Archaea and Eukarya, it is likely to have emerged from a common ancestor (Ponting et al. 1999). In three model photosynthetic organisms, the numbers of the predicted TPR proteins were estimated from the fully sequenced genomes (Kaneko et al. 1996; GI Arabidopsis 2000; Merchant et al. 2007). This estimation revealed that the Arabidopsis genome encodes for about 2-fold and 7-fold more TPR proteins than the genomes of *C.reinhardtii* and *Synechocystis* 6803, respectively (Table 15). Hence, the genome of *C.reinhardtii* contains 3 times more TPR protein encoding genes than those of *Synechocystis* 6803. This might be associated with the increasing complexity of cellular functions in green algae and higher plants compared to cyanobacteria, for which the tandem repeat proteins are required (Andrade et al. 2001). The percentage of TPR proteins among total proteins shows similar values for the photosynthetic organisms analyzed, supporting a critical and essential role of TPR proteins during the evolution. Interestingly, two protein families containing multiple tandem repeats as well, namely the PPR (pentatricopeptide repeat) and

OPR proteins (octatricopeptide repeat), were exclusively found in eukaryotic organisms (Schmitz-Linneweber and Small 2008; Rochaix 2011). Based on the similarity of the secondary structures of TPR, PPR and OPR motifs (Small and Peeters 2000; Kroeger et al. 2009), these repeat-containing proteins might have been recruited during evolution, by adaptation of a modular protein fold, to recognize new interaction partners (Merendino et al. 2006). Furthermore, the PPR proteins appear to be derived from the TPR proteins which are considered to be more ancient (Kroeger et al. 2009). The OPR protein family in *C.reinhardtii* was speculated to act as the counterpart of the repeats of the TPR and PPR proteins involved in the RNA maturation (Merendino et al. 2006) according to the predicted number (Table 15).

Table 15. The predicted numbers and percentages of TPR, PPR and OPR proteins among *A.thaliana*, *C.reinhardtii* and *Synechocystis* 6803 (Kaneko et al. 1996; GI Arabidopsis 2000; Merchant et al. 2007; Nickelsen et al. unpublished)

Organism	Total proteins	TPR (%)	PPR (%)	OPR (%)
<i>A.thaliana</i>	28581	172 (0.602)	450 (1.575)	1 (0.003)
<i>C.reinhardtii</i>	15142	79 (0.522)	11 (0.073)	114 (0.753)
<i>Synechocystis</i> 6803	3168	23 (0.726)	0 (0)	0 (0)

7.2 Sll1946, a TPR protein potentially involved in early steps of PS II assembly

Sll1946 was chosen for further studies due to the effected photosynthetic performances of the mutant. Protein sequence analysis of Sll1946 reveals the presence of 11 predicted transmembrane domains (TMD) in the N-terminus and 2 hypothetical TPR units in the C-terminus (Figure 10A). Loss of Sll1946 has dramatic effects on photosynthetic performance, especially on PS II related functions (Figure 12 and 13). In *sll1946* cells, a reduction of D1 and CP43 levels and slight accumulation of CP47 level were observed in whole cell protein extracts analyzed by immunoblot (Figure 17). The obvious decrease of RCC I (PS II monomer) in BN-PAGE/SDS-PAGE (Figure 17A) and RC 47 as well as RC complexes in the pulse labeling experiment (Figure 17B) implied that, by loss of Sll1946, the formation of RCC I might be affected but the amount of RCC II (PS II dimer) was not changed. Taken together, these results could assume that the assembly step from RC47 to RCC I is impaired. This assumption was further supported by analysis of protein sublocalization using membrane fractionation experiments (Figure 18), in which Sll0933 was found to be localized to a larger proportion in PDMs in *sll1946* compared to WT. Sll0933 is the homolog of PAM68, which was suggested to interact with several PS II subunits like D1, D2, CP43, CP47, PsbH and PsbI and assembly factors like HCF136/YCF48 and was thus proposed to be involved in PS II assembly in *A. thaliana* (Armbruster et al. 2010). Moreover, in *Synechocystis* 6803, Sll0933 was found to interact with YCF48 to form part of a complex involved in RC 47 assembly (Rengstl et al. 2011). To further study and confirm the role of Sll1946 in PS II assembly, two major points have to be addressed in future studies: (1) interaction partners of Sll1946 and (2) sublocalization of Sll1946 in the membrane fractions.

The multiple alignment of protein sequences reveals a hypothetical PMT domain (amino acid 7-274, Figure 14) in the N-terminus. The family of PMTs (Protein O-mannosyltransferases), firstly reported in yeast, catalyzes the transfer of mannose from dolichyl activated mannose to seryl or threonyl residues of secretory proteins starting in the endoplasmic reticulum (ER) (Strahl-Bolsinger et al. 1999). The PMT protein family is evolutionarily conserved in Eukarya, Bacteria and Archea (Abu-Qarn et al. 2008) with the exceptions of *Caenorhabditis elegans* and higher plants like *Arabidopsis thaliana* and *Oryza sativa* (Lommel and Strahl 2009). Moreover, PMT proteins are crucial for numerous physiological processes, like cell wall rigidity and cell integrity (Gentzsch and Tanner 1996). Among all PMTs, *Saccharomyces cerevisiae* Pmt1 is characterized best, which is an integral ER membrane glycoprotein with seven TMDs (Strahl-Bolsinger and Scheinost 1999; Figure 32). Two invariant Arg64 and Arg138 residues of TMD1 and TMD2 were found to be essential for the formation and/or stability of PMT complexes by site-directed mutagenesis analysis, respectively (Girrbachet al.

2000; Girrbach and Strahl 2003). Structural analyses of Ptmp1 make clear that amino acids Asp77 and Glu78 located in loop 1 are crucial for substrate binding and enzyme activity (Girrbach and Strahl 2003). These so-called DEx/Dex-like motifs were shown to play a key role for catalysis in many glycosyltransferases, suggesting that loop 1 represents the catalytic domain (Lommel and Strahl 2009). Moreover, deletion of loop 5 resulted in the complete loss of transferase activity, showing that loop 5 is critical for the catalytic activity as well. However, the loop5 is not present in bacterial PMTs (Girrbach et al. 2000). Despite progress on the roles of PMT proteins in eukarya, less information is available on the function of protein O-mannosylation in bacteria (Lommel and Strahl 2009). In cyanobacteria, a number of proteins are predicted to contain the PMT domain according to sequence alignments and similarity searches, but none of them has been elucidated in more details yet. Unfortunately, the DEx/Dex-like motifs are not found with any loops in the hypothetical PMT domain (Figure 14). To confirm that Sli1946 is indeed an active Protein O-mannosyltransferase, enzyme activity measurements should be performed in the future.

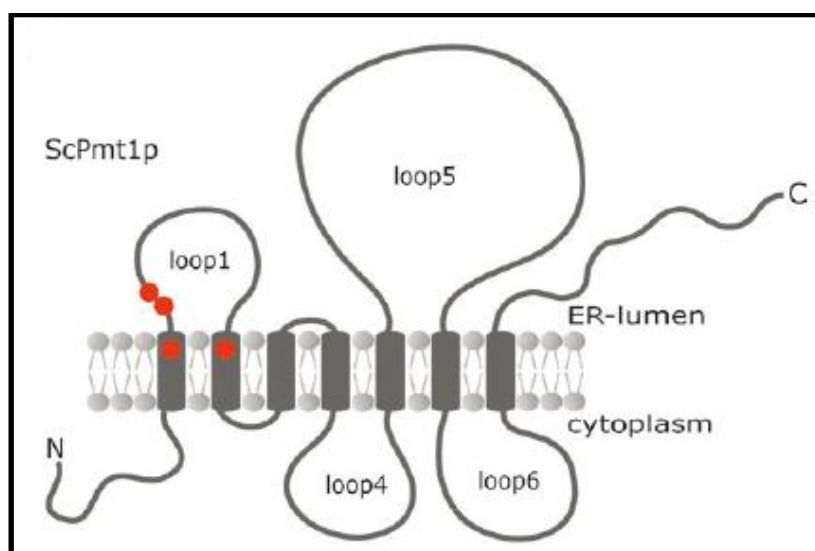


Figure 32. Topology models of *Saccharomyces cerevisiae* Pmt1 (ScPmt1). Conserved Arg (amino acids 64 and 138) residues within transmembrane domain one and two and conserved Asp-Glu motif (amino acids 77 and 78, DEx/Dex-like motif) in loop 1 that are crucial for enzymatic activity are indicated in red (Lommel and Strahl 2009).

7.3 Slr0483 is a thylakoid membrane organization factor

7.3.1 Loss of Slr0483 leads to defective TM organization and reduced photosynthetic performance

In this study, *slr0483* was shown to exhibit dramatic defects in TM organization and photosynthetic activity (Figure 24, Table 13; Figure 30). In previous studies, three genes (*vipp1*, *alb3* and *slr1768*) in *Synechocystis* 6803 have been identified, whose deletion resulted in substantial loss of the thylakoid membrane system as well (Westphal et al. 2001; Spence et al. 2004; Bryan et al. 2011, Figure 33). The products of these three genes are localized in the PM, in contrast to the TM-localized Slr0483. Complete deletion of *vipp1* and *alb3* in the genome could not be achieved, suggesting that these are two essential genes (Westphal et al. 2001; Spence et al. 2004), but *slr1768* was found to be fully segregated in the mutant (Bryan et al. 2011). So far, it remains uncertain whether the knock-down of *vipp1* and *alb3* primarily effects the production of the thylakoid membranes themselves. However, the loss of Slr1768 results in a variegated phenotype: a proportion of the $\Delta slr1768$ cells shows complete absence of TMs and chlorophyll, while the rest of the cells seems to be completely normal in terms of their pigment and TM content as well as photosynthetic performance under either low growth light or high light (Bryan et al. 2011).

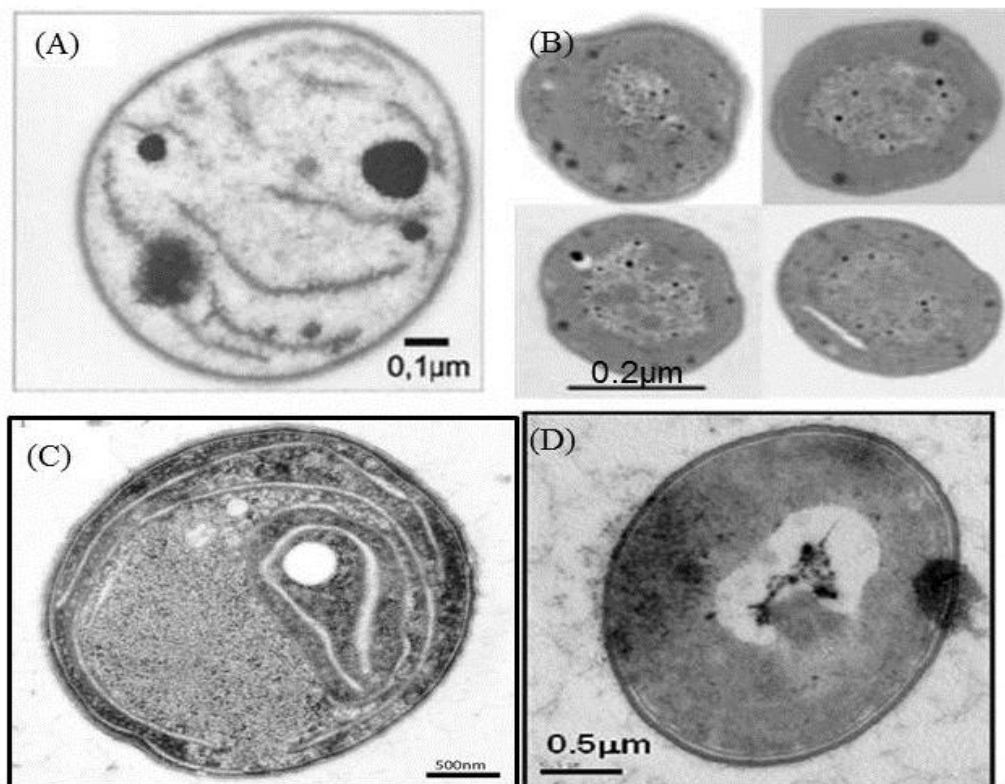


Figure 33. Comparison of morphology from various mutants of *Synechocystis* 6803. Transmission Electronic Microscopy (TEM) images of $\Delta vipp1$ cell (A, Westphal et al. 2001), $\Delta alb3$ cells (B, Spence et al. 2004), $slr0483^-$ cell (C) growing under normal conditions ($30 \mu\text{mol m}^{-2} \text{s}^{-1}$ photon irradiance) and $\Delta slr1768$ cell (D, Bryan et al. 2011) growing under high light ($130 \mu\text{mol m}^{-2} \text{s}^{-1}$). The scale bars are shown in the images.

Slr0483 is clearly not essential for TM biogenesis (Figure 22), since mutant cells are able to survive under photoautotrophic conditions. Moreover, the phenotype of the morphology of $slr0483^-$ indicates that the role of Slr0483 is significantly different from Vipp1, Alb3 and Slr1768. The measurements show longer doubling time, less oxygen production, lower maximum PSII quantum yield and decreased chlorophyll concentration in $slr0483^-$ cells in comparison to WT (Figure 24, Table 13). These observations could be explained by reduced PS II subunits levels (Figure 25) and the almost absence of fully functional PS II dimers (Figure 26A, B). There are two possibilities for the dramatic decrease of PS II dimers: (1) the PS II dimer could not be formed or (2) the PS II dimer is unstable. To test the first assumption, pulse labeling experiments were carried out (Figure 26C). Unfortunately, the signals of PS II dimers were not pronounced even in WT due to the inefficient radioactive labeling of the cells. However, no accumulation of PS II monomers was observed. To verify the second assumption regarding the stability of PS II dimers, the Psb I and Psb M levels have to be estimated in future experiments since both proteins are critical for the formation and stability of PS II (Kawakami et al. 2010).

However, the declined PS I / PS II ratio appears to be contradictory to the lower PS II amount measured by the emission spectra at 77 K with intact WT and $slr0483^-$ cells. Meanwhile, the PsaA level was not changed in $slr0483^-$ cells. Concerning the fact that in *Synechocystis* 6803, about 80 % Chl is bound to PS I (Dobáková et al. 2009), the possibility of this contradiction might result from the reduction of chlorophyll amount (Figure 24D).

In WT cells, the TMs are organized in multiple concentric shells (Figure 30A; Nierzwicki-Bauer et al. 1983) that possess distinct convergence sites to the PM at the cell periphery (Stengel et al. 2012). However, it is still unknown how the connections between the cell interior and the PM are maintained, and how the different shells or layers of the TMs communicate with each other to ensure concerted responses to environmental changes or to incoming stimuli. By contrast, the TMs in $slr0483^-$ cells are organized in either parallel or irregular sheets without obvious convergence sites to the PM, which means that the connection and communication between TMs and PM are disrupted by the loss of Slr0483. This observation is rather distinguished from $\Delta vipp1$ and $\Delta alb3$ under normal conditions and

$\Delta slr1768$ at high light intensity. In $\Delta vip1$, $\Delta alb3$ and $\Delta slr1768$ cells, the formation or development of TMs appears to be affected by mutagenesis (Figure 33).

So far, many questions remain to be answered concerning TM biogenesis in both cyanobacteria and chloroplasts. A recent study analyzing the localization of PratA and pD1 by ultrastructural and immunogold labeling experiments describes a specialized PratA-dependent membrane structure at convergence sites between TMs and PM, called biogenesis center, on which PratA and pD1 are localized and the initial steps of PS II biogenesis occur (Stengel et al. 2012). Concerning the total absence of convergence sites between TMs and PM in $slr0483$ cells, several questions remain to be answered: (1) where are PratA and pD1 localized in $slr0483$? (2) Where and how does pD1 processing into mature D1 occur? (3) How do D1 (iD1) and D2 interact to form RC complexes? To answer at least part of these questions, immunogold labeling experiments in $slr0483$ cells should be performed in future experiments.

The enlargement of $slr0483$ cells observed under both optical microscope (Figure 29) and TEM (Figure 30) might be resulted from the increased doubling time (Figure 24 and Table 13).

7.3.2 Slr0483 is conserved in photosynthetic organisms

As shown by BLAST searches and multiple alignments of protein sequences (Figure 21B), Slr0483 homolog proteins are found universally in cyanobacteria, green algae, mosses and higher plants, but not in non-photosynthetic organisms. This suggests that Slr0483 homolog proteins play crucial cellular photosynthesis-related functions, as these proteins have been conserved during evolution. The multiple alignments demonstrate that the sequences are especially highly conserved at the C-terminus, indicating that this part might include a functional region (Figure 21B). Six polar (N₁₀₁, P₁₀₄, M₁₁₅, Y₁₁₇, T₁₁₈, Y₁₂₄) amino acids and 3 charged (R₁₂₃, R₁₃₂, E₁₃₄) amino acids were found among this region with high identity and similarity. While polar amino acids are thought to be involved in hydrogen bonding with side chains or main chain atoms or with water, charged amino acids often interact with each other to form salt bridges. These interactions are considered to preserve the tertiary structure of the protein (Engelman et al. 1986). To understand the function and role of conserved amino acids, site-directed mutagenesis could be performed in the future.

7.3.3 Defective respiratory performance

The cyanobacterial TM system contains both photosynthetic and respiratory electron transport chains (Vermaas 2001) where *Cyt_b₆f* is a key and indispensable complex in linear and cyclic photosynthetic as well as respiratory electron transport (Schultze et al. 2009). The core of this complex is composed of four subunits, cytochrome *b*, cytochrome *f*, subunit IV and the Rieske protein (PetC). In the present study, the respiratory performance was found to be affected by measuring the oxygen consumption in *slr0483* cells. Compared with the oxygen evolution, the oxygen consumption revealed an even more obvious decrease (Figure 24B). To analyze possible effects of the loss of Slr0483 on the amount or composition of the Cyt *b*₆*f* complex, the protein level of cytochrome *f* was monitored by immunoblots. However, no difference compared to WT was observed (Figure 25). Protein levels of other subunits involved in the respiratory electron transport chain should be further analyzed. Although the exact effects of the loss of Slr0483 on the respiratory complexes remain to be investigated, the defective TM organization in *slr0483* cells caused by the irregular arrangement of the TMs leads to the hypothesis that the electron transport chains via the electron carriers or the proton gradient across the membranes are influenced.

7.3.4 Changes of pD1 and CP47 localization in *slr0483*

The PDM is a specialized membrane fraction identified in *Synechocystis* 6803 in which the early steps of PS II assembly were proposed to occur (Schottkowski et al. 2009). PratA was demonstrated to play an essential role in the spatial organization of PDMs to serve as a platform for PS II biogenesis, because the loss of PratA severely affects the sublocalization of other PSII assembly factors, like Slr1471, YCF48, and SlI0933 (Rengstl et al. 2011). The role of PDMs in early PS II assembly steps was further substantiated by the sublocalization of the PS II subunits themselves: (1) pD1 accumulates in this fraction upon deletion of PratA (Schottkowski et al. 2009); (2) D1 and D2 are found in both PDMs and TMs (Schottkowski et al. 2009; Rengstl et al. 2011); (3) CP47 and CP43, the antennae proteins that are assembled in later steps of PS II biogenesis are by contrast exclusively localized in TMs (Rengstl et al. 2011). These observations are consistent with the current models of PSII biogenesis based on the analysis of PSII assembly intermediates by BN-PAGE/SDS-PAGE (Figure 7, Nixon et al. 2010). In *slr0483* cells, PratA was still detected in a “PDM fraction” in *slr0483* cells, suggesting that specialized membrane regions still exist, although no PM/TM convergence sites are found by ultrastructural analysis of *slr0483* cells (Figure 30). Surprisingly, pD1 was not detectable in PDMs and CP47 was on the contrary slightly shifted towards the PDMs, however, the sublocalizations of D1, D2 and CP43 were not affected (Figure 27). The loss of

pD1 in the PDMs and the change in localization of CP47 suggest that the distribution of pD1 and CP47 in the TMs was disrupted by inactivation of *slr0483*, which might be a secondary effect caused by disordered TM organization. Interestingly, membrane domains with specialized functions have been localized even in the PM of the ancient cyanobacterium *Gloeobacter violaceus*, the only known organism performing oxygenic photosynthesis without internal TMs (Rexroth et al. 2011). Hence, the exact localization of PrtA and potential PS II biogenesis regions in *slr0483* will be a task for further experiments.

7.3.5 Crucial role of Slr0483 under salt stress

Slr0483 was initially detected by investigation of salt-stress induced changes in PM proteins of *Synechocystis* 6803 using a proteomic approach (Huang et al. 2006). The PM fractions from control and salt-treated (4 % NaCl, w/v, 684 mM) cells were isolated and the proteins were separated by 2-dimensional gels and analyzed by MALDI MS (Matrix-assisted laser desorption/ionization mass spectrometry). The results demonstrate that the Slr0483 amount increased upon salt stress, suggesting a salt-induced regulation (Huang et al. 2006). Other proteins, including components of ABC transporters and Vipp1, were induced at least 2-fold in salt-acclimated cells. The clear enhancement of NrtA (nitrate/nitrite-binding protein, increased more than 2 fold) and of some putative nitrate /sulfonate /bicarbonate /taurine /binding proteins observed in salt-treated cells might be in agreement with the observation that high salinity in the media appears to lead to nutrient deficiency caused by compositional and structural changes in the PM (Willkinson and Northcote 1980, Huang et al. 2006). The 5-fold increase of Vipp1 was assumed to be required of reorganization of the TMs in salt-acclimated cells (Huang et al. 2006) due to the essential function of Vipp1 in the formation of TMs (Westphal et al. 2001). In the present study, the Slr0483 level in whole cell proteins was found to be increased, confirming that Slr0483 is induced in salt-treated cells (Figure 31). Therefore, it can be hypothesized that Slr0483 might function together with Vipp1 in the TM biogenesis. To verify this hypothesis, the protein level of Vipp1 in whole cell proteins extracts and the potential interaction between Slr0483 and Vipp1 will be studied by immunoblots and co-immunoprecipitation in the next steps. Furthermore, Slr0483 is localized in the TMs as well as PDMs (Figure 27), suggesting that Slr0483 might partly be transferred from TMs to PM via PDMs under salt stress condition. To investigate this transfer, membrane fractionation of salt-stressed cells should be performed in the next step. However, the exact function of Slr0483 in the salt acclimation is still unknown. It also remains to be investigated whether the sensitivity to salt stress is a secondary effect due to the distorted membrane structure or whether – vice versa – the changes in membrane organization are caused by the

salt sensitivity. The *slr0483* cells show an extremely high salt sensitivity as even 1 % NaCl (w/v, 171 mM, Figure 31B) seems to be fatal to the mutant cells. The protection mechanism against salt stress of *slr0483* cells is supposed to be lost, due to either the defective TM arrangement, or the inactivation of *slr0483* or both.

7.4 Conclusion

The results shown in this thesis contributed to a better understanding of TM biogenesis and of the functions of TPR proteins in *Synechocystis* 6803. However, several questions concerning the roles of TPR proteins and Slr0483 remain open. For Sll1946, more details about the early step of PS II assembly will be understood by localization of Sll1946 in PS II complexes as well as identification of interaction partners. For Slr0483, it is tempting to speculate that one of its roles could be maintaining the convergence sites between the PM and TMs. Investigation of the precise role of Slr0483 under salt-stressed conditions will be an interesting and challenging task in the future.

8. References

- Abu-Qarn, M., J. Eichler, et al. (2008). "Not just for Eukarya anymore: protein glycosylation in Bacteria and Archaea." *Current Opinion in Structural Biology* 18(5): 544-550.
- Allakhverdiev, S. I. and N. Murata (2008). "Salt stress inhibits photosystems II and I in cyanobacteria." *Photosynthesis research* 98(1): 529-539.
- Allakhverdiev, S. I. and N. Murata (2004). "Environmental stress inhibits the synthesis de novo of proteins involved in the photodamage–repair cycle of Photosystem II in *Synechocystis* sp. PCC 6803." *Biochimica et Biophysica Acta (BBA) - Bioenergetics* 1657(1): 23-32.
- Allakhverdiev, S. I., A. Sakamoto, et al. (2000). "Ionic and osmotic effects of NaCl-induced inactivation of photosystems I and II in *Synechococcus* sp." *Plant Physiology* 123(3): 1047-1056.
- Allen, F.-J., W.-B.-M. de Paula, et al. (2011). "A structural phylogenetic map for chloroplast photosynthesis." *Trends in Plant Science* 16(12): 645-655.
- Almela, L., J. -A. Fernández-López, et al. (2000). "High-performance liquid chromatographic screening of chlorophyll derivatives produced during fruit storage." *Journal of Chromatography A* 870: 483–489.
- Amunts, A., O. Drory, et al. (2007). "The structure of a plant photosystem I supercomplex at 3.4 Å resolution." *Nature* 447(7140): 58-63.
- Amunts, A., H. Toporik, et al. (2010). "Structure determination and improved model of plant Photosystem I." *Journal of Biological Chemistry* 285(5): 3478-3486.
- Andrade, M. A., C. Perez-Iratxeta, et al. (2001). "Protein repeats: structures, functions, and evolution." *Journal of Structural Biology* 134(2-3): 117-131.
- Armbruster, U., J. Zühlke, et al. (2010). "The Arabidopsis thylakoid protein pam68 is required for efficient D1 biogenesis and photosystem II assembly." *The Plant Cell Online* 22(10): 3439-3460.
- Arnon, D. (1949). "Copper enzymes in isolated chloroplasts. Polyphenoloxidase in *Beta vulgaris*." *Plant Physiology* 24(1): 1-15.

- Aro, E.-M., I. Virgin, et al. (1993). "Photoinhibition of photosystem II. Inactivation, protein damage and turnover." *Biochimica et Biophysica Acta (BBA) - Bioenergetics* 1143(2): 113-134.
- Arthur, R.-S. (1969). "A low-viscosity epoxy resin embedding medium for electron microscopy." *Journal of Ultrastructure Research* 26(1-2): 31-43.
- Awai, K., K. Takatoshi, et al. (2006). "Comparative genomic analysis revealed a gene for monoglucosyldiacylglycerol synthase, an enzyme for photosynthetic membrane lipid synthesis in cyanobacteria." *Plant Physiology* 141(3): 1120-1127.
- Barber, J. (2006). "Photosystem II: an enzyme of global significance." *Biochemical Society Transactions* 34: 619–631.
- Barber, J. and Nield, J. (2002). "Organization of transmembrane helices in photosystem II: comparison of plants and cyanobacteria." *Philosophical Transactions of the Royal Society B: Biological Sciences* 357(1426): 1329-1335.
- Biesiadka, J., B. Loll, et al. (2004). "Crystal structure of cyanobacterial photosystem II at 3.2 Å resolution: a closer look at the Mn-cluster." *Physical Chemistry Chemical Physics* 6(20): 4733-4736.
- Blankenship, R. E. (1992). "Origin and early evolution of photosynthesis." *Photosynthesis research* 33(2): 91-111.
- Boudreau, E., J. Nickelsen, et al. (2000). "The *Nac2* gene of *Chlamydomonas* encodes a chloroplast TPR-like protein involved in psbD mRNA stability." *EMBO J* 19(13): 3366-3376.
- Boudreau, E., Y. Takahashi, et al. (1997). "The chloroplast *ycf3* and *ycf4* open reading frames of *Chlamydomonas reinhardtii* are required for the accumulation of the photosystem I complex." *EMBO J* 16(20): 6095-6104.
- Bennoun, P. (1982). "Evidence for a respiratory chain in the chloroplast." *Proceedings of the National Academy of Sciences* 79: 4352-4356.
- Bradford, M. M. (1976). "A rapid and sensitive method for the quantitation of microgram quantities of protein utilizing the principle of protein-dye binding." *Analytical biochemistry* 72: 248-254.
- Bryan, S. J., N. J. Burroughs, et al. (2011). "Loss of the SPHF homologue Slr1768 leads to a catastrophic failure in the maintenance of thylakoid membranes in *Synechocystis* sp. PCC 6803." *PLoS ONE* 6(5): e19625.

- Chen, S., V. Prapapanich, et al. (1996). "Interactions of p60, a mediator of progesterone receptor assembly, with heat shock proteins Hsp90 and Hsp70." *Molecular Endocrinology* 10(6): 682-693.
- Chen, Z. and X. Xu (2009). "DnaJ-like protein gene *sll1384* is involved in phototaxis in *Synechocystis* sp. PCC 6803." *Chinese Science Bulletin* 54(23): 4381-4386.
- Chew, A. G. M. and D. A. Bryant (2007). "Chlorophyll biosynthesis in bacteria: the origins of structural and functional diversity." *Annual Review of Microbiology* 61(1): 113-129.
- Chung, Y.-H., M.-S. Cho, et al. (2001). "*ctr1*, a gene involved in a signal transduction pathway of the gliding motility in the cyanobacterium *Synechocystis* sp. PCC 6803." *FEBS letters* 492(1-2): 33-38.
- Cramer, W. A., G. M. Soriano, et al. (1996). "Some new structural aspects and old controversies concerning the cytochrome *b₆f* complex of oxygenic photosynthesis." *Annual review of plant physiology and plant molecular biology* 47(1): 477-508.
- Das, A.-K., P.-W. Cohen, et al. (1998). "The structure of the tetratricopeptide repeats of protein phosphatase 5: implications for TPR-mediated protein-protein interactions." *EMBO J* 17(5):1192-1199.
- D'Andrea, L. D. and L. Regan (2003). "TPR proteins: the versatile helix." *Trends in Biochemical Sciences* 28(12): 655-662.
- Demand, J., J. Lüders, et al. (1998). "The carboxy-terminal domain of Hsc70 provides binding sites for a distinct set of chaperone cofactors." *Molecular and cellular biology* 18(4): 2023-2028.
- Dietzel, L., K. Bräutigam, et al. (2011). "Photosystem II supercomplex remodeling serves as an entry mechanism for state transitions in *Arabidopsis*." *The Plant Cell Online* 23(8): 2964-2977.
- Dobáková, M., R. Sobotka, et al. (2009). "Psb28 protein is involved in the biogenesis of the photosystem ii inner antenna CP47 (PsbB) in the cyanobacterium *Synechocystis* sp. PCC 6803." *Plant Physiology* 149(2): 1076-1086.
- Dobáková, M., M. Tichý, et al. (2007). "Role of the Psbl protein in photosystem II assembly and repair in the cyanobacterium *Synechocystis* sp. PCC 6803." *Plant Physiology* 145(4): 1681-1691.

- Dühning, U., F. Ossenbühl, et al. (2007). "Late assembly steps and dynamics of the cyanobacterial photosystem I." *Journal of Biological Chemistry* 282(15): 10915-10921.
- Dyall, S. D., M. T. Brown, et al. (2004). "Ancient invasions: from endosymbionts to organelles." *Science* 304(5668): 253-257.
- Engelman, D. M., T. A. Steitz, et al. (1986). "Identifying nonpolar transbilayer helices in amino acid sequences of membrane proteins." *Annual Review of Biophysics and Biophysical Chemistry* 15(1): 321-353.
- Eubel, H., J. Heinemeyer, et al. (2004). "Respiratory chain supercomplexes in plant mitochondria." *Plant Physiology and Biochemistry* 42: 937–942.
- Ferjani, A., L. Mustardy, et al. (2003). "Glucosylglycerol, a compatible solute, sustains cell division under salt stress." *Plant Physiology* 131(4): 1628-1637.
- Ferreira, K. N., T. M. Iverson, et al. (2004). "Architecture of the photosynthetic oxygen-evolving center." *Science* 303(5665): 1831-1838.
- Fuhrmann, E., S. Gathmann, et al. (2009). "Thylakoid membrane reduction affects the photosystem stoichiometry in the cyanobacterium *Synechocystis* sp. PCC 6803." *Plant Physiology* 149(2): 735-744.
- Gentzsch, M. and Tanner, W. (1996). "The PMT gene family: protein O-glycosylation in *Saccharomyces cerevisiae* is vital." *EMBO J* 15(21): 5752–5759.
- Girrbach, V. and S. Strahl (2003). "Members of the evolutionarily conserved PMT family of protein O-mannosyltransferases form distinct protein complexes among themselves." *Journal of Biological Chemistry* 278(14): 12554-12562.
- Girrbach, V., T. Zeller, et al. (2000). "Structure-function analysis of the Dolichyl Phosphate-Mannose: protein O-mannosyltransferase ScPmt1p." *Journal of Biological Chemistry* 275(25): 19288-19296.
- Grigorieva, G. and S. Shestakov (1982). "Transformation in the cyanobacterium *Synechocystis* sp. 6803." *FEMS Microbiology Letters* 13(4): 367-370.
- Grossman, A. R., M. R. Schaefer, et al. (1993). "The phycobilisome, a light-harvesting complex responsive to environmental conditions." *Microbiological Reviews* 57(3): 725-749.
- Hagemann, M. (2011). "Molecular biology of cyanobacterial salt acclimation." *FEMS Microbiology Reviews* 35(1): 87-123.

- Hagemann, M., S. Richter, et al. (1997). "The *ggtA* gene encodes a subunit of the transport system for the osmoprotective compound glucosylglycerol in *Synechocystis* sp. strain PCC 6803." *Journal of Bacteriology* 179(3): 714-720.
- Hansson, M. and A. V. Vener (2003). "Identification of three previously unknown *in vivo* protein phosphorylation sites in thylakoid membranes of *Arabidopsis thaliana*." *Molecular & Cellular Proteomics* 2(8): 550-559.
- Heber, U. and D. Walker (1992). "Concerning a dual function of coupled cyclic electron transport in leaves." *Plant Physiology* 100(4):1621-1626.
- Huang, F., S. Fulda, et al. (2006). "Proteomic screening of salt-stress-induced changes in plasma membranes of *Synechocystis* sp. strain PCC 6803." *Proteomics* 6(3): 910-920.
- Ikeuchi, M. and S. Tabata (2001). "*Synechocystis* sp. PCC 6803 — a useful tool in the study of the genetics of cyanobacteria." *Photosynthesis research* 70(1): 73-83.
- Inaba, M., A. Sakamoto, et al. (2001). "Functional expression in *Escherichia coli* of low-affinity and high-affinity Na⁺ (Li⁺)/H⁺ antiporters of *Synechocystis*." *Journal of Bacteriology* 183(4): 1376-1384.
- Initiative, T. A. G. (2000). "Analysis of the genome sequence of the flowering plant *Arabidopsis thaliana*." *Nature* 408(6814): 796-815.
- Jensen, P. E., R. Bassi, et al. (2007). "Structure, function and regulation of plant photosystem I." *Biochimica et Biophysica Acta (BBA) - Bioenergetics* 1767(5): 335-352.
- John G.K, W. (1988). "Construction of specific mutations in photosystem II photosynthetic reaction center by genetic engineering methods in *Synechocystis* 6803." *Methods in Enzymology*. 167: 766-778.
- Johnson, X., K. Wostrikoff, et al. (2010). "MRL1, a conserved pentatricopeptide repeat protein, is required for stabilization of *rbcL* mRNA in *Chlamydomonas* and *Arabidopsis*." *The Plant Cell* 22(1): 234-248.
- Jordan, P., P. Fromme, et al. (2001). "Three-dimensional structure of cyanobacterial photosystem I at 2.5 Å resolution." *Nature* 411(6840): 909-917.
- Kamiya, N. and J.-R. Shen (2003). "Crystal structure of oxygen-evolving photosystem II from *Thermosynechococcus vulcanus* at 3.7 Å resolution." *Proceedings of the National Academy of Sciences* 100(1): 98-103.

- Kaneko, T., S. Sato, et al. (1996). "Sequence analysis of the genome of the unicellular cyanobacterium *Synechocystis* sp. Strain PCC 6803. II. Sequence determination of the entire genome and assignment of potential protein-coding regions." *DNA Research* 3(3): 109-136.
- Kaneko, T. and S. Tabata (1997). "Complete genome structure of the unicellular cyanobacterium *Synechocystis* sp. PCC 6803." *Plant and Cell Physiology* 38(11): 1171-1176.
- Karplus, P., M. Daniels, et al. (1991). "Atomic structure of ferredoxin-NADP⁺ reductase: prototype for a structurally novel flavoenzyme family." *Science* 251(4989): 60-66.
- Kashino, Y., W.-M. Lauber, et al. (2002). "Proteomic analysis of a highly active photosystem II preparation from the cyanobacterium *Synechocystis* sp. PCC 6803 reveals the presence of novel polypeptides." *Biochemistry* 41(25):8004-8012.
- Kawakami, K., Y. Umena, et al. (2011). "Roles of PsbI and PsbM in photosystem II dimer formation and stability studied by deletion mutagenesis and X-ray crystallography." *Biochimica et Biophysica Acta (BBA) - Bioenergetics* 1807(3): 319-325.
- Khrouchtchova, A., M. Hansson, et al. (2005). "A previously found thylakoid membrane protein of 14 kDa (TMP14) is a novel subunit of plant photosystem I and is designated PSI-P." *FEBS letters* 579(21): 4808-4812.
- Klinkert, B., F. Ossenbühl, et al. (2004). "PratA, a periplasmic tetratricopeptide repeat protein involved in biogenesis of photosystem II in *Synechocystis* sp. PCC 6803." *Journal of Biological Chemistry* 279(43): 44639-44644.
- Kobayashi, K., M. Kondo, et al (2007). "Galactolipid synthesis in chloroplast inner envelope is essential for proper thylakoid biogenesis, photosynthesis, and embryogenesis." *Proceedings of the National Academy of Sciences* 104(43):17216-17221.
- Komenda, J., J. Nickelsen, et al. (2008). "The cyanobacterial homologue of HCF136/YCF48 is a component of an early photosystem II assembly complex and is important for both the efficient assembly and repair of photosystem II in *Synechocystis* sp. PCC 6803." *Journal of Biological Chemistry* 283(33): 22390-22399.
- Komenda, J., V. Reisinger, et al. (2004). "Accumulation of the D2 protein is a key regulatory step for assembly of the photosystem II reaction center complex in *Synechocystis* PCC 6803." *Journal of Biological Chemistry* 279(47): 48620-48629.

- Kong, R., X. Xu, et al. (2003). "A TPR-family membrane protein gene is required for light-activated heterotrophic growth of the cyanobacterium *Synechocystis* sp. PCC 6803." *FEMS Microbiology Letters* 219(1): 75-79.
- Kroeger, T. S., K. P. Watkins, et al. (2009). "A plant-specific RNA-binding domain revealed through analysis of chloroplast group II intron splicing." *Proceedings of the National Academy of Sciences* 106(11): 4537-4542.
- Korzyńska, A. and M. Zychowicz (2008). "A method of estimation of the cell doubling time on basis of the cell culture monitoring data." *Biocybernetics and Biomedical Engineering* 28(4): 75–82.
- Kroll, D., K. Meierhoff, et al. (2001). "VIPP1, a nuclear gene of *Arabidopsis thaliana* essential for thylakoid membrane formation." *Proceedings of the National Academy of Sciences* 98(7): 4238-4242.
- Lässle, M., G. L. Blatch, et al. (1997). "Stress-inducible, murine protein mSTI1: Characterization of binding domains for heat shock proteins and *in vitro* phosphorylation by different kinases." *Journal of Biological Chemistry* 272(3): 1876-1884.
- Liberton, M., B.-R. Howard, et al. (2006). "Ultrastructure of the membrane systems in the unicellular cyanobacterium *Synechocystis* sp. strain PCC 6803." *Protoplasma* 227(2-4):129-138.
- Liu, H., J. L. Roose, et al. (2011). "A genetically tagged Psb27 protein allows purification of two consecutive photosystem II (PSII) assembly intermediates in *Synechocystis* 6803, a Cyanobacterium." *Journal of Biological Chemistry* 286(28): 24865-24871.
- Loll, B., J. Kern, et al. (2005). "Towards complete cofactor arrangement in the 3.0 Å resolution structure of photosystem II." *Nature* 438(7070): 1040-1044.
- Lommel, M. and S. Strahl (2009). "Protein O-mannosylation: Conserved from bacteria to humans." *Glycobiology* 19(8): 816-828.
- Marion M, B. (1976). "A rapid and sensitive method for the quantitation of microgram quantities of protein utilizing the principle of protein-dye binding." *Analytical biochemistry* 72(1-2): 248-254.
- Merchant, S. S., S. E. Prochnik, et al. (2007). "The *Chlamydomonas* genome reveals the evolution of key animal and plant functions." *Science* 318(5848): 245-250.

- Merendino, L., K. Perron, et al. "A novel multifunctional factor involved in trans-splicing of chloroplast introns in *Chlamydomonas*." *Nucleic acids research* 34(1): 262-274.
- Meskauskiene, R., M. Nater, et al. (2001). "FLU: A negative regulator of chlorophyll biosynthesis in *Arabidopsis thaliana*." *Proceedings of the National Academy of Sciences* 98(22): 12826-12831.
- Meurer, J., H. Plucken, et al. (1998). "A nuclear-encoded protein of prokaryotic origin is essential for the stability of photosystem II in *Arabidopsis thaliana*." *EMBO J* 17(18): 5286-5297.
- Mohamed, H.-E., A.-M. van de Meene, et al. (2005). "Myxoxanthophyll is required for normal cell wall structure and thylakoid organization in the cyanobacterium *Synechocystis* sp. strain PCC 6803." *Journal of Bacteriology* 187(20):6883-6892.
- Munekage, Y., M. Hashimoto, et al. (2004). "Cyclic electron flow around photosystem I is essential for photosynthesis." *Nature* 429(6991): 579-582.
- Murata, N., S. Takahashi, et al. (2007). "Photoinhibition of photosystem II under environmental stress." *Biochimica et Biophysica Acta (BBA) - Bioenergetics* 1767(6): 414-421.
- Naver, H., E. Boudreau, et al. (2001). "Functional studies of Ycf3: Its role in assembly of photosystem I and interactions with some of its subunits." *The Plant Cell Online* 13(12): 2731-2745.
- Nelson, N. and A. Ben-Shem (2004). "The complex architecture of oxygenic photosynthesis." *Nat Rev Mol Cell Biol* 5(12): 971-982.
- Nelson, N. and C. F. Yocum (2006). "Structure and function of photosystems I and II." *Annu Rev Plant Biol* 57(1): 521-565.
- Nickelsen, J., B. Rengstl, et al. (2011). "Biogenesis of the cyanobacterial thylakoid membrane system--an update." *FEMS Microbiol Lett* 315(1): 1-5.
- Nierzwicki-Bauer, S. A., D. L. Balkwill, et al. (1983). "Three-dimensional ultrastructure of a unicellular cyanobacterium." *The Journal of cell biology* 97(3): 713-722.
- Nixon, P. J., F. Michoux, et al. (2010). "Recent advances in understanding the assembly and repair of photosystem II." *Annals of Botany* 106(1): 1-16.

- Park, S., P. Khamai, et al. (2007). "REP27, a tetratricopeptide repeat nuclear-encoded and chloroplast-localized protein, functions in D1/32-kD reaction center protein turnover and photosystem II repair from photodamage." *Plant Physiology* 143(4): 1547-1560.
- Peng, L., J. Ma, et al. (2006). "LOW PS II ACCUMULATION1 is involved in efficient assembly of photosystem II in *Arabidopsis thaliana*." *The Plant Cell Online* 18(4): 955-969.
- Pierre, J. and G.-N. Johnson (2011). "Regulation of cyclic and linear electron flow in higher plants." *Proceedings of the National Academy of Sciences* 108(32): 13317-13322.
- Pfeiffer, S. and K. Krupinska (2005). "Chloroplast ultrastructure in leaves of *Urtica dioica* L. analyzed after high-pressure freezing and freeze-substitution and compared with conventional fixation followed by room temperature dehydration." *Microscopy Research and Technique* 68(6): 368-376.
- Ponting, C. P., L. Aravind, et al. (1999). "Eukaryotic signaling domain homologues in Archaea and Bacteria. Ancient ancestry and horizontal gene transfer." *Journal of Molecular Biology* 289(4): 729-745.
- Raines, C. A. (2003). "The Calvin cycle revisited." *Photosynthesis Research* 75(1): 1-10.
- Reed, R. H. and W. D. P. Stewart (1985). "Osmotic adjustment and organic solute accumulation in unicellular cyanobacteria from freshwater and marine habitats." *Marine Biology* 88(1): 1-9.
- Reed, R. H., S. R. C. Warr, et al. (1985). "Multiphasic osmotic adjustment in a euryhaline cyanobacterium." *FEMS Microbiology Letters* 28(3): 225-229.
- Rengstl, B., U. Oster, et al. (2011). "An intermediate membrane subfraction in cyanobacteria is involved in an assembly network for photosystem II biogenesis." *Journal of Biological Chemistry* 286(24): 21944-21951.
- Rexroth, S., C. W. Mullineaux, et al. (2011). "The plasma membrane of the cyanobacterium *Gloeobacter violaceus* contains segregated bioenergetic domains." *The Plant Cell Online* 23(6): 2379-2390.
- Reynolds, E. S. (1963). "The use of lead citrate at high pH as an electron-opaque stain in electron microscopy." *The Journal of cell biology* 17(1): 208-212.
- Rhee, K.-H., E. P. Morris, et al. (1998). "Three-dimensional structure of the plant photosystem II reaction centre at 8 Å resolution." *Nature* 396(6708): 283-286.

- Rippka, R., J. Deruelles, et al. (1979). "Generic assignments, strain histories and properties of pure cultures of cyanobacteria." *Journal of General Microbiology* 111(1): 1-61.
- Rochaix, J.-D. (2011). "Assembly of photosynthetic complexes." *Plant Physiology* 155 (4):1493-1500.
- Roose, J.-L. and H.-B. Pakrasi (2008). "The Psb27 protein facilitates manganese cluster assembly in photosystem II." *Journal of Biological Chemistry* 283(7):4044-4050.
- Ruf, S., H. Kössel, et al. (1997). "Targeted inactivation of a tobacco intron-containing open reading frame reveals a novel chloroplast-encoded photosystem I-related gene." *The Journal of cell biology* 139(1): 95-102.
- Sambrook, J. and D. Russell (2001). "Molecular Cloning: A laboratory manual." Cold Spring Harbour Laboratory Press.
- Scheller, H. V., P. E. Jensen, et al. (2001). "Role of subunits in eukaryotic Photosystem I." *Biochimica et Biophysica Acta (BBA) - Bioenergetics* 1507(1-3): 41-60.
- Schmitz-Linneweber, C. and I. Small (2008). "Pentatricopeptide repeat proteins: a socket set for organelle gene expression." *Trends in Plant Science* 13(12): 663-670.
- Schottkowski, M., S. Gkalypoudis, et al. (2009). "Interaction of the periplasmic PrtA factor and the PsbA (D1) protein during biogenesis of photosystem II in *Synechocystis* sp. PCC 6803." *Journal of Biological Chemistry* 284(3): 1813-1819.
- Schottkowski, M., J. Ratke, et al. (2009). "Ptt, a novel tetratricopeptide repeat protein involved in light-dependent chlorophyll biosynthesis and thylakoid membrane biogenesis in *Synechocystis* sp. PCC 6803." *Molecular plant* 2(6): 1289-1297.
- Schultze, M., B. Forberich, et al. (2009). "Localization of cytochrome *b₆f* complexes implies an incomplete respiratory chain in cytoplasmic membranes of the cyanobacterium *Synechocystis* sp. PCC 6803." *Biochimica et Biophysica Acta (BBA)-Bioenergetics* 1787(12): 1479-1485.
- Schwabe, T. M. E., K. Gloddek, et al. (2003). "Purification of recombinant BtpA and Ycf3, proteins involved in membrane protein biogenesis in *Synechocystis* PCC 6803." *Journal of Chromatography B* 786(1-2): 45-59.
- Sikorski, R. S., M. S. Boguski, et al. (1990). "A repeating amino acid motif in CDC23 defines a family of proteins and a new relationship among genes required for mitosis and RNA synthesis." *Cell* 60(2): 307-317.

- Small, I. D. and N. Peeters (2000). "The PPR motif - a TPR-related motif prevalent in plant organellar proteins." *Trends in Biochemical Sciences* 25(2): 45-47.
- Smith, R. L., M. J. Redd, et al. (1995). "The tetratricopeptide repeats of Ssn6 interact with the homeo domain of alpha 2." *Genes and Development* 9(23): 2903-2910.
- Spence, E., S. Bailey, et al. (2004). "A homolog of Albino3/Oxal is essential for thylakoid biogenesis in the cyanobacterium *Synechocystis* sp. PCC6803." *Journal of Biological Chemistry* 279(53): 55792-55800.
- Stöckel, J., S. Bennewitz, et al. (2006). "The evolutionarily conserved tetratricopeptide repeat protein Pale Yellow Green7 is required for photosystem I accumulation in *Arabidopsis* and Copurifies with the Complex." *Plant Physiology* 141(3): 870-878.
- Strahl-Bolsinger, S., M. Gentzsch, et al. (1999). "Protein O-mannosylation." *Biochimica et Biophysica Acta (BBA) - General Subjects* 1426(2): 297-307.
- Strahl-Bolsinger, S. and A. Scheinost (1999). "Transmembrane topology of Pmt1p, a member of an evolutionarily conserved family of protein O-mannosyltransferases." *Journal of Biological Chemistry* 274(13): 9068-9075.
- Stengel, A., I.-L. Guegel, et al. (2012). "Initial steps in photosystem II *de novo* assembly and preloading with manganese take place in biogenesis centers in *Synechocystis*." *The Plant Cell*, in press.
- Tamura, K., D. Peterson, et al. (2011). "MEGA5: molecular evolutionary genetics analysis using maximum likelihood, evolutionary distance, and maximum parsimony methods." *Molecular biology and evolution* 28(10): 2731-2739.
- The Arabidopsis Genome Initiative (2000). "Analysis of the genome sequence of the flowering plant *Arabidopsis thaliana*." *Nature* 408(6814): 796-815.
- Thomas, C.-S. (2000). "Membrane heredity and early chloroplast evolution." *Trends in Plant Science* 5(4): 174-182.
- Umena, Y., K. Kawakami, et al. (2011). "Crystal structure of oxygen-evolving photosystem II at a resolution of 1.9 Å." *Nature* 473(7345): 55-60.
- Vaistij, F. E., E. Boudreau, et al. (2000). "Characterization of Mbb1, a nucleus-encoded tetratricopeptide-like repeat protein required for expression of the chloroplast *psbB/psbT/psbH* gene cluster in *Chlamydomonas reinhardtii*." *Proceedings of the National Academy of Sciences* 97(26): 14813-14818.

- van de Meene, A., M. Hohmann-Marriott, et al. (2006). "The three-dimensional structure of the cyanobacterium *Synechocystis* sp. PCC 6803." *Archives of Microbiology* 184(5): 259-270.
- Vassiliev, I. R., Y.-S. Jung, et al. (1998). "PsaC subunit of photosystem I is oriented with iron-sulfur cluster FB as the immediate electron donor to ferredoxin and flavodoxin." *Biophysical journal* 74(4): 2029-2035.
- Vermaas, W. F. J. (2001). Photosynthesis and respiration in cyanobacteria. *Encyclopedia of Life Sciences* 1-7.
- Wang, Q., S. Jantaro, et al. (2008). "The high light-inducible polypeptides stabilize trimeric photosystem I complex under high light conditions in *Synechocystis* PCC 6803." *Plant Physiology* 147(3): 1239-1250.
- Watanabe, M., M. Iwai, et al. (2009). "Is the photosystem II complex a monomer or a dimer?" *Plant Cell Physiol* 50(9): 1674-1680.
- Wegener, K. M., E. A. Welsh, et al. (2008). "High sensitivity proteomics assisted discovery of a novel operon involved in the assembly of photosystem II, a membrane protein complex." *Journal of Biological Chemistry* 283(41): 27829-27837.
- Westphal, S., L. Heins, et al. (2001). "Vipp1 deletion mutant of *Synechocystis*: A connection between bacterial phage shock and thylakoid biogenesis?" *Proceedings of the National Academy of Sciences* 98(7): 4243-4248.
- Wilde, A., K. Lünser, et al. (2001). "Characterization of the cyanobacterial *ycf37*: mutation decreases the photosystem I content." *Biochemistry J.* 357(1):211-216.
- Williams, J.-G.-K. (1988). "Construction of specific mutations in photosystem II photosynthetic reaction center by genetic engineering methods in *Synechocystis* 6803." *Methods in Enzymology* 167:766-778.
- Wittig, I. and H. Schägger (2005). "Advantages and limitations of clear-native PAGE." *Proteomics* 5(17): 4338-4346.
- Wollman, F. A., L. Minai, et al. (1999). "The biogenesis and assembly of photosynthetic proteins in thylakoid membranes." *Biochimica et biophysica acta* 1411: 21-85.
- Xiong, J. and C. E. Bauer (2002). "Complex evolution of photosynthesis." *Annu Rev Plant Biol* 53(1): 503-521.

- Xu, W., H. Tang, et al. (2001). "Proteins of the cyanobacterial photosystem I." *Biochimica et Biophysica Acta (BBA) - Bioenergetics* 1507(1-3): 32-40.
- Yoshihara, S., X. Geng, et al. (2002). "*pilG* gene cluster and split *pilL* genes involved in pilus biogenesis, motility and genetic transformation in the cyanobacterium *Synechocystis* sp. PCC 6803." *Plant and Cell Physiology* 43(5): 513-521.
- Yu, J. and W. Vermaas (1990). "Transcript levels and synthesis of photosystem II components in cyanobacterial mutants with inactivated photosystem II genes." *The Plant Cell Online* 2(4): 315-322.
- Yu, Q.-B., G. Li, et al. (2008). "Construction of a chloroplast protein interaction network and functional mining of photosynthetic proteins in *Arabidopsis thaliana*." *Cell Res* 18(10): 1007-1019.
- Zak, E., N. Birgitta, et al. (2001). "The initial steps of biogenesis of cyanobacterial photosystems occur in plasma membranes" *Proceedings of the National Academy of Sciences* 98(23): 13443–13448.
- Zhu, X., S.-P. Long, et al. (2008). "What is the maximum efficiency with which photosynthesis can convert solar energy into biomass?" *Current Opinion in Biotechnology* 19(2): 153-159.
- Zinchenko, V.-V., I.-V. Piven, et al. (1999). "Vectors for the complementation analysis of cyanobacterial mutants." *Russian Journal of Genetics* 35(3): 228-232.
- Zouni, A., H.-T. Witt, et al. (2001). "Crystal structure of photosystem II from *Synechococcus elongatus* at 3.8 Å resolution." *Nature* 409(6821): 739-743.

9. List of abbreviations

Å	Angstrom
Alb3	albino3 mutant of Arabidopsis
ATPase	ATP Synthase complex
BN-PAGE	blue native polyacrylamide gel electrophoresis
Ca	Calcium
Car	carotene
CAB	chlorophyll a/b-binding
CBB	Coomassie Brilliant Blue
CEF	cyclic electron flow
Chl	chlorophyll
CN-PAGE	clear/colorless native polyacrylamide gel electrophoresis
C-terminus	carboxyl terminus
Cyt <i>b₆f</i>	Cytochrome <i>b₆f</i>
DGDG	digalactosyldiacylglycerol
<i>E.coli</i>	<i>Escherichia coli</i>
Fd	ferredoxin
FNR	ferredoxin-NADP reductase
HCF	high chlorophyll fluorescence
iD1	intermediate D1
Km ^R	kanamycin resistant cassette
LHCs	Light-Harvesting Complexes
Met	Methionine
MGDG	monogalactosyldiacylglycerol
Mn	manganese
NrtA	nitrate/nitrite-binding protein
N-terminus	amino terminus
OD	optical density
OEC	oxygen evolving complex

OM	outer membrane
OPR	octatricopeptide repeat
ORF	open reading frame
PBS	phycobilisome
pD1	D1 precursor
PC	plastocyanin
PCR	Polymerase Chain Reaction
PD	peptidoglycan layer
PDM	PratA-defined membrane
Pitt	POR-interacting TPR protein
PM	plasma membrane
PMT	Protein O-mannosyltransferase
POR	light-dependent <u>p</u> rotochlorophyllide <u>o</u> xido <u>r</u> eductase
PPP4	Putative Photosynthetic Protein 4
PPR	pentatricopeptide repeat
PQ	plastoquinone
PratA	processing-associated TPR protein A
PS I	Photosystem I
PS II	Photosystem II
RbcL	large subunit of ribulose-1,5-bis-phosphate carboxylase/oxygenase
RC	reaction center
RC 47	reaction center lacking CP43
RCC I	reaction center complex I (PS II monomer)
RCC II	reaction center complex II (PS II dimer)
SCPs	small CAB-like proteins
TEM	transmission electronic microscopy
TLC	thin layer chromatography
TM	thylakoid membrane
TMD	transmembrane domain
TMP14	Thylakoid Membrane Phosphoprotein of 14 kDa

TPR	tertratricopeptide-repeat
Vipp1	vesicle-inducing protein in plastids 1
WT	wild type
Ycf	hypothetical chloroplast ORF

10. Acknowledgements

First of all, I would like to thank my supervisor Prof. Dr. Jörg Nickelsen for giving me the opportunity to perform my PhD project in his group. Furthermore, I am grateful for his constant, critical and constructive discussion with me and my project.

I appreciate the CSC (China Scholarship Council) and SFB TR1 for the financial supports.

I want to give my special thanks to Dr. Anna Stengel for numerous, fruitful and valuable discussions and suggestions coming up from my experiments and dissertation.

I also want to thank Dr. Marco Schottkowski for his helpful guidance and the constant readiness to help and answer my questions at the beginning of my project. I would like to thank Birgit Rengstl for her useful help and discussions on my experiments.

I am grateful to Dr. Irene Gügel for supplying the nice transmission electronic microscopy images and her kind assistance in the ongoing immunogold labeling experiments. I am also grateful to all the people who contributed during the physiological measurements of mutants: Dr. Ulrike Oster, Dr. Christian Stelljes and Alexander Hertle. I also thank the people from AG Koop for the frequent loan of the Mini-BeadBeater.

Many thanks to my lab colleagues: Dr. Alexandra-Viola Bohne, Fei Wang, Abdullah Jalal, Dr. Christian Schwarz and Karin Findeisen.

I am grateful to Prof. Dario Leister and Dr. Ute Armbruster for the assistance and suggestions on the project about Slr0483.

I am also grateful to my Chinese friends: Ming Zhao, Dr. Weihua Qin, Dr. Yafei Qi, Xia Ha, Yan Li, Wen Deng, Nannan Li, Qiuping Liu, Jing Wang, Yuanyuan Liang and Wenteng Xu. Thank you all for giving me the helpful suggestions and encouragement when I lose my confidence.

Last but not least, my greatest thanks are dedicated to my parents for their lifelong understanding and support. I love you!

11. Curriculum Vitae

Family name: Shao

Surname: Lin

Working address: Biozentrum LMU München, Grosshaderner Straße 2-4,
82152, Planegg-Martinsried, Germany

E-Mail: soulshao@hotmail.com

Date and place of birth: Oct. 7th. 1982 in Bei' an, Hei Longjiang, China

Nationality: Chinese

Family status: Single

Education:

since Oct. 2008 Ph.D student
Ludwig-Maximilians-Universität München
(University of Munich)
Faculty of Biology
Department of Botany
Supervisor: Prof. Dr. Jörg Nickelsen

Sept. 2005-June 2008 Master of Science
Ocean University of China
College of Marine Life Science
Department of Genetics
Thesis: Molecular analysis of periplasmic manganese superoxide dismutase from *Porphyra yezoensis* Ueda (Rhodophyta)
Supervisor: Prof. Dr. Mao, Yunxiang

Sept. 2000-June 2004 Bachelor of Science
Shandong Agricultural University
College of Life Sciences
Department of Biotechnology

12. Ehrenwörtliche Versicherung

Ich versichere hiermit ehrenwörtlich, dass die vorgelegte Dissertation von mir selbständig und ohne unerlaubte Beihilfen angefertigt wurde.

München, den 30. Januar 2012

Shao, Lin

Erklärung

Hiermit erkläre ich, dass ich zuvor nicht versucht habe, anderweitig eine Dissertation einzureichen oder mich einer Doktorprüfung zu unterziehen. Die vorliegende Dissertation wurde keiner weiteren Prüfungskommission weder in Teilen noch als Ganzes vorgelegt.

München, den 30. Januar 2012

Shao, Lin